

UNITED STATES DEPARTMENT OF COMMERCE

Alexander B. Trowbridge • *Acting Secretary*

NATIONAL BUREAU OF STANDARDS • A. V. Astin, *Director*

Nuclear Science and Technology for Ceramists

Proceedings of a Symposium

April 7-12, 1966

Held under the auspices of the Ceramic Educational Council of the American Ceramic Society, with the cooperation of the National Bureau of Standards, and under the sponsorship of the Office of Naval Research. The symposium took place at the 68th Annual Meeting of the American Ceramic Society in Washington, D.C.



National Bureau of Standards Miscellaneous Publication 285

Issued May 26, 1967

Library of Congress Catalog Card Number: 67-60013

Contents

	Page
Introduction	iv
1. Material Radiation Environment	1
Carl O. Muehlhause National Bureau of Standards Washington, D. C.	
2. Radiation Damage in Ceramics	7
Alan B. Lidiard United Kingdom Atomic Energy Research Establishment Harwell, Didcot, Berkshire, England	
3. Physical Properties of Irradiated Ceramic Materials	21
Paul W. Levy Brookhaven National Laboratory Upton, L. I., New York	
4. Chemical Problems Associated with Lattice Defects	33
R. J. Thorn and G. H. Winslow Argonne National Laboratory Argonne, Illinois	
5. Nuclear Fuel Materials	45
D. W. Readey and J. H. Handwerk Argonne National Laboratory Argonne, Illinois	
6. Reactor Materials Design	61
Don R. deHalas, W. D. Freshley and W. C. Morgan Pacific Northwest Laboratories Battelle Memorial Institute Richland, Washington	

Introduction

Our rapidly advancing technology continually presents demands to the materials scientist and engineer to make present materials do new things or to devise new materials. To meet these ever-expanding challenges, the ceramist must be able to bring to bear in his field the most advanced and sophisticated ideas and techniques available from other fields. To assist in this task, a series of Symposia was established through the joint efforts of the National Bureau of Standards, the American Ceramic Society, and the Office of Naval Research. Additional support for the first two in the series was also provided by the Edward Orton, Jr. Ceramic Foundation.

These symposia have all been held at Annual Meetings of the American Ceramic Society, under the auspices of the Ceramic Educational Council, joined in 1964 by the National Institute of Ceramic Engineers. The first three Symposia were:

Mechanical Behavior of Crystalline Solids
New York, 1962
NBS Monograph 59

Microstructure of Ceramic Materials
Pittsburgh, Pennsylvania, 1963
NBS Miscellaneous Publication 257

Systems Engineering in Ceramics
Chicago, Illinois, 1964
NBS Miscellaneous Publication 267

One of the new technologies for which ceramics hold great promise is that of nuclear reactors. Among the material properties desirable in this technology are chemical inertness, the ability to operate at elevated temperatures, and dimensional stability under loads applied for long periods. These general requirements suggest the potential usefulness of ceramics. Thus as nuclear reactor technology grows and expands, important new uses for ceramics may be expected to appear.

The requirements placed upon nuclear materials are quite naturally related to the radiation environment. Materials are chosen to perform certain functions - as fuel, moderator, control, etc., and must operate under the intense bombardment from neutrons and other high-energy radiation. Direct damage to the crystal structure by the radiation brings about changes in dimensions and in physical properties. Chemical reactivities are altered, and thus the chemical stability of the materials and the compatibility of one material with another are influenced. Successful development of nuclear materials requires an understanding of the nuclear properties and reactions, the physical processes involved in radiation damage, and the chemistry of materials under operating conditions of temperatures, atmosphere, and loading.

The purpose of this Symposium is to provide an introductory survey of those properties involved in the choice and use of materials. In the first chapter, Dr. C. O. Muehlhause describes the radiation fields present in reactors and the features of these fields most important to the development of nuclear materials, touching upon the principal physical effects induced in materials by the radiation. A. B. Lidiard, in the second chapter, discusses the solid state physics of radiation damage processes, with examples drawn partly from ceramics. The effects these processes have on physical properties is then described by P. Levy. Turning to chemical problems, R. J. Thorn and G. H. Winslow discuss the thermodynamics of non-stoichiometry, a particularly significant problem encountered with nuclear fuels. Finally, in the last two chapters, D. W. Readey and J. H. Handwerk, and D. R. deHalas, W. C. Morgan, and M. D. Freshley take up the problems encountered in the development of nuclear fuels on the one hand, and structural and moderator materials on the other, thus displaying the application of the basic ideas presented in the first four chapters.

It is the hope of the editors that this volume may prove to be of value as an introductory survey to the subject, and as a reference useful in the teaching of ceramic science. The editors would like to take this opportunity to thank the authors for the generous contribution of time and energy represented by each paper.

Floyd A. Hummel, Chairman
Pennsylvania State University

Alan D. Franklin
National Bureau of Standards

Cyrus Klingsberg
Office of Naval Research
(Now at the National Academy of Sciences)

Material Radiation Environment

C. O. Muehlhause

Institute for Materials Research

National Bureau of Standards

Washington, D. C. 20234

Abstract

Materials used in radiation systems are in general restricted by a wide variety of boundary conditions. For example, in reactor systems the materials are required not only to possess suitable nuclear properties, but also to display adequate stability against radiation damage. Ceramic materials are important in this technology. Radiation fields to which reactor materials are subjected are described, and principal physical effects induced by the radiation are identified. The elucidation of these effects by materials scientists and engineers is important not only to nuclear technology, but also to a general understanding of structure sensitivity of solids.

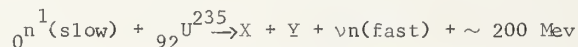
C. O. Muehlhause

Except for a few scattered speculations and one experiment, work on the interaction of radiation with bulk matter prior to the advent of atomic energy was confined to the effects on radiation by matter, i.e., just the other way around from those considerations which will be given today. I refer to the attenuation of radiation, the stopping of charged particles, the diffraction and scattering of radiation, and other similar considerations which come to mind when the radiation field intensities are low. Large scale disruption of bulk matter by radiation was regarded as remote not only because the radiation densities were low, but also because it was recognized that most of the energy deposited by charged particles induced transitory electronic and ionization changes from which the matter quickly recovered. This is to say that nearly all of the energy lost by nuclear radiation quickly appears as thermal energy. If this were not so, we would have a formidable, if not impossible, technological problem on our hands today. This will be illustrated with a few numbers.

Consider the case of fission wherein approximately 200 Mev of energy is released primarily via the short range ($\sim 5\mu$) fission products. This is a prime example of the enormous ratio, $\sim 10^8$, between nuclear and chemical energies. Even if the fuel is alloyed or otherwise contained in a material having 100 times as many atoms and the energy to disrupt a lattice site is ~ 20 ev, one might only be able to burn one fuel atom in 10^5 before the material integrity disappeared. Fortunately, this is not the case.

The high inherent energy ratio between nuclear and chemical processes should, however, constitute a warning that if even a small fraction of the energy deposit goes into a permanent change in the bulk properties of matter, one could be faced with a serious problem in the engineering of nuclear systems. This was first recognized and stated by E. P. Wigner in the early phases of the Manhattan Project. Since then a large effort has been spent studying these phenomena in a wide variety of materials. Though much of the motivation has been technological in nature, the subject is of great interest to solid state physicists, chemical physicists, metallurgists, ceramists and other materials scientists who find the inducement of defects by radiation of singular importance to their understanding of the structure sensitivity of solids. How and why this comes about will be indicated in other chapters. The purpose here will be to give some idea of the radiation environment prevailing in reactor systems and some notion of the primary physical effects which accompany that radiation.

We note first that the fission reactor is based upon the following nuclear process:



X and Y represent the fission products, (Fig. 1) and ν the average number of fast neutrons produced per fission. This number is ~ 2.5 and is the means by which the reaction is made self-sustaining. The fact that the reaction is exothermic accounts for its ability to generate power. Approximately 3×10^{19} fissions per second are required to produce one watt.

Accompanying this reaction are some prompt γ -rays. Other γ -rays result from the decay of the fission products, X and Y, and also from neutron capture in other materials composing the reactor. Not all uranium absorptions lead to fission. On the average a little more than two neutrons (η) are released per neutron absorbed, one of which is needed to sustain the reaction. The other neutron is either absorbed in the control rods or some structural component, or else it leaks from the system. In fact, the critical condition for steady power can be written:

$$\eta f p = 1$$

" η " is the average number of neutrons (fast) emitted per neutron absorbed (slow) in uranium; "f" is the fraction of neutrons absorbed in uranium compared with other materials; and "p" is the neutron non-leakage probability, a quantity dependent upon the size of the system.

The f-factor appearing above formally displays the requirement that materials comprising the reactor other than uranium fuel (i.e., moderator, structure, etc.) be of low neutron absorption. The minimum allowable value for "f" is $\cong 0.5$.

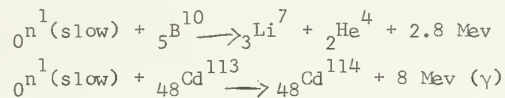
A basic reactor system consists of a core of fuel assemblies, i.e., fuel elements containing uranium; a coolant to remove the power or heat from the core; a moderator to slow the fast fission neutrons down to thermal energies (so that they may be reabsorbed by the fuel); control rods whose position in the core maintains the critical condition (largely by adjusting "f" above); a reactor vessel to contain the primary system; and a biological shield to reduce radiation levels to tolerance outside the system.

Neutrons born at the instant of fission are fast. Their average energy is ~ 1 Mev, but the distribution extends to ~ 10 Mev. (Fig. 2). In a thermal reactor it is necessary to slow them down by moderation so that they may rereact with the fuel. The reason for this is that the probability for neutron absorption generally varies inversely as the neutron velocity. Neutrons cannot be slowed down to an average energy less than the thermal energy (~ 0.025 ev) of the moderator. At this energy (\sim kT) they are in thermal equilibrium with their environment. Roughly speaking then there are three principal neutron energy regions, i.e., parts to the energy spectrum, in which neutrons are found. These correspond to: the very fast or virgin fission neutrons, the intermediate or slowing down neutrons, and the thermal or slowed down neutrons.

The spectrum (Fig. 3) is, of course, continuous and varies in detail with the specific reactor design. It also varies with position inside a given reactor. For example, the average neutron energy is highest near the fuel elements. The thermal portion is described by a Maxwell-Boltzman distribution, the intermediate portion varies as $\sim E^{-1}$, and the fast portion is like the fission spectrum of Fig. 2. The distance over which all of the transport, slowing down, and diffusion takes place varies from a few feet to several tens of feet depending on the design and size of the core.

Usually the uranium is either alloyed with another metal or embodied as an oxide in a metal to form a cermet. This is then clad with a metal to form a plate or pin. A successful type of ceramic fuel is $U_3O_8 + Al$ clad with Al. The plates are assembled to form a so-called fuel element or assembly. Some appropriate number of these are in turn required to constitute the core. They are placed in a specific geometrical array and individually cooled by the flow over their plates of some primary heat transfer fluid. This might be gas, water, or even liquid metal. Between the assemblies and for some distance beyond them is the moderator. This could be water, graphite, BeO, etc. Sometimes it is identical with the coolant, e.g., water.

Also between the assemblies are located the control rods. These absorb slow neutrons and are automatically adjusted to guarantee the critical or steady state power condition. The absorption of the rods is usually via one of the two following processes:



The first reaction produces new species (Li and He) and the second a heavier isotope plus γ -rays.

Beyond the moderator region is the reactor vessel and perhaps an additional water cooled metal shield. Finally, the entire system is contained by the biological shield, usually composed of concrete. This last structure is one in which radiation damage is not controlling. Due to its poor thermal conductivity, radiation levels must be kept low anyway to avoid excessive heating and an accompanying temperature rise which would lead to a prohibitive thermal stress.

A general picture should now be evident to you in which we have a system composed of at least five main components: the fuel assemblies, the core support structure, (usually steel grid plates), the moderator-coolant, the control rods, and the reactor vessel. All of these components are subject to various and intense radiations: fast neutrons, intermediate neutrons, slow neutrons, and γ -rays with their accompanying Compton electrons. In addition, the fuel proper is subject to fission product bombardment. Also, the control rods, if composed of boron, are subject to alpha particle bombardment.

Requirements on the fuel are most severe. This is where the bulk of the power is generated and from which the heat must be transferred to the coolant. Proper fuel materials possess the following characteristics: 1) high fuel content, 2) low parasitic neutron absorption, 3) high thermal conductivity, 4) high temperature stability, and 5) high radiation stability. Sometimes 2) is violated purposefully to improve 1) by the addition to the fuel of so-called burnable poison (e.g., boron carbide, a ceramic). This increases the life of the assembly by requiring a higher fuel loading. Ceramic fuels, though lacking the conductivity of metallic fuels, can function at higher temperatures. They also offer the advantage of being able to contain a higher fuel fraction than alloys.

Control rod materials are probably second in receiving intense radiation and are somewhat similar to the fuel element problem in that a large fraction of their special material burns up and may also generate foreign atoms.

The moderator-coolant receives intense radiation also, but this is usually a radiochemical problem. If the fluid is water, for example, the disassociated molecules are either vented or made to recombine.

The core support and reactor vessel both receive considerable radiation exposure over the lifetime of the system. These are expensive items, difficult to replace, and therefore should be designed to survive the life of the plant.

With this brief outline of the radiation conditions prevailing within a general reactor system, we will proceed to a more specific identification of the kinds of primary processes which these radiations can induce. These are all nuclear in character. The secondary processes are the ones which lead to the various and subtle solid state or chemical physics effects, and it is these which will be dealt with in greater detail in other chapters.

Before describing such things as neutron scattering, capture, transmutation and some of their consequences, it should be pointed out that the principal radiation effect is the inducement of power. Earlier it was stated that nearly all of the nuclear energy released is ultimately transformed by ionization, electron-electron interaction, and electron-phonon interaction into thermal energy or heat. This is, of course, what one wants to happen in the fuel plates, but not also throughout the system. About 85 percent of the total energy is released directly to the fuel plates and primary coolant. About 10 percent of the energy is generated in the control rods and grid plates, and another 5 percent in the reactor vessel. The γ -rays alone in the reactor core heat structural members at the rate of 1 to 10 watts per gm.

The inducement of power within the body or volume of structural members is a phenomenon not ordinarily encountered in engineering practice. It sets up additional thermal stresses which can limit or even prohibit certain types of construction. For example, a high pressure - high temperature loop contained by a cylindrical steel or other metal shell requires a certain wall thickness in the absence of the radiation field. In the field an additional thermal stress is induced, thereby requiring a greater wall thickness. This in turn generates yet greater thermal stress and it may not be possible to contain the loop by such a design at all.

The inducement of power by the radiation field in the various components can be analyzed at least initially, i.e., in a new clean system. This is to say that if the classic parameters of the materials are known along with the nuclear cross sections, the initial performance of the materials can be predicted. The difficulties arise with time when the materials or their properties are changed by the radiation. In the case of the pressure vessel cited above, it is evident one must know how the mechanical properties change with exposure in order to design a possible system. The situation with respect to creep, fatigue, and thermal cycling is even more complex.

Let us now cite the primary radiation processes of importance. These are:

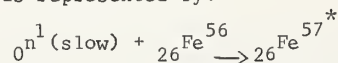
1. Slow neutron absorption.

This process was illustrated earlier in the examples of fission, n-alpha, and n- γ capture. The process can either transform a nucleus into a different species or merely add to its atomic weight and emit γ -rays. The rate at which this process or any nuclear process takes place is determined by the cross section of the nucleus, σ , and the flux of the radiation, ϕ . The cross section is the effective size of the nucleus for the process in question, and the flux is the number of bombarding particles, in this case neutrons, passing through a unit area in a unit time. Thus, if there are N nuclei per unit volume of cross section σ in a flux ϕ , the rate at which the process takes place per unit volume is given by $N\sigma\phi$. Also, the meanlife for survival of the nucleus is given by $(\sigma\phi)^{-1}$.

In a typical power reactor thermal fluxes are $\sim 10^{13}/\text{cm}^2\text{sec}$. B^{10} which has a cross section of ~ 4000 barns ($1 \text{ barn} \equiv 10^{-24}\text{cm}^2$) would have a meanlife in this flux of $\sim 2.5 \times 10^7$ sec, or approximately one year. The U^{235} cross section is ~ 600 barns.

In the case of fuel atoms, such as uranium, the fission process leads to a variety of fission products, some of which are gasses, e.g., Xe, Kr. In the case of boron-containing control rod materials one of the reaction products is also a gas, namely He. These foreign atoms usually reside in interstitial positions within the lattice and thereby alter the density and other bulk properties of the material. The gases are particularly troublesome, especially in the case of ceramics. They can accumulate to form bubbles and generate a high internal pressure. This induces swelling, cracking, rupture, and leakage. This is perhaps the most serious radiation effect in fuel and control rod materials. Of course, the passage of these fission or other fragments through the lattice also causes damage, but this appears as a background effect in the presence of the other more serious one.

In the case of structural materials, neutron absorption usually results in producing a heavier isotope and γ -rays. For steel this is represented by:



where the * represents a highly excited state of Fe^{57} . This promptly decays by cascade γ -emission according to:



The emitted γ -rays cause the Fe^{57} nucleus to recoil. The amount of energy T_γ which can be transferred in this manner is given by:

$$T_\gamma \cong \frac{5 \times 10^{-10}}{A} E_\gamma^2$$

where A is the atomic weight and E_γ is the γ -ray energy emitted. If $A \sim 50$ and $E_\gamma \sim 2$ Mev, $T_\gamma \sim 40$ ev, a quantity able to dislodge the atom from its site. The next process to be described is able to transfer considerably more energy to such atoms.

2. Fast neutron scattering.

A billiard ball type elastic scattering takes place between neutrons and all nuclei, the cross section for this process being typically several barns. The recoil or knockon ion travels for a short distance ($\sim 1\mu$) through the lattice. The maximum energy, T_M , which can be transferred by this process is given by:

$$T_M = \frac{4A}{(A+1)^2} E_n$$

where A is the atomic weight and E_n is the bombarding neutron energy.

T_M results from a head on collision. In the case of iron and a 1 Mev neutron, T_M has the value ~ 70 Kev. The transferred energy, T , varies from zero (grazing incidence) to T_M . If the scattering is isotropic, the differential probability distribution for transfer over this energy band is constant. That is:

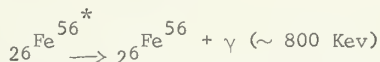
$$dp = \frac{dT}{T_M}$$

If $T \geq 25$ ev the nucleus can be dislodged from the lattice. The passage of this ion through the lattice creates both ionization and Frenkel pairs. This, however, is the subject of the other chapters.

Fast neutrons can also inelastically scatter from materials like iron. This is a process in which the neutron suffers a marked degradation in energy by exciting the nucleus to a higher state. For iron:



and the subsequent prompt reaction:



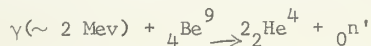
which takes the iron back to its ground state by γ -emission. The recoil energy from these two steps is less than in the elastic case, but can be $\sim E_n/A$, a significant fraction of the former case.

3. Electron scattering

Nuclear recoil from electron scattering is another possible process; however, due to the light electron mass the recoil energy is small and of the same order as T_γ , above.

4. Gamma ray transmutation.

For sufficiently high γ -ray energies (resulting from fission product decay and neutron capture) certain low binding nuclei can photo-disintegrate. For example, in beryllium or its oxide:



Fast neutrons can also induce this reaction. Again foreign atoms and, in particular gases, appear in the matrix via this process.

These constitute the principal primary interactions. In a general way it can be seen that neutron and γ -radiation disassociates matter at the chemical level. Before closing this chapter three secondary effects will be just briefly cited. These are:

1) In moderators such as graphite radiation scattering results not only in altered mechanical properties, etc., but also in the inducement of stored energy. Graphite moderated power reactors must be periodically annealed to relieve this condition.

2) Neutrons and γ -rays cause chemical disassociation, a certain amount of which will back react or anneal at the operating temperature.

3) Neutrons and γ -rays can augment chemical combination by forming chemically active species such as free radicals. This phenomenon can be put to use to fix nitrogen as in the so-called

chemonuclear systems. On the other hand it can operate to disadvantage by augmenting corrosion rates as in the graphite-moderated, sodium-cooled systems.

General References

R. Strumane, J. Nihoul, R. Gevers, and S. Amelinckx, The Interaction of Radiation with Solids, North Holland Publishing Co. (Amsterdam, 1964)

J. F. Kirchner and R. E. Bowman, Effects of Radiation on Materials and Components, Reinhold Publishing Co. (New York, 1964)

D. S. Billington and J. H. Crawford Jr., Radiation Damage in Solids, Princeton University Press (Princeton, 1961)

Reactor Material, Division of Technical Information, United States Atomic Energy Commission

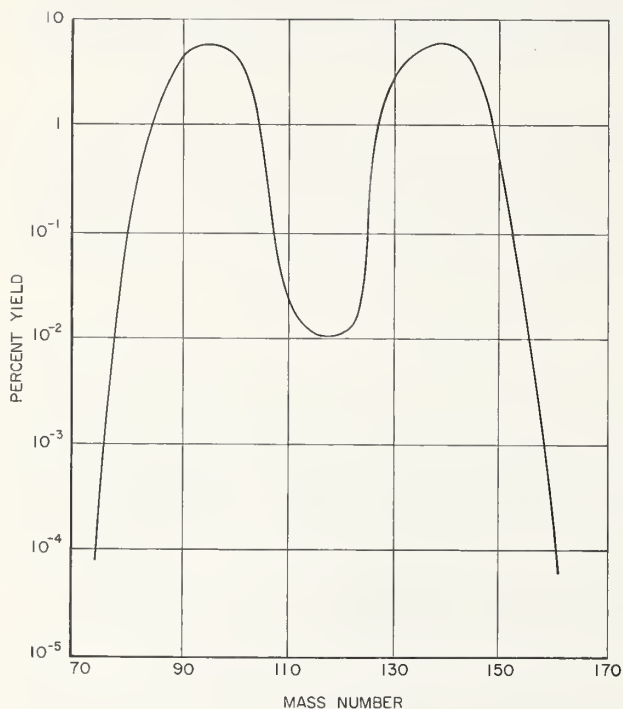


Figure 1. Fission Product Yield vs Mass

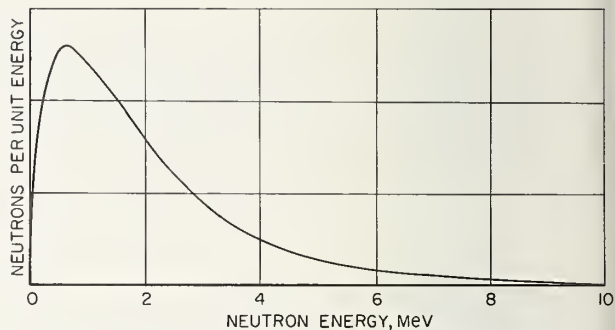


Figure 2. Fission Neutron Spectrum

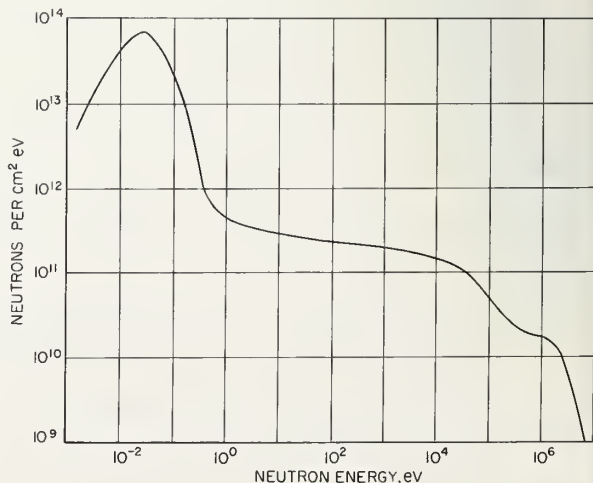


Figure 3. Reactor Neutron Spectrum

Fundamentals of Radiation Damage in Ceramics

A. B. Lidiard

United Kingdom Atomic Energy Research Establishment
Harwell, Didcot, Berks., England

Abstract

Processes of radiation damage in ceramic materials of interest in nuclear technology are reviewed. These materials include those used as fuels (e.g. UO_2 solid solutions) as fuel coatings (e.g. SiC , Al_2O_3) and as moderators (e.g. graphite, BeO). Radiation damage in these materials consists firstly of the production of interstitial atoms and vacancies and, in fuels, of the introduction of foreign atoms notably the fission products. Secondly, at normal reactor temperatures the aggregation of these defects into clusters occurs and in non-cubic materials this leads to anisotropic changes in physical properties of the component, crystallites of which the most striking may be dimensional changes (e.g. in graphite). In fuels the growth of bubbles of fission gas can also lead to important dimensional changes. The theory of the growth of defect clusters will be described in relation to some of these problems.

Fundamentals of Radiation Damage in Ceramics

A.B. Lidiard

1. Introduction

Nuclear technology provides an interest in a variety of ceramic materials and requires us to study changes in their physical properties under reactor irradiation. However, these materials do not form a coherent group from the point of view of solid state physics, but show a wide variety of electronic and crystal structures. Examples are:

- (i) carbides, nitrides, etc. of fissile elements, e.g. UC, UN; these have a metallic electronic structure and a NaCl crystal lattice;
- (ii) the stoichiometric oxides BeO, MgO, Al₂O₃, ThO₂, etc. which are insulators;
- (iii) non-stoichiometric oxides, e.g. UO₂, (U,Pu)O₂ which are semiconductors;
- (iv) SiC, which is a semiconductor;
- (v) graphite, which has a semi-metallic electronic structure.

The principle radiations to which these substances are subjected in a reactor are:

- (i) neutrons, especially fission neutrons whose average energy is about 1.5 MeV (neutron distributions are shown in Figures 2 and 3 on p. 20).
- (ii) γ -rays, which can lead in turn to the production of Compton electrons and also cause photonuclear reactions;
- (iii) (in fissile materials) fission fragments, which carry off most of the energy liberated in fission (~ 200 MeV per U²³⁵ fission).

This variety of radiations and materials means that it is only at a rather general and qualitative level that we can describe all the situations of interest. The important processes that we must consider are the following.

(1) Atomic Displacements. Atoms are displaced from their normal lattice positions as a result of receiving large amounts of kinetic energy - most frequently as a result of elastic collisions with energetic neutrons or fission fragments. In such collisions the struck nucleus may receive energy up to a maximum E_{\max} given by

$$E_{\max} = \frac{4Mm}{(M+m)^2} E_n, \quad (1.1)$$

where M = mass of the struck atom

m = mass of the neutron (or fission fragment)

E_n = energy of the incident neutron (or fission fragment).

This energy can be very high, e.g. for a C atom struck by a 1.5 MeV fission neutron E_{\max} is 475 keV, and such a displaced atom ("primary") has the potentiality to displace many other atoms ("secondaries") as it moves through the crystal. These displaced atoms eventually come to rest in interstitial positions in the lattice; the existence of these "interstitials" and the corresponding vacant lattice sites ("vacancies") changes the physical properties of the solid - including those which are important in reactor design, e.g. thermal conductivity and physical dimensions.

(2) Introduction of Foreign Atoms. Foreign atoms are introduced into fissile materials in greatest number as a result of the fission process itself. Figure 1 on p.20 shows the distribution of elements produced by the fission of U²³⁵. The rare gases Kr and Xe are especially important because of their very low solubility in all solids.

In non-fissile materials transmutations occur as a result of nuclear reactions induced by the neutrons and many of these also lead to the production of insoluble rare gases, e.g.

(a) in BeO



followed by



(b) in MgO



(c) in all oxides



Since the solubility of these gases is invariably exceeded they may collect into bubbles at high temperatures and cause swelling of the solid.

(3) Annealing Reactions. Interstitial atoms and vacancies can migrate through the lattice as a result of thermal activation and can therefore recombine, with consequent removal of the damage. Recombination can also occur when a new displacement sequence penetrates into a region of previous damage. Thermally activated recombination means that less damage is retained at higher than at low temperatures, while irradiation-induced recombination means that proportionally less damage occurs at high doses than at low doses ("saturation").

(4) Clustering Reactions. Thermally activated motion of the interstitials and vacancies leads not only to their mutual annihilation but also to the clustering of defects of like kind, e.g. interstitials may cluster together to form a new lattice plane. Such processes occur almost universally at the temperatures of reactor operation and the study of their nucleation and growth is important. The nucleation and growth of rare gas bubbles and other precipitate phases may be equally important at higher temperatures.

In this review we shall survey the elements of the quantitative description of these four major processes, illustrating the principles as far as possible by examples in ceramic materials. Our attention will be mainly on neutron damage; this will focus the discussion on the fundamentals of the subject. Even here we shall find large gaps in our knowledge and understanding of ceramic materials. It does not therefore seem appropriate to elaborate greatly on the more complicated fission fragment damage - even though this is of great importance in fuels. Where possible we shall try to indicate the differences from neutron damage.

It is not our object to review knowledge of the effects of radiation upon physical properties nor to discuss the principles behind different experimental methods of studying defects for which there are other sources, in particular the article by Levy on p. 21[1]¹.

2. The Displacement of Atoms

In passing through matter neutrons cause no direct ionisation or electronic excitation and collide elastically with the nuclei with only very low cross-section (total elastic cross-sections σ typically $\sim 10^{-24} \text{ cm}^2$). Since the number of nuclei per cm^3 in a solid, N , is roughly 10^{22} it follows that the mean free path $\lambda = 1/N\sigma$ is $\sim 100 \text{ cm}$. Thus the primary displacements are well separated independent events. The probability that an atom receives energy between E and $E+dE$ as a result of a collision between its nucleus and a neutron of energy E_n is governed by the differential cross-section $\sigma(E_n, E)$ for this transfer. To a good approximation $\sigma(E_n, E)$ is generally independent of E up to E_{max} - beyond which it is zero, of course ("hard-sphere" collisions). This has the consequence that the average energy of atoms struck by neutrons of energy E_n is $E_{\text{max}}/2$, which is very high for fission neutrons. Each primary displaced atom of energy E therefore gives rise to a cascade of collisions in the lattice, leading ultimately to $\nu(E)$ displaced atoms altogether.

¹Figures in brackets indicate the literature references at the end of this paper.

2.1 Total number of displaced atoms

(a) The Collisions. It is a major part of our problem to calculate $\nu(E)$ for each of the kinds of atom making up the lattice. The greater part of the discussions of $\nu(E)$ have however been made for monatomic substances and we shall first describe the salient features of this simpler situation. A useful and adequate simplification which is often made in approaching this problem is to treat the collisions between atoms as hard-sphere collisions - even though the actual potential of interaction will not be infinitely hard but will be Coulombic at close distances of approach and something like screened Coulombic or Born-Mayer (i.e. exponential) at larger distances. This hard-sphere approximation is generally a fair one to use for collisions leading to large angular deflections if we equate the classical distance of closest approach of two atoms in a head-on encounter to the sum of their equivalent hard-sphere radii, i.e. to their diameter D when they are chemically the same. This means that the effective diameter of an atom moving through the lattice is a function of its energy, $D(E)$, which decreases as its energy increases. A fast atom therefore sees a more open lattice than a slow one

For atoms of atomic weight, A , greater than about 50 the mean energy of a primary produced by fission neutrons is low enough that, in subsequent collisions, the screening effect of the electrons is always important. All collisions are then effectively hard-sphere collisions. On the other hand light atoms ($A < 50$) receive more energy from the neutrons and in the subsequent collisions the nuclei may penetrate right inside the screening electron cloud. The interaction potential is then Coulombic, with the consequence that the cross-section for energy transfer E' is proportional to $1/(E')^2$, so that low energy transfers are much more probable than the hard-sphere approximation would predict. This causes an important difference in the distribution of defects, although for a special reason it turns out not to affect very much the total number of displacements. We shall therefore proceed first on the basis that all collisions are hard-sphere collisions.

Fission fragments are of sufficiently high initial energy (light ~ 95 MeV and heavy ~ 67 MeV) that here too the collisions with the atoms of the solid are Coulombic, at least to begin with; as Figure 1 shows they become hard-sphere type when they have slowed down to ~ 160 keV (light) and ~ 400 keV (heavy). This figure shows the energy at which the scattering becomes mainly Coulomb scattering as a function of the atomic number of the colliding atoms. The boundary between Coulomb encounters and hard-sphere encounters has been calculated using a screened Coulomb potential proposed by Bohr.

(b) The Displacement Energy. In terms of $\nu(E)$ we can write down an expression for the displacement cross-section σ_d , defined so that

$$\text{No. of displaced atoms} = (\sigma_d N) \times (\text{neutron dose}) , \quad (2.1)$$

where N is the number of atoms per unit volume of solid and

$$\text{Dose} = (\text{time of irradiation}) \times \int_0^{\infty} \phi(E_n) dE_n , \quad (2.2)$$

in which $\phi(E_n) dE_n$ is the flux of neutrons having energies in the interval between E_n and $E_n + dE_n$. This spectrum depends upon the reactor being used and the position of the specimen relative to the fuel elements (an example is Figure 3 on p. 20). The expression for σ_d is

$$\sigma_d = \frac{\int_0^{\infty} \phi(E_n) dE_n \int_{E_d}^{E_{\max}(E_n)} \nu(E) \sigma(E_n, E) dE}{\int_0^{\infty} \phi(E_n) dE_n} . \quad (2.3)$$

In this expression we have introduced a lowest energy E_d which an atom must receive if it is to be displaced from its normal lattice site; this energy is several times the sum of the thermodynamic formation energies of interstitials and vacancies - the extra energy being dissipated as heat in the displacement process. The cross-section $\sigma(E_n, E)$ may be taken as $\sigma_{\text{total}}/E_n$.

To calculate $\nu(E)$ we need the following:

- (i) the fundamental displacement probability $P(E) dE$ of an atom which has received energy between E and $E+dE$;
- (ii) a knowledge of the loss of energy by an energetic atom by ionisation.

A typical displacement probability may be as shown in Figure 2. There will be a lower threshold corresponding to the direction of easiest displacement in the lattice. The function will then rise in one or more steps corresponding to directions of more difficult displacement (more closely packed crystal directions) before it approaches the asymptote $P=1$ at high energies. A much simpler model than this is often used; $P(E)$ is replaced by a simple step function

$$\begin{aligned} P(E) &= 0 & E < E_d, \\ P(E) &= 1 & E > E_d. \end{aligned} \tag{2.4}$$

For simple analytical calculations it is difficult to use more complex forms and we shall therefore use (2.4) here. Although some reasonable calculations of the energy E_d have now been made for metals [2,3], this is best determined experimentally and this is generally done by electron irradiation. The small mass of the electron allows only low energy transfers. The energy of the electron beam can therefore be adjusted until a radiation damage threshold is found. In practice, since $P(E)$ is not generally a simple step function the exact value obtained may depend on the sensitivity of the method used to study the radiation damage. An example of this occurs in graphite, as shown by the following illustrative results.

TABLE I. Displacement Energies

Substance	Displacement energy	Method
C, graphite	33 eV threshold	Sensitive chemical method [4]
C, graphite	60 eV	Electrical resistivity change [5]
C, diamond	80 eV	7410 Å Colour centres [6]
SiC	~ 30 eV	Change in carrier concentration [7]

In compounds there is necessarily more than one displacement energy, but so far there are no examples of substances for which these have been determined. In Al_2O_3 there is a colour centre which absorbs at 6 eV. Electron irradiation experiments [8] lead to the conclusion that if (as seems more likely) this is an oxygen defect then

$$E_d(O) = 40 \text{ eV},$$

whereas if it is an Al defect then

$$E_d(Al) = 22 \text{ eV}.$$

Such uncertainties are at present characteristic of the materials we are interested in here and more work needs to be done on the identification of defects and the determination of E_d parameters. Errors in $\nu(E)$ are in proportion to those in E_d . In materials such as BeO , MgO , SiC , etc. where the two kinds of atoms lie on equivalent sites we might expect their displacement energies to be closely equal.

(c) Ionisation. The third point we have to discuss before calculating $\nu(E)$ is loss of energy by ionisation and electronic excitation. This is unimportant at low energies where the electrons of the solid can follow the motion of the atom as it travels through. At high energies, by contrast, it is dominant. The energies of light atoms (say atomic weight < 50) displaced by fission neutrons are such that ionisation losses are significant; this applies to all of the substances on our list. Unfortunately, detailed knowledge of ionisation losses is not very extensive. Theoretical expressions give order of magnitude agreement for $10^4 < E < 10^6$ eV. The relation between the rates of loss of energy by electronic excitation and by elastic collisions is shown schematically in Figure 3. Electronic excitation rapidly dominates above a certain critical energy, E_i , and is unimportant below it. Commonly therefore one takes

$$\nu(E) = \nu(E_i), \quad E > E_i. \tag{2.5}$$

A crude, but often used, approximation is to take

$$E_i = M \text{ keV} \quad (2.6)$$

where M is the atomic weight of the moving atom. This relation between E and M results from equating the dominant excitation frequency of the solid to the principal frequency associated with the motion of the fast atom through it; the coefficient of proportionality, which strictly is dependent upon the properties of the solid, turns out generally to be roughly 1 keV. For light atoms under fast neutron irradiation, $E_{\max} > E_i$.

A more satisfactory procedure is to calculate both the rate of loss of energy in collisions with the lattice and the rate of loss by ionisation as the primary is slowed down. This then gives us the effective energy available for the production of displacements by the primary.

It is implicit in what we have just said that ionisation or electronic excitation per se will not lead to displacements of atoms from the lattice. While this is generally correct it is not true of at least some alkali halides and other alkali salts. Here there is no doubt that ionisation of the solid leads to displacements of anions. The exact mechanism by which this occurs is still not settled, but the various models proposed agree in not expecting the effect to be significant in oxides. There is some indication that it may occur to a small extent in BeO [9].

(d) The Calculation of $\nu(E)$. With this simple model we can now determine the function $\nu(E)$ by a simple argument. We assume that after collision an atom continues through the lattice if its energy $E > E_d$, otherwise not. Thus if an atom having energy $< 2E_d$ collides with a stationary atom at least one of the pair has energy $< E_d$ after collision and there is no multiplication in the number of displaced atoms. Thus

$$\nu(E) = 1, \quad E_d < E < 2E_d. \quad (2.7)$$

When $E > 2E_d$ we arrive at the following equation for $\nu(E)$ based on the fact that after a collision each of the two atoms gives rise to further displacements which on average total $\nu(E)$. For hard sphere collisions all energy transfers are equally probable and

$$\nu(E) = \int_0^E \nu(E') \frac{dE'}{E} + \int_0^E \nu(E-E') \frac{dE'}{E},$$

i.e.

$$E \nu(E) = 2 \int_0^E \nu(E') dE',$$

or

$$E \frac{d\nu}{dE} = \nu(E).$$

By (2.7) this gives

$$\nu(E) = E/2E_d, \quad E > 2E_d. \quad (2.8)$$

This result is due to Kinchin and Pease [10]. Other formulations, either making slightly different assumptions about the conditions for displacement or about the distribution of energy in the collisions, lead to closely similar results.

In fact this result (2.8) may even be good when the primary is so energetic that its collisions with the atoms of the solid are no longer hard-sphere collisions but Coulomb collisions. The reason is that by the nature of Coulomb collisions the primary then loses its energy principally in a series of low angle collisions in each of which there is a relatively small transfer of energy. The secondaries are on average energetic enough to produce further displacements, but are well within the range of hard-sphere encounters. The result is that the energy of the primary is spread out over a large number of secondaries each of which then produces more displacements in accordance with (2.8). Since $\nu(E)$ is linear in E we therefore arrive at the same total number of displacements as if we had assumed (2.8) for the primary itself. This is especially fortunate in the present context since at the high energies which light atoms may receive from fission neutrons the encounters are almost entirely Coulombic.

Equation (2.8) has been widely used for the calculation of displacement cross-sections. An example of its use together with (2.6) is that for graphite ($E_d = 60$ eV):

$$\sigma_d = 0.677 \times 10^{-21} \times (\text{equivalent Ni dose})$$

for a position in a hollow fuel element in the Harwell Pluto reactor [11]. The equivalent Ni-dose is a measure of the fast neutron flux in this reactor. A more careful treatment of the relative energy losses by electronic excitation and by displacement (e.g. not completely omitting displacement losses when $E > E_d$) leads to a higher estimate [11]

$$\sigma_d = 1.313 \times 10^{-21} \times (\text{equivalent Ni dose}) .$$

Such results, although evaluated for a particular material and a particular neutron spectrum, are typical. For order of magnitude estimates we may take it that this kind of calculation predicts every atom to be displaced once by doses in the range $10^{20} - 10^{21}$.

This kind of simple cascade theory has not been developed for diatomic (or more complex solids) except for a model solid of type AB in which E_d is the same for both atoms [12]. As noted previously we may expect this to be a fair model in some cases, e.g. for BeO and MgO. The total number of displacements does not vary much with the ratio of masses of the two atoms. For example when the mass ratio parameter $\lambda \equiv 4 M_A M_B / (M_A + M_B)^2$ is $\frac{1}{4}$ (heavier atom ~ 13 times the mass of the lighter) the total number of displaced atoms is $\sim 0.44 (E/E_d)$ in place of (2.8). The difference between the numbers of displaced atoms like and unlike the primary however increases more slowly than linearly with the energy of the primary. Thus primaries of very high energy effectively produce only displacements of their own kind. Since, in neutron irradiation, the mean primary energy is high this result implies that the numbers of displaced atoms of different kinds are in proportion to their neutron elastic scattering cross-sections.

2.2 Lattice Effects

It is known from work on radiation damage in metals (especially Cu and other noble metals) that even where good threshold values E_d are known the expression (2.8) leads to overestimates of the number of displaced atoms [13]. It is generally believed that this is due to the neglect of the lattice structure in the calculation and, in particular, to the phenomenon of "channelling". It has been observed both experimentally and in computer simulations that a proportion of the fast displaced atoms become focussed into open channels through the lattice and that they then continue in these channels in fairly stable trajectories. An obvious example of a channel is obtained by looking along the c-axis of a wurtzite lattice, e.g. BeO. Atoms moving in these channels at velocities greater than phonon velocities lose energy by the generation of a phonon shock-wave; the energy received by the atoms of the lattice, although large, is then not large enough to cause displacements (a few times 10 eV per plane).

Robinson and Oen [14] have developed the theory leading to (2.8) to include a probability P that either of the two atoms involved in a collision becomes channelled afterwards. Channelled atoms are assumed to produce no further displacements. Then in place of (2.8) they get

$$\nu(E) = \frac{1}{(1-2P)} \left[(1-P) \left(\frac{E}{2E_d} \right)^{1-2P} - P \right]. \quad (2.9)$$

In Cu $P \sim 0.07$ empirically. Nothing appears to be known about this quantity theoretically. It is assumed in the above calculation to be independent of E and this may be fair for a close-packed lattice when collisions are hard-sphere collisions - the situation one is interested in for Cu. However, for light atoms struck by neutrons the subsequent collisions will generally be Coulomb collisions and these give predominantly small angle deflections. It therefore seems unlikely that P is significantly different from zero for many of the solids of interest here.

2.3 Distribution of Defects

The simple cascade theory of §2.1 can be developed to provide estimates of the range of an energetic atom and thus of the size of the region containing the defects produced by a given primary. Such calculations have been done in the approximation of hard-sphere scattering but they are not independent of the potential of interaction between the atoms since the collision radius enters in directly; this, as we have noted above depends on energy in a way fixed by the interaction potential. Reasonable potentials exist and have been used. For example, the average Cu primary

under fission neutron irradiation has energy of 64 keV and in Cu metal this gives rise to a damaged region about 250 Å long; extension of the calculations to give the lateral spread leads to a width about half this. The atomic fraction of defects in this volume is thus about 2%. These estimates agree with the rate at which one observes saturation of irradiation damage at high doses due to the overlap of separate damage regions.

The channelling of the fast atoms will undoubtedly lead to a more diffuse distribution than calculated in this way; channelled atoms will come to rest (as interstitials) well outside the damaged region, which will therefore contain an excess of vacancies. There are also low energy processes - "replacement sequences" - leading to the same effect [15]. Collision sequences propagate coherently down close-packed rows of atoms as a result of either purely geometrical ("Silsbee") focussing of successive collisions toward the axis or focussing assisted by the neighbouring rows of atoms. These are low energy effects because when the collision radii become too small (high energies) the lattice effectively becomes too open to restrain the sequence of collisions along a row. These maximum energies may be a few times the displacement energy E_d . The point for the present discussion is that for energies greater than E_d (for the relevant direction) these sequences propagate as replacement sequences, each atom taking the place of the next one along the row. This process thus also produces interstitials on the outside of the damaged region. Of course, in strongly ionic compounds these replacement sequences can only propagate along rows of one kind of atom.

These features thus lead to a picture of neutron damage as consisting of relatively high defect density with a diffuse distribution of interstitials on the outside. This is the commonly assumed model which applies to materials of atomic number Z greater than about 25. However as we have already seen the energies of light atoms displaced by fission neutrons are generally so high that their collisions with atoms of the solid are primarily Coulomb, rather than hard-sphere, collisions. The distribution of defects produced by a primary is then very different and consists not of a single region of defects but of a greater number of clumps of a few interstitials and vacancies. One can make detailed predictions of the range of a primary and the mean size of these clumps once an interaction potential is assumed. We may contrast results for Ge ($Z=32$) with those for C ($Z=6$). Thus a 10 keV Ge (about $\frac{1}{4}$ the mean energy of Ge primaries produced by 1.5 MeV fission neutrons) gives generally a single dense group of interstitials and vacancies ~ 200 Å diameter [16]. On the other hand a 100 keV C primary (again about $\frac{1}{4}$ the mean energy of primaries produced by 1.5 MeV fission neutrons) has a range ~ 2000 Å and the secondary defects are produced in small groups of 10 or less, separated by ~ 60 Å [17]. In the example of a C primary it is not until it has slowed down to a few keV that it enters the hard sphere range of collisions (Figure 1); its path will therefore end in a larger group of defects. For heavier atoms, e.g. Mg or Al, this final group will be larger. In the corresponding situation which arises at the end of a fission fragment path it may be very large indeed, containing several thousand defects.

We can summarise the general picture thus:

(1) In ceramics containing only light atoms - most of those in our list - the defects resulting from neutron irradiation are distributed in a large number of small groups. This is a much more nearly random distribution than the usual picture of neutron damage in materials of medium and high atomic weight.

(2) In ceramics containing both heavy and light atoms, say UO_2 , we expect the U primaries to displace mainly the U atoms and so give large clusters of U-vacancies and U-interstitials. Similarly the O primaries will displace mainly O atoms, but, lead to a much larger number of small groups of O interstitials and vacancies.

This picture of course applies to very low temperatures where the defects are frozen-in and cannot move after their production. Most experiments on these materials have, however, been done at reactor temperature and above; some of the defects are then expected to be mobile as a result of thermal activation. We must therefore consider the effect this has.

3. Annealing Processes

The picture of radiation damage which we have described in §2 only strictly applies at exceedingly low temperatures, where no thermally activated atomic migrations are possible. At temperatures where these migrations can occur various annealing processes will go on, e.g. interstitial-vacancy recombination, the formation of small mobile clusters and eventually of large immobile clusters. A basic knowledge of defect migration rates is needed to understand these processes and in this section we shall briefly discuss defect activation energies, since these are the most important parameters determining these migration rates.

We shall elaborate on the following three features:

(i) the activation energies for interstitials are often less than those for the corresponding vacancies (Table II).

(ii) activation energies are different for different electronic states and degrees of ionisation of the same defect.

(iii) close-pairs of vacancies and interstitials may recombine with very low activation energies.

TABLE II. Some Defect Migration Activation Energies

Substance	Vacancy, E_{mv}	Interstitial, E_{mi}	Remarks
Cu	1.05 eV	0.71 eV	E_{mi} is energy of Stage III annealing
Ag	0.88	0.67	"
Au	0.82	0.80	"
Graphite	>2.5	~0.5	[17]
Si	0.33	~0	[18]
AgCl	(Ag^+) 0.33	(Ag^+) 0.15	
AgBr	(Ag^+) 0.36	(Ag^+) 0.15	
KCl	(Cl^-) 0.95	(Cl^-) ~0.07	[19,20]
CaF ₂	(F^-) <0.9	(F^-) 1.7	n.b. $E_{mi} > E_{mv}$ [21]

(i) Defect activation energies are known experimentally with varying degrees of certainty for different substances. In the noble metals the vacancy activation energies are known accurately; the interstitial activation energies are probably those characterising the famous annealing stage III, even though the evidence for this is still qualitative and subject to dispute. That the interstitial in graphite has a lower activation energy than the vacancy is shown by the formation of interstitial clusters - identified in the electron microscope - at lower temperatures than vacancy clusters. A similar situation is observed also in some irradiated metals and oxides, thus confirming $E_{mi} < E_{mv}$ here too.

For the Ag^+ -ion defects in AgCl and AgBr both vacancy and interstitial activation energies are accurately known; even details of the mode of interstitial movement are known experimentally [22]. In the alkali halides - and by implication perhaps also in the alkaline earth oxides - calculations predict [22],

$$E_{mv} \sim E_{mi} \text{ for the cation defects}$$

$$E_{mv} > E_{mi} \text{ for the anion defects.}$$

The interstitial ions are predicted to move by a replacement or interstitialcy mechanisms - as do the Ag^+ ions in AgBr and AgCl. The anion interstitial in the alkali halides is predicted to move with a low activation energy and thus to anneal out at very low temperatures, e.g. below liquid N_2 temperature.

(ii) In insulators, of course, interstitials and vacancies can exist in various charge states and the activation energy for migration may alter considerably when the centre is ionised or in an excited state. Thus in KCl the F-centre appears less mobile than the empty anion vacancy, but the activation energy for an F-centre in its first excited electronic state is very low indeed. On the other hand the interstitial halogen atom - the so-called H-centre - migrates as easily as the interstitial halogen ion. There is a considerable variety of possible behaviour with only a few pointers to the general rules at the present time.

(iii) The processes of the recombination of close pairs of vacancies and interstitials may go with very low activation energies. Indeed in many substances there are many positions of an interstitial around a vacancy that are unstable, so that no activation is required for recombination. These unstable volumes determine the speed with which radiation damage saturates at very low temperatures. In Cu, saturation measurements lead to an unstable volume of about 80 atomic volumes. Beyond these unstable positions of the interstitial lie positions from which the activation energy is only about 0.1 eV (cf. Table II) and from these positions thermally activated recombination takes place at or below ~ 50 K. The recombination of close pairs of anion vacancies and anion interstitials takes place at even lower temperatures in KCl and KBr. Again, of course, such processes depend on the charge states of the defects concerned; Coulomb forces between charged defects can easily be dominant.

These remarks and examples have been largely drawn from materials much more fully studied than those of concern here. But it seems clear that even in ceramic materials we would expect processes involving interstitial-vacancy recombination and other rearrangements, e.g. formation of interstitial pairs, at temperatures below room temperature. Some examples are:

(1) BeO. We know from work on diffusion and ionic conductivity by Austermann [23] that the Be^{2+} ion vacancy moves with an energy of ~ 1.5 eV. By analogy with the theoretical results for the alkali halides we might assume that Be^{2+} interstitials move with roughly the same activation energy as the Be^{2+} vacancy, so that their migration will not be significant below, say, 200°C . On the other hand by this same analogy O^{2-} interstitials may have an activation energy of not more than 0.5 eV and they will consequently be mobile as low as $\sim 200^\circ\text{K}$. The recombination of close interstitial-vacancy pairs is expected at even lower temperatures; indeed some recovery of thermal conductivity in irradiated BeO is seen [25] between 100°K and 300°K (irradiation temperature $\sim 100^\circ\text{K}$). Further evidence for the mobility of defects at low temperatures in BeO comes from the observation of defect clusters in BeO after irradiation at reactor temperature. In addition long wavelength ($>$ say 5\AA) neutron scattering experiments [25] show that material irradiated at 150°C contains only a few per cent of the predicted number of defects. (These experiments can give absolute values of the total defect concentration when good estimates of the lattice distortion around the defects can be made). Many more low temperature studies need to be made in order to understand the basic annealing processes going on.

(2) MgO. In irradiated MgO a number of vacancy defect centres have been identified by optical methods and spin resonance. These include:

(a) F-centres [27];

(b) aggregate centres having the same symmetry and probably the same structure as the M, R and N centres in alkali halides [28];

(c) trapped hole centres [27].

However, with one possible exception [27] there appear to be no observations of interstitial centres by these means, although large clusters formed at high temperatures have been identified as interstitial. There is very little information about activation energies or annealing processes in this material, but again studies [28] of material irradiated at $\sim 100^\circ\text{C}$ show only a few per cent of the defects expected from theory (using $E_d \sim 25$ eV) and there is little doubt that thermally activated annealing occurs below room temperature.

(3) UO₂. In UO₂ the interstitial oxygen ion migrates with an activation energy of ~ 1.3 eV, as is known from a combination of oxygen diffusion studies and thermodynamic studies on non-stoichiometric UO_{2+x}. Owing to the difficulty of obtaining accurately stoichiometric material it has not so far proved possible to study point defects optically in this substance. The electrical conductivity of UO_{2+x} is due to the migration of electron holes and in irradiated material the conductivity decreases, presumably as a result of the trapping of holes. A recovery stage, believed to be second order, occurs around 700°C with an activation energy of 2.3 eV. This temperature is much higher than the 100°C or so to be expected if the interstitial oxygen ion were responsible (1.3 eV) and may correspond to the motion of the uranium vacancy (which could also be a hole trap). However, irradiation at reactor temperature leads to the presence of defect clusters visible in the electron microscope and by annealing at higher temperatures these have been identified as interstitial clusters without stacking fault, i.e. containing both U and O in the correct proportion. At the present time it does not seem easy to put the defect clusters seen in the electron microscope in relation to point defects. There does not seem to be evidence for the different primary distributions of U and O defects expected in §2. This may be because one or more of the primary defects is mobile below reactor temperature [30].

(4) Graphite. Of the materials in our list, graphite is undoubtedly the best understood [17]. Here the vacancies do not become appreciably mobile until $\sim 600^\circ\text{C}$ whereas at room temperature the interstitials are undoubtedly very mobile and form small clusters, both mobile and immobile. The mobile interstitials which may be pairs or triplets, have an activation energy of 1.2 eV and nucleate larger clusters. These grow on continued irradiation, forming extra discs between the hexagonal layers. These large clusters are visible in the electron microscope and they have been verified to be interstitial layers by this means.

It is clear from these examples that in all the materials of interest here defect clusters are formed in material irradiated at reactor temperature and above. Except in graphite, the basic mechanisms by which these form and grow are so far largely unstudied; much of the necessary basic knowledge about the point defects is missing. However it is clear that these clusters are an important aspect of radiation damage and we shall therefore discuss them in further detail in the next section.

4. Defect Cluster Formation

The general pattern of clusters seen in neutron irradiated materials is that at lower temperatures (reactor temperature and above) the density of clusters is high but their size is small. They are visible in the electron microscope, but not resolvable as more than dots. At higher temperatures of irradiation their density is low but they are much bigger and their type - e.g. interstitials or vacancies, with or without stacking fault - may be determined. The total number of point defects retained in the form of clusters after a given dose is less the higher the temperature of irradiation.

In anisotropic materials, e.g. graphite, BeO, U-metal, the collection of interstitial defects - the more mobile - on to the basal plane of a crystal leads to a macroscopic growth in the perpendicular direction. This does not saturate with dose so rapidly as properties dependent on point defects or dislocation line length, e.g. thermal conductivity. It is clear therefore that the nucleation and growth of these clusters is important in practice and we make some remarks about these aspects. These are mainly derived from a detailed study which we have made for graphite [31] but are probably of wider application. We may, however, remark that the conditions of nucleation and growth in other ceramic systems have not yet been sufficiently well studied experimentally for this to be certain.

In this connection it should also be noted that ionic and charged defects can only cluster in the correct stoichiometric proportions. On the other hand uncharged defects can cluster without preserving stoichiometry, e.g. the clustering of F-centres to give M-, R-, N-centres and, ultimately, metal particles in the alkali halides.

4.1 Nucleation

In graphite this is known to be intrinsic or "homogeneous", i.e. the nuclei are formed by the random aggregation of the defects. The general characteristic of homogeneous nucleation is the temperature variation described above. At high temperatures the density of homogeneously formed nuclei becomes lower than the density of impurity or boundary nucleation sites. A changeover to heterogeneous nucleation at higher temperatures has also been observed in graphite.

Now the density of homogeneously formed nuclei involves the mobility of the point defects which form the cluster. In the early stages the rate of formation of nuclei must follow an equation describing random encounters of the mobile defects, i.e.

$$\frac{d}{dt} (\text{nuclei}) = (\text{mobility constant}) \times c^2, \quad (4.1)$$

where c is the concentration of mobile defects. Once formed, the nuclei grow as the irradiation proceeds. The density of nuclei increases until a point is reached where a newly created defect is more likely to reach an existing cluster than it is to encounter another migrating defect. At this point nucleation ceases and something closely approaching a steady state is established. As the clusters grow their efficiency of collection of the defects increases and the steady-state concentration of point defects falls, thus making the formation of further nuclei less and less probable as the irradiation proceeds. The density of nuclei arising in a solid (cubic) is proportional to D^{-2} where D is the diffusion coefficient of the defect. In a strongly anisotropic material such as graphite in which the defect migration is effectively two-dimensional the density of nuclei again is almost but not exactly proportional to D^{-2} . The nucleation of fission gas bubbles by the aggregation of fission gas atoms is similar [32].

4.2 Growth

Since the interstitials execute a random walk through the lattice until they either disappear by recombination with a vacancy or become attached to a cluster we can describe their concentration, c , by a diffusion equation

$$\frac{\partial c}{\partial t} = D \nabla^2 c + G_0 - \Gamma \delta c, \quad (4.2)$$

which contains the rate of generation by the radiation G_0 and the interstitial-vacancy recombination term $\Gamma \delta c$. Here Γ is the jump frequency of the interstitial ($D \propto \Gamma$) and δ is the probability of annihilation at any jump - proportional to the vacancy concentration and thus dependent on the time (of irradiation). The boundary conditions to be observed are:

- (i) $c=0$, at the cluster periphery at all t ,
- (ii) $c=0$, everywhere at $t=0$,
- (iii) $\nabla c=0$, midway between clusters.

In graphite we have effectively a two-dimensional problem since the interstitials migrate much more easily between the hexagonal layers than in the a-axis direction. Some general features of a detailed study of the graphite problem are however worth noting.

(a) The solution for c is very flat over the greater part of the region between clusters. It is therefore independent of their arrangement.

(b) The mean concentration of the mobile point defects is very low - due to the fine distribution of sinks which the clusters represent. Thus in graphite at 200°C the mean spacing between clusters is only 800 Å; as a result, after 5×10^{19} fast neutrons, the atomic fraction of mobile interstitials is only $\sim 10^{-7}$. Hence the existence of sizeable radiation effects which cannot be accounted for by the clusters may imply the existence of small immobile clusters of interstitials in addition to the mobile ones. This situation certainly occurs in graphite and probably in BeO and a number of other substances as well.

(c) D is not important in determining the rate of growth of the clusters once nucleation is settled. This rather surprising result arises because once nucleation has stopped there is a nearly steady state, the time dependence of c arising only through the (slow) growth of the defect cluster. It is therefore a good approximation to put $\partial c / \partial t \sim 0$ in (4.2) whence, since D is proportional to Γ ,

$$c = \frac{G_0}{D} \times \text{function of } (\delta, r, t) . \quad (4.3)$$

The rate of arrival of defects at the cluster is then

$$\int_{\Sigma} \underline{J} \cdot d\underline{S} = - \int_{\Sigma} D(\nabla c) \cdot d\underline{S} \quad (4.4)$$

where J is the flux and Σ is the cluster surface. Hence by (4.3) and (4.4) the cluster growth is independent of D in this approximation. Of course, the total number of defects retained as clusters will be proportional to D^{-2} through the density of nuclei.

The important parameters for the growth of clusters are G_0 , the rate of introduction of defects, and δ their recombination probability. The former may be taken from the theory of §2.1; δ varies with dose. Since the vacancy concentration may saturate at high doses the rate of growth of interstitial clusters may show an increase at high doses. This effect occurs in graphite. There it also appears that small vacancy clusters, even divacancies, may collapse and no longer act as sinks for interstitials, but this may be a special property of this covalent structure.

The total number of defects retained as clusters at a given dose will therefore depend on temperature through the density of nuclei, which is proportional to D^{-2} , and through the growth rate i.e. δ . Roughly speaking then we may expect to find the total number of defects retained as

clusters to depend on temperature as $\exp \frac{1}{kT} \left(\frac{Q_D}{2} - Q_\delta \right)$ where Q_D is the activation energy of D and Q_δ is that for the annealing of δ .

4.3 Gas Bubbles

The same general approach which we have taken above can be applied also to the growth of bubbles of the insoluble gases formed in fission or by other reactions (§1). In general bubbles visible in the electron microscope form at considerably higher temperatures than interstitial defect clusters - an effect probably due to the need for vacancies to migrate if the bubbles are to grow. Theories of the influence of gas bubbles on the swelling of solid fuels have been published [33] but the conditions for their validity do not seem to have been very thoroughly tested.

Experiments on the release of Xe fission gas from UO_2 can be used to obtain the Xe diffusion coefficient [34]. There seems little doubt that trapping of Xe occurs at defect clusters produced by the irradiation, since the apparent diffusion coefficient falls by very large factors, $\sim 10^4$, at high doses - an effect which has also been seen with the analogous system Ar in CaF_2 ($Ca^{44} + n \rightarrow Ar^{41} + \alpha$). However this seems to be another region where the work on defects visible in the electron microscope is still waiting to be put in close correspondence with that on the point defects, in this case the interstitial gas atoms.

5. Conclusion

In this article we have briefly reviewed a number of basic ideas in radiation damage with special reference to ceramic materials of nuclear interest. These ideas have been extensively used up to now mainly for metals and require some elaboration for ceramic compounds. The work on metals, however, also shows that experiments on ceramics are still at a rather early stage. Despite the large amount done from a technological interest, basic studies on these substances are still very

incomplete and comparatively crude. In order to achieve proper understanding of radiation damage in ceramics it is necessary to study irradiation effects at low temperatures especially using methods susceptible to point defects (e.g. optical, electron spin resonance, thermal conductivity) and to achieve an understanding of the formation of clusters in terms of point defects. Once the properties of point defects are determined with reasonable certainty (as e.g. the F-centre in MgO) these should then be employed to study defect reactions, especially the formation of small aggregates. More careful work on diffusion and mass transport properties at high temperatures also needs doing.

Acknowledgements

In the construction of this review I have benefited much from a number of discussions with Dr. B. Henderson, Dr. A.M. Stoneham and Mr. R.S. Wilks and other colleagues at A.E.R.E.

References

- [1] For more extensive accounts see (a) D.S. Billington and J.H. Crawford, *Radiation Damage in Solids* (University Press, Princeton, 1961); (b) D.S. Billington, Editor, *Radiation Damage in Solids* (Italian Physical Society and Academic Press, New York and London 1962); (c) R. Strumane et al, Editors, *The Interaction of Radiation with Solids* (North Holland, Amsterdam, 1964)
- [2] C. Erginsoy, *The Interaction of Radiation with Solids*, Editors R. Strumane et al (North Holland, Amsterdam, 1964), p.51.
- [3] H.H. Anderson and P. Sigmund, *Risø Report No. 103* (1965).
- [4] G. Montet, G. Myers and F. Feates (to be published).
- [5] M.W. Lucas and E.W.J. Mitchell, *Carbon*, 1, 345 (1964).
- [6] E.W.J. Mitchell, *Radiation Damage in Solids*, Editor D.S. Billington, (Academic Press, New York and London, 1962) p.518.
- [7] M.J. Moore and E.W.J. Mitchell, *7th International Conference on the Physics of Semiconductors, Part 3, Radiation Damage in Semiconductors* (Dunod, Paris, 1965), p.235.
- [8] E.W.J. Mitchell and P.D. Townsend, *Disc. Far. Soc.* No.31, p.259 (1961). See also W.D. Compton and G.W. Arnold, *Ibid*, p.130.
- [9] R.S. Wilks and F.J.P. Clarke, *J. Nucl. Materials*, 14, 179 (1965).
- [10] G.H. Kinchin and R.S. Pease, *Rep. Prog. Phys.*, 18, 1 (1955).
- [11] M.W. Thompson and S.B. Wright, *J. Nucl. Materials*, 16, 146 (1965).
- [12] E.M. Baroody, *Phys. Rev.*, 112, 1571 (1958).
- [13] See e.g. D.K. Holmes, *The Interaction of Radiation with Solids*, Editors R. Strumane et al (North Holland, Amsterdam, 1964) p.147.
- [14] M.T. Robinson and O.S. Oen, *Appl. Phys. Letts.* 2, 83 (1963).
- [15] See e.g. M.W. Thompson, *The Interaction of Radiation with Solids*, Editors R. Strumane et al (North Holland, Amsterdam, 1964) p.84.
- [16] M. Yoshida, *J. Phys. Soc. Japan*, 16, 44 (1961).
- [17] J.H.W. Simmons, *Radiation Damage in Graphite* (Pergamon, Oxford, 1965).
- [18] G.D. Watkins, *7th International Conference on the Physics of Semiconductors, Part 3, Radiation Damage in Semiconductors*, (Dunod, Paris, 1965) p.97.
- [19] R.G. Fuller, *Phys. Rev.* 142, 524 (1966).
- [20] N. Itoh, B.S.H. Royce and R. Smoluchowski, *Phys. Rev.* 137, A1010 (1965).
- [21] R.W. Ure, *J. Chem. Phys.* 26, 1363 (1957).
- [22] See e.g. A.B. Lidiard, *Handbuch der Physik*, 20, 246 (1957).
- [23] K. Tharmalingam, *J. Phys. Chem. Solids*, 25, 255 (1964).
- [24] S.B. Austerman and J.W. Wagner, *J. Amer. Ceram. Soc.* 49, 94 (1966).
- [25] D.L. McDonald, *Appl. Phys. Letts.* 2, 175 (1963).
- [26] D.G. Martin, *Proc. Brit. Ceram. Soc.* (in the press).
- [27] J.E. Wertz, G.S. Saville, L. Hall and P. Auzins, *Proc. Brit. Ceram. Soc.*, 1, 59 (1964).
- [28] I.K. Ludlow and W.A. Runciman, *Proc. Phys. Soc.* 86, 1081 (1965); I.K. Ludlow *Proc. Phys. Soc.* 88 (in the press); R.D. King and B. Henderson, *Proc. Phys. Soc.* (in the press).
- [29] B.S. Hickman and D.G. Walker, *Phil. Mag.* 11, 1101, (1965).
- [30] A.D. Whapham and B.E. Sheldon, *Phil. Mag.* 12, 1179 (1965).
- [31] A.B. Lidiard and R. Perrin, *Phil. Mag.* (in the press).

[32] G.W. Greenwood, A.J.E. Foreman and D.E. Rimmer, *J. Nucl. Materials*, **4** 305 (1959).

Effects in Solids held at Ashville, North Carolina in September 1965).

[33] R.S. Barnes and R.S. Nelson, AERE Report R.4952 (to be published in the Proceedings of the Conference on Radiation

[34] See e.g. Thermodynamic and Transport Properties of UO_2 and Related Phases, I.A.E.A. Technical Reports Series No.39 (Vienna 1965).

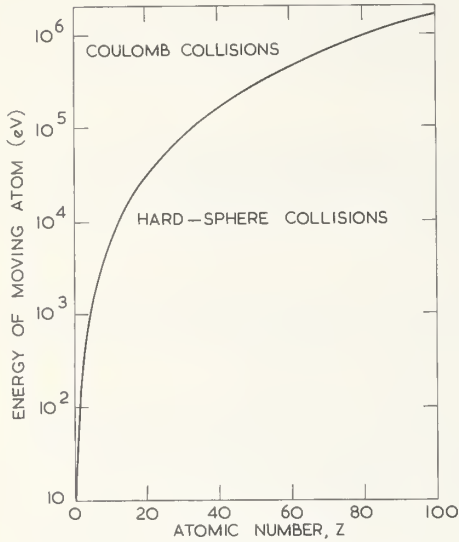


FIGURE 1. The boundary between the region of energy where the collisions are Coulomb encounters and that where they are hard-sphere collisions. The collisions are assumed to take place between two equal atoms of atomic number Z . This boundary line has been calculated using the screened Coulomb potential of Bohr in which the screening parameter is a smooth function of Z . In reality one expects electron shell periodicity to cause this line to be wavy and not exactly as shown here. The boundary is in any case not sharp. (after Billington and Crawford, Ref.1).

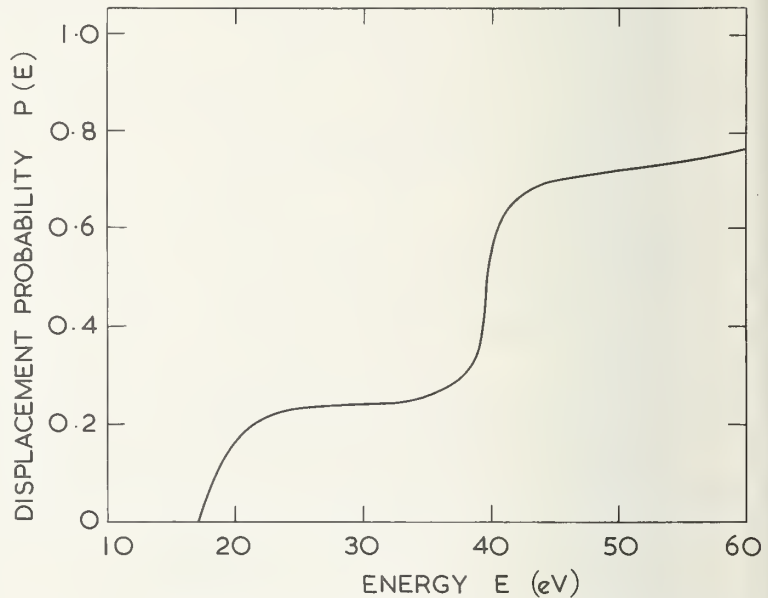


FIGURE 2. The integrated displacement probability for an atom of energy E as calculated for α -Fe (after Erginsoy, Ref 2).

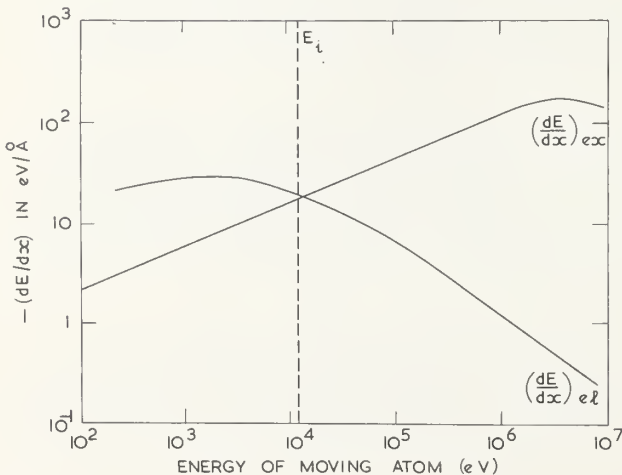


FIGURE 3. Diagram showing the rates of loss of energy per unit distance dE/dx by (i) electronic excitation and ionisation, $(dE/dx)_{ex}$, and (ii) elastic collisions, $(dE/dx)_{el}$. Scales for C atoms. For other elements the diagram is schematic (after Thompson and Wright, Ref.11).

Physical Properties of Irradiated Ceramic Materials

Paul W. Levy

Brookhaven National Laboratory

Upton, N. Y.

Abstract

Materials are subjected to two principal types of radiation effects during reactor irradiation. First, there are ionization effects which result from electron and (electronic) hole movement and trapping. Second, there are displacement effects resulting from the movement of atoms. Reactor irradiation introduces vacancies, interstitials, and more complex defects consisting of combinations of these simple defects. Some of these act as charge traps.

Numerous examples of radiation induced changes in the physical properties of ceramic materials can be cited. The most common phenomena associated with ionization effects is the coloring of glasses by irradiation. Displacement effects occur when atoms are ejected from their lattice sites by energetic electrons, gamma-rays, slow neutrons; fast neutrons (very efficiently); and, rarely, by other radiations. Almost all of the fast neutron damage is caused by energetic lattice atom recoils which are created by elastic collisions with fast neutrons. As the recoil passes through the lattice it produces numerous vacancies and interstitials along its trajectory.

Both the ionization effects and the formation of individual point defects are illustrated by color-center studies on very pure fused silica. The defect regions occurring along the trajectory of the lattice atom recoil can be related to changes in the low temperature thermal conductivity in single crystal Al_2O_3 . The collective effect of numerous damage-creating events, produced by long irradiations, result in a density decrease in crystal quartz and density increase in fused silica.

In addition, the physical properties of materials are changed during irradiation. During bombardment the defect concentration is increased and this will, in turn, increase any defect-dependent diffusion processes. For example, the diffusion of Be in BeO is greatly accelerated during reactor irradiation.

Paul W. Levy

1. Introduction - Basic Radiation Damage Processes

When solids are exposed to nuclear radiations usually one or more of their physical properties are changed. This simple fact is the basis for the branch of nuclear engineering concerned with materials used in reactors or otherwise subjected to radiation. Also, it is the reason for a large basic physics and chemistry research effort to understand the fundamental mechanisms involved in these changes. Most often the radiation induced effects are referred to as "radiation damage" and both the engineering and basic investigations are referred to as "radiation damage research". This paper will consider the effects of radiation on certain properties of a small number of ceramic materials that were carefully selected to demonstrate the more important basic radiation processes. [1,2,3]¹ First, they were chosen to emphasize the difference between the ionizing processes and the atomic displacement processes which occur in reactor radiation fields. Second, the choices demonstrate the difference between three classes of radiation induced defects. These classes can be conveniently characterized since they differ greatly in size. They are: 1) the point defects, which, at most, involve only a few atoms or vacancies. 2) the totality of defects along the trajectory of a given recoil, sometimes called a spike and which the writer likes to call a Wigner region. And, 3) macroscopic changes, i.e., effects which are measurable as a property of the entire damaged substance.

Before describing the "damaged" substance, consider first the radiation which produces "radiation damage". The radiation field in a typical reactor may be divided into three components. One component consists of neutrons with energies extending from a few MeV down to tenths of eV's. The slow flux may be as large or even larger than the fast flux, and is important when certain elements are present. A second component is the electron flux. The electron energies also extend from a few MeV to less than an eV. Lastly, there is the intense photon component which includes gamma rays, X-rays, and ultraviolet, visible, and infra-red light. And again the energy range is from several MeV to a fraction of an eV.

Each of the various radiation field components interacts with a crystal or glassy solid in a characteristic fashion. The fast neutrons and more energetic electrons are a primary source of radiation damage since they can displace atoms from their normal lattice positions. Most often the neutron damage will occur as a two step process. The initial step is an elastic, or rarely an inelastic, collision between a fast neutron and a lattice atom. In ceramics, where the lattice atoms usually have relatively low masses, a one MeV fast neutron will create recoiling lattice atoms in the 0.1 to 0.3 MeV range. The second step occurs as the recoiling atom literally "plows" through the lattice. It creates a large number of vacancies and interstitials along its trajectory. The resulting damage region will be a straight or slightly curved oblate spheroid from 10 to 100 atom spacings wide and a few thousand atom spacings in total length. Occasionally, the spike or damage region will be branched. In aluminum oxide, for example, a one MeV neutron could produce a 0.2 MeV Al or O recoil that would form three or four hundred vacancies, and a corresponding number of interstitials, in each spike or Wigner region. The total number of spikes will be proportional to the total fast neutron flux and to the elastic scattering cross section. Since the mean free path for typical reactor fast neutrons is several centimeters or more the damage region will be quite uniformly distributed in centimeter size samples.

Many reactors have an appreciable slow or thermal neutron flux. In fact, some reactors have facilities for irradiating samples with only slow neutrons. The slow neutron reactions can be a copious source of lattice defects. In an (n,γ) reaction a slow neutron is captured by the nucleus and one or more gamma rays are emitted. Conservation of momentum requires that when a gamma ray is emitted in one direction the nucleus recoils in the opposite direction. If the kinetic energy of the recoiling nucleus, i.e. the recoil atom, exceeds the displacement energy it will eject itself from the lattice. Most often this will create a single vacancy with a nearby interstitial. Also, slow neutrons will produce damage by energetic nuclear reactions when the target contains certain elements. Examples are the $\text{Li}^6(n,\alpha)\text{T}^3$ and $\text{B}^{10}(n,\alpha)\text{Li}^7$ reaction in which both the α particles and recoil nuclei are emitted with energies in the MeV range. In this case the damage creating process is similar to that caused by nuclei recoiling from elastic collisions with fast neutrons.

The distribution of (n,γ) and (n,α) reactions in the bombarded substance will depend on the total neutron absorption cross-section. If it is low, and the neutron mean free path is large compared to the sample size, the distribution of damage will be relatively uniform. If the cross-section is large, most of the reactions (damage) will occur at the surface and the reaction density (damage) will decrease toward the sample center. Glasses containing boron or lithium are good examples of materials in which

1. Figures in brackets indicate the literature references at the end of this paper.

slow neutron produced damage is important. Also, in these substances the damage tends to be greatest near the surface and decreases toward the interior.

The energetic electron and gamma-ray components will also displace atoms from the lattice. An incident fast electron will displace an atom from the lattice only if sufficient energy is transferred in the collision. The minimum energy that must be imparted, the displacement energy, is approximately 25eV. To displace an oxygen atom the electron energy must exceed 0.16 MeV, and 0.25 MeV is required to remove a silicon atom from the lattice.

Energetic gamma rays can produce displacements in two distinct ways. First, the gamma rays produce fast electrons because of the Compton, and to a very slight extent photoelectric and pair production, processes. Once formed, such electrons are indistinguishable from fast electrons produced in any other way and can undergo elastic scattering with lattice atoms. Second, gamma rays may make (γ, n) reactions with a nucleus, i.e. a gamma ray is absorbed and a neutron is emitted by the nucleus. In this case, conservation of momentum requires that - when the neutron is emitted in one direction - the nucleus recoils in the opposite direction. When the energy of the recoiling nucleus exceeds the displacement energy it will eject itself from the lattice.

The electron displacement processes occur infrequently. Once formed, the moving electron rapidly loses energy by ionization and is quickly degraded below the energy required to displace an atom. In reactors the (γ, n) process is negligible even for the lightest elements. The flux of sufficiently energetic gamma rays, and the reaction cross-section are both very small. The electron and gamma-ray processes create single vacancies and interstitials which are randomly distributed in the irradiated material.

The second major process which occurs in the reactor radiation is ionization. A large fraction of the total ionization is produced by the lattice atom recoils as they "plow" through the lattice. In fact when the recoils are produced by reactor neutrons roughly half of the recoil energy is used up in producing ionization electrons and holes along the recoil trajectory. Superimposed on this is the ionization provided by the reactor electron, and photon - mostly gamma-ray - radiation field. It is extremely important to realize that the normal ionization process involves only electrons and (electronic) holes, not the lattice atoms. The total number of ionization events which occur in most reactors is very large; roughly one ion pair - per atom - per second.

A critical analysis of the different aspects of the ionization process indicates that it would not produce lattice defects. Yet, it is clear that 10 to 50 KeV X-rays produce F-centers, i.e. anion vacancies, in the alkali halides and even ultra-violet light produces F centers in KI [4]. This is one, of many, radiation effects that is not understood at this time.

The defect properties of any irradiated material will be influenced by both the temperature during irradiation and the subsequent thermal history. The ambient temperature in most reactors is usually between 20 and 200 or 300 degrees C. Special irradiation facilities are available for irradiation between liquid nitrogen temperature and more than 1000°C. During and immediately after the passage of a recoiling lattice atom the closely surrounding lattice is in violent thermal agitation. Very roughly half of the energy lost by the recoiling atom appears in the agitated region, usually called a thermal spike. It may reach a temperature of several thousand degrees, but only for a period of less than 10^{-9} sec. Obviously thermal spikes will affect any temperature dependent processes. Vacancies, interstitials, and other defects will undergo accelerated diffusion. Electrons and holes will be released from shallow traps, strains will be annealed, etc. Certainly thermal spikes will promote the diffusion of induced defects, and annealing processes which are operative near the ambient reactor temperature will tend toward completion. It would be convenient to attribute a spike-produced temperature increment, to be added to the ambient temperature, to describe the effects of the thermal spikes. However, it appears that such a simple approach has a very limited, if any, utility.

2. Point Defects - Color Centers in Fused Silica.

The first radiation damage process to be considered in detail is the formation of color centers in fused silica. [5,6] This example is included to illustrate several things. First, the production of point defects by either neutrons or gamma rays. Second, the role of ionization in converting defects to color centers. Third, to give an illustration, albeit an incomplete one, of the annealing of radiation damage. Fourth, to include some mention of point defects in glasses.

The absorption spectrum of irradiated Corning 7940 fused silica is shown in Fig. 1. This type of spectrum, i.e., the coloring of a solid by radiation, is definitely due to color centers. The classical color center, the F-center, is an electron trapped on a negative ion vacancy in an alkali halide crystal. Other types of color centers are formed when electrons are trapped on more complicated negative ion defects, when holes are trapped on positive ion defects, etc. Conceivably every combination of negative and positive ion defects can trap one or more charge carriers of proper sign and each of these centers would have a characteristic absorption band. Once a band is identified with a particular defect, color center measurements can become a useful tool for determining the concentrations of that defect. However, it is important to realize that the defect alone usually does not give rise to an absorption band. The band appears only when the appropriate carrier is trapped. Also, to

make precise concentration measurements it is essential that all, or a known fraction, of the defects have been converted to color centers.

Color centers are also formed when charges are trapped by some of the impurities in the lattice. The maximum intensity of an impurity-related band is fixed by the impurity concentration. This fact can be the basis for the identification of these bands. Under proper circumstances the defect-related bands can be increased by exposure to radiation while the impurity band will remain constant.

Absorption bands have been observed in a large variety of crystals, the number of bands varying from one to more than ten. Very few of these bands have been correlated with specific defects. Thus, as the number of correlations becomes larger color center measurements should become an increasingly useful tool for studying defects.

The absorption spectrum of gamma-ray irradiated fused silica is very close to the spectrum obtained by reactor irradiation. The rate of color center formation differs greatly. The reactor gamma-ray component colors this material at about the rate as a comparable flux of Co^{60} gamma rays. Superimposed on this is a large number of additional defects created by the reactor neutron component.

Color center formation in single crystal Al_2O_3 is entirely different [7]. During gamma-ray irradiation 3 or 4 bands are formed. Reactor irradiation forms 6, 7, or 8, entirely different bands. Furthermore, the bands induced by gamma rays reach maximum intensity at a dose of $3 \times 10^4 \text{R}$ and remain at this level for irradiations up to 10^9R . In the fused silica the gamma-ray coloring increases at a steadily decreasing rate up to $2 \times 10^8 \text{R}$ and is increasing linearly above that dose. In reactor irradiated Al_2O_3 the bands increase linearly with dose after a slight amount of rapid initial growth. This linear growth continues until more than 10^{18} defects per cm^3 have been created. Above this concentration the formation rate decreases slowly with increasing defect concentration.

This fused silica and Al_2O_3 data is consistent with the following interpretation: Co^{60} gamma rays do not create defects in Al_2O_3 . At least, they do not produce defects that are stable at room temperature. The color centers produced by gamma rays are formed by carrier trapping on defects or impurities or both. There is a reasonable explanation for the absence of a color center increase at large doses. The displacement energy of both the Al and O atoms is higher than the maximum energy that can be transferred from the most energetic Compton electrons created by the Co^{60} gamma rays. The fused silica situation is different. The displacement energy of either or both the O or Si atoms is below the maximum energy that can be imparted by the Compton electrons from Co^{60} gamma rays. Thus, defects are formed in fused silica, but at a comparatively low rate. Once formed they are converted to color centers by electron or hole capture. Obviously, the reactor radiations, particularly the fast neutron component, are sufficiently energetic to produce defects in both materials.

This interpretation, especially the difference between the defect formation and charge trapping processes, is supported by annealing studies on these materials [8]. When reactor colored Al_2O_3 is heated, e.g. at 300°C for several hours, the optical absorption decreases during the first 20 minutes and remains constant during the remainder of the heating period. If the crystal is then exposed to gamma rays, a relatively low dose will restore some, but not all, of the color removed. Additional gamma-ray irradiation does not increase the color center density.

A similar annealing procedure was applied to fused silica [9,10] to obtain the upper curve in Fig. 2. First, the sample was reactor irradiated until a convenient optical density level was attained. Second, it is heated at 550°C for 40 minutes. Preliminary measurements had shown that this was the shortest annealing time at this temperature (which was the lowest temperature) required to remove all of the absorption bands with peaks below 6.2 eV. Next, it was irradiated with gamma rays. The upper curve is the growth of the 5.82 eV peak as a function of gamma-ray dose.

The lower curve in Fig. 2 shows the growth of the same peak in a sample that had not been previously exposed to radiation. Above $5 \times 10^7 \text{R}$, the two curves are similarly shaped except that the top one is displaced upward by a relatively constant amount. Near the origin the upper curve increases very rapidly with increasing gamma-ray dose. When the optical density reaches 0.35 it starts to level off and becomes nearly parallel to the lower curve. The extremely rapid increase near the origin can be attributed to charge trapping by existing defects. If defects were not present prior to irradiation the rapid increase would not occur. This annealing data also indicates that the heat treatment has removed some defects and released all of the charges that were trapped on the remaining defects. When the sample was subsequently exposed to gamma rays the remaining defects rapidly trapped charges. Continued gamma-ray irradiation caused additional defects to be formed at the same rate observed in samples exposed only to gamma rays.

3. The Damage Region Created by a Recoiling Lattice Atom

The next subject to discuss in detail is the region of damage, i.e., the spike or Wigner region, created by an energetic recoiling lattice atom. Two things are to be emphasized. First, the fact that experimental data is available to substantially verify the descriptions of the spike region given above. Second, the same example will illustrate how these regions influence the physical properties of an

insulator. The example chosen is the effect of fast neutron irradiation on the low temperature thermal conductivity of single crystal Al_2O_3 , technically, synthetic sapphire or corundum. The work to be described was published by Berman, Foster and Rosenberg in 1954 [11]. It is surprising that this is still an appropriate, if not the best, example that could be cited.

At room temperature the thermal conductivity of all insulators is almost entirely due to the transport of energy by lattice or phonon waves. The factors that limit the heat conductivity are usually referred to as the thermal resistance. Above 20 or 30°K this resistance results from the interactions of one phonon wave with all of the others. Usually, this thermal resistance is given by the expression

$$W_U = A T^{-\nu} e^{-\theta/2T}$$

where T = temperature in °K, θ = Debye temperature, A and ν are constants, the latter near unity. This expression for the phonon-phonon interaction is usually written

$$W_U = \frac{A}{T} e^{-\theta/2T}$$

Below 10 or 20°K the thermal resistance is the result of the interactions of the phonon waves with the sample boundary or surface, not with themselves. This contribution to the resistance will depend on the shape and size of the sample. The usual expression for this part of the thermal resistance is given by

$$W_B = BT^{-3}$$

where B is a constant that depends on the shape and size of the sample.

The W_U and W_B thermal resistance contributions must occur in all substances. Additional thermal resistance W_R will arise if the sample contains inclusions, lattice defects, impurities, etc., that can scatter the phonon waves. Thus, the thermal resistance of a substance should be increased by any treatment that introduces additional scattering centers. If this added resistance is called W_R the total thermal resistance is given by

$$W = \frac{A}{T} e^{-\theta/2T} + \frac{B}{T^3} + W_R$$

Most often, heat conduction data is expressed as thermal conductivity, in units of Watts/cm/deg, which is the reciprocal of the thermal resistance.

The thermal conductivity of single crystal Al_2O_3 both prior to irradiation and after a series of irradiations with fast neutrons is shown in Figs. 3 and 4. The first figure very clearly shows the decrease in conductivity. The second figure relates the conductivity curves to the various terms in the thermal resistance expression. In the temperature range 1.5 to 10°K which corresponds to the straight section on each curve the resistance is due to the boundary term W_B , the radiation has decreased the conductivity in this range. Also, above 10°K the resistance due to the term W_U , has increased.

From this data the radiation induced increase in thermal resistance W_R has been computed. This is shown in Fig. 5. The next step is to use these curves to determine the size and shape of the radiation induced defect region. The following simple expression for the thermal conductivity, K , is obtained from elementary kinetic theory.

$$K = \frac{1}{3} cvl \text{ or } W = \frac{1}{K} = \frac{3}{cvl}$$

where c = specific heat, v = velocity of the lattice waves, and l = mean free path, i.e. the average distance between scattering points of the lattice waves. The radiation induced change in thermal resistance, at any given temperature, is given by a similar expression

$$W_R = \frac{3}{cvl_D}$$

Where l_D is the mean free path for scattering by the defects. From the data in Fig. 5, and computing the number of damage regions from the fast neutron scattering cross-section, the scattering power (for phonons) of the damage regions can be estimated. In turn, from the scattering power, the size of each damage region is obtained. The result obtained is approximately 1000 atoms, a number that agrees well with other determinations [1,2,3].

The shape of the spike or recoil damage region can also be inferred from Fig. 5. In determining the size of the damage region, given above, it was assumed that the region was spherical. This is not consistent with the very nearly constant value of W_R between, approximately, 20 and 40°K shown in Fig. 5. The constant W_R in this temperature range is consistent with phonon scattering by long thin

obstacles. The size of these regions, computed from the thermal resistance data, is roughly 100 angstroms in length by 10 angstroms in diameter. Again, these values are in accord with other estimates of the recoil damage region dimensions.

Thermal conductivity is also influenced by exposure to purely ionizing radiation. When Al_2O_3 is exposed to gamma rays the thermal resistance is increased. This is shown in Fig. 6. The change is like that produced by fast neutron irradiation. However, it differs in one respect. The initial exposure produced all of the observed change. Additional exposure did not increase the resistance. This is similar to the coloring of Al_2O_3 by gamma rays. An initial exposure of $3 \times 10^4 R$ produced saturation coloration, i.e., additional irradiation did not produce an increase in color center concentration. These observations indicate that the gamma-ray created thermal resistance change is related to charge trapping. It is not clear why this should influence the conductivity. Furthermore, the resistance increase is surprisingly large, it is approximately equal to the change produced by the first neutron irradiation. It appears that additional work of this type on Al_2O_3 and other materials could be very interesting.

4. Macroscopic Radiation Effects

The macroscopic or external properties of ceramics are affected by sufficiently large irradiations. These macroscopic changes result from the cumulative effects of a large number of individual point defects, of spikes, or both. The external physical dimensions which are often changed can be conveniently and accurately measured. Small density changes are particularly easy to detect. A very good example of this type of measurement is the work of Primak [12,13] and his co-authors who have systematically studied the irradiation induced dimensional changes in crystal quartz and fused or glassy silica. This work will be briefly described to illustrate the macroscopic radiation effects.

Before doing this, the section on the basic radiation damage process must be expanded slightly. To begin, consider the effect of an interstitial atom on the atoms that surround it in a crystal lattice. Intuitively one sees that the interstitial will push the surrounding atoms outward and a large number of interstitials will tend to expand the crystal. Compare this with the effect of a vacancy on the lattice. There will be a tendency for the void produced by the removal of an atom to be partially filled as the surrounding atoms tend to push in. A large number of vacancies would be expected to produce an overall contraction of the lattice. However, this picture is almost certainly too simple. When an atom is removed from the lattice the attractive forces it exerts on the surrounding atoms are no longer present to hold them together. Consequently the atoms nearest or next nearest tend to move outward. These inward and outward movements will, at least partially, cancel and the total distortion around a vacancy is relatively small. In fact, in some crystals it is not known if the distortion around a vacancy expands or contracts the lattice.

On the basis of these arguments, which are definitely oversimplified, it can be concluded that radiation damage will cause most crystal lattices to expand. This conclusion is more readily understood by pointing out that the impinging radiation creates one interstitial atom for each vacancy formed.

When glasses are subjected to atom-displacing radiation the effects of vacancy and interstitial formation will be somewhat different. The glass network is less compact than the corresponding crystal structure. For example, glassy silica is considerably less dense than crystal silica, i.e. quartz. The open spaces, or voids, in the network can accommodate interstitials and the lattice is strained very little or not at all. The displacement of a network modifier should have relatively little effect on the network stability. In contrast, the displacement of a bridging oxygen or a silicon atom from the network will have a larger effect. In a loose structure the network could move either in or out; this would depend on local forces.

The most common network-forming atoms are strong chemical reactants. In fact, this is the reason for the strength of most glasses. This chemical reactivity should give rise to a strong tendency for the reestablishment of the network after disruption by radiation. Thus the violent thermal agitation, and perhaps even a short lived gas-like state, associated with the spike created by a recoil atom could be conducive to a network rearrangement. *A priori*, it cannot be said that this rearrangement will lead to a compacted or expanded lattice. It might be worth while to point out that this radiation-induced lattice rearrangement might be characteristic of equilibrium temperature and pressure conditions that are not attained in the usual glass forming equipment. If a glass which has been modified by radiation is subjected to the temperature and pressure conditions occurring when it was originally formed, it should revert to its previous state. Obviously, this does not apply to materials like crystal quartz which, as is very well known, transforms to glassy quartz or fused silica when heated to the melting point.

What happens when crystal quartz and fused silica are exposed to fast neutrons? Figure 7, taken from the work of Primak et al., [13] shows that the density of crystal quartz decreases with increasing exposure to fast neutrons. This indicates the lattice expansion tendencies predominate over the contraction tendencies. The opposite occurs with fused silica. This is shown in Fig. 8. The density of the fused silica increases as the exposure to fast neutrons increases. This contraction could result from the rearrangement of the network into a more dense lattice, Considering that fused

silica is all network former. Or, it could result from the following combination: the interstitials do not expand the lattice since they find their way to the lattice voids and the vacancies permit the lattice to contract enough to produce an overall density increase. Other explanations for the radiation induced contraction can be given. At this time, the phenomena is not entirely understood.

As the quartz and fused silica are subjected to increasing doses of reactor radiations the densities approach one another. For exposure in excess of 10^{20} or 10^{21} nvt both materials acquire the same density or very nearly so.

When the samples with small or moderate radiation induced density changes are heated the radiation effect is reversed. The crystal quartz density increases and the fused silica decreases. Heating to a sufficiently high temperature removes all the density changes. These annealing changes are shown in Figures 9 and 10.

When the crystal quartz is heated the mobility of any vacancies or interstitials that are present is greatly increased. If the interstitials are more mobile they will diffuse, in a random walk fashion, until they encounter and combine with vacancies. In this way the lattice will be restored. Since some interstitials may be more tightly trapped than others only a fraction may be mobile at a given temperature. This is one possible explanation for the observation that prolonged heating well below 900 or 1000°C will anneal only part of this damage.

The processes contributing to the annealing of irradiated fused silica are not completely understood at this time. If the density change involves only defects annealing would occur in a manner described above for crystal quartz. If the density involves network rearrangement then the annealing processes are different and probably much more complicated.

A very interesting thing occurs upon annealing crystal quartz which has been very heavily irradiated until it has nearly the same density as highly irradiated fused silica. It does not revert to crystal quartz but becomes fused silica. It would appear that this nearly common density is characteristic of the state in which the atoms have undergone such a large number of displacements that both the original crystal lattice and the thermodynamically controlled glass structure have been transformed into a common state. Upon heating the thermodynamics favor the glassy state and this is the state formed during annealing. In some recent work Primak has shown that an additional complication occurs [14], in that the density change is influenced by the presence of ionizing radiation. Obviously, this is an area for additional interesting work.

5. Radiation Enhanced Diffusion

The diffusion of atoms in a solid is a relatively slow process that is difficult to measure. In many materials the diffusion rate depends on the concentration of vacancies in the lattice and if this is changed the diffusion rate is changed. The examples given in the preceding sections were chosen to emphasize both the different ways that radiation interacts with a solid and the different kinds of damage remaining in the lattice after irradiation. This required considerable discussion of the physical process that occurs during the short period that the bombarding particle is interacting with the solid. The process which occurs during reactor irradiation that is most pertinent to a discussion on diffusion is the creation of vacancies. Each incident particle will create some vacancies, the number depending on its mass and energy. Usually for each vacancy there will be a corresponding interstitial. Both of these will diffuse in the solid. Each time that an interstitial encounters a vacancy they will recombine and the respective concentrations will decrease. During irradiation the vacancy concentrations will depend on the radiation level. At low levels it will be linear with dose but considerably less than linear at high levels.

The relation between radiation-induced vacancies and the diffusion process can be stated explicitly in terms of the well-known diffusion equations. The general diffusion equation is usually written for isotropic materials

$$D\nabla^2 [C] - \frac{d}{dt} [C] = 0$$

where $[C]$ is the concentration of the diffusing entity, t is the time, ∇^2 is the Laplacian operator, and D is the diffusion coefficient. Very often the diffusion of atoms in solids occurs by way of the "vacancy mechanism". One of the atoms (next to a vacancy) jumps into the vacancy and both the atom and vacancy have moved or "diffused". In this case the diffusion coefficient, D , in the above expression is given by

$$D = D_0 e^{-E_m/kT},$$

where k and T have the usual meaning, E_m is the activation energy for vacancy migration; and

$$D_0 = A[V_0],$$

where A is a constant and V_0 the intrinsic vacancy concentration. During irradiation there will be an additional vacancy concentration which will depend on the dose rate; call this $[V_R]$. Then D_0 is

$$D_o = A [V_o + V_R]$$

and it is apparent that the diffusion constant D depends directly on the relative size of V_o and V_R . The intrinsic vacancy concentration is dependent on the temperature, and is given by a relation of the form

$$V_o = B e^{-E_f/kT},$$

where B is a constant and E_f is the activation energy for vacancy formation. If at a high enough temperature $V_o > V_R$ the radiation induced component of the diffusion is unimportant.

Many examples of radiation-enhanced diffusion in metals and alloys can be found in the literature [1,2] Only recently the preliminary results of a radiation-enhanced diffusion experiment in a ceramic material were made available.² This is a study of the self diffusion of Be in BeO by de Bruin, Roman, Watson, and Blood. [16] Classical tracer diffusion techniques were used. Be⁷ tracer was deposited on the surface of the samples. The samples were heated to various temperatures, or irradiated in a reactor at the same temperature. The diffusion which occurs during these treatments is determined from the final distribution of tracer Be⁷. This is obtained by sectioning the sample and counting each layer. Apparently, the diffusion occurs in the usual way since plots of $\log [Be^7]$ versus the square of the penetration depth are linear.

A number of diffusion constant determinations are shown in Fig. 11. Each of the points refers to different radiation conditions and the straight line indicates how the diffusion constant of unirradiated samples depends on temperature. Above 1200°C the radiation field does not increase the coefficient. Apparently, above this temperature, the intrinsic vacancy concentration is large enough to control the diffusion rate. Between 1200° and 800°C the results are not easily understood. The data factitiously suggests that the diffusion increases as the temperature is lowered. In this region the annealing of the radiation-induced defects is strongly temperature dependent. Also, the sample may be slightly amorphous. It is apparent, upon reflection, that these and other effects can invalidate the simple vacancy diffusion model in this temperature range. Below 800°C the diffusion coefficients during irradiation are comparable to those obtained at 1100 to 1400°C in samples not exposed to radiation. This appears to be unmistakable evidence for a large amount of radiation-enhanced diffusion. It is conceivable that the observed increase is due to grain boundary diffusion, although de Bruin et al. believe it is not.

The effects of radiation on diffusion rates will undoubtedly be studied intensively in the future. It will be particularly important in ceramic moderators and fuel elements.

2. The author is extremely grateful to Dr. H. J. de Bruin for making these results available prior to publication; consequently, they are still subject to modification.

References

- [1] This and the following 2 references are general books on radiation damage and related subjects. G. J. Dienes and G. H. Vineyard, Radiation Effects in Solids, Interscience, New York (1957).
- [2] D. S. Billington and J. H. Crawford, Radiation Damage in Solids, Princeton Univ. Press., Princeton (1961).
- [3] L. T. Chadderton, Radiation Damage in Crystals, Methuen, London (1965).
- [4] T. P. P. Hall, D. Pooley, W. A. Runciman, P. T. Wedepohl, Proc. Phys. Soc., 84, 719 (1964).
- [5] J. H. Shulman and W. D. Compton, Color Centers in Solids, Macmillian, New York (1962). This is a general treatment of color centers.
- [6] P. W. Levy, to be published.
- [7] P. W. Levy, Phys. Rev. 124, 1226 (1961).
- [8] P. W. Levy, Discussions Faraday Soc. 31, 118 (1961).
- [9] P. W. Levy, Chemical and Physical Effects of High Energy Radiation on Inorganic Substances, Amer. Soc. for Testing and Materials, Philadelphia (1964) p.3.
- [10] P. W. Levy, to be published.
- [11] R. Berman, E. L. Foster and H. M. Rosenberg, Defects in Crystalline Solids, The Physical Soc. London (1955) p.321.
- [12] W. Primak, L. H. Fuchs, and P. Day, J. Amer. Cer. Soc., 38, 135 (1955).
- [13] W. Primak, Phys. Rev. 110, 1240 (1956).
- [14] W. Primak and E. Edwards, Phys. Rev. 128, 2580 (1962).
- [15] M. Wittels and F. A. Sherrill, Phys. Rev. 93, 1117 (1954).
- [16] H. J. de Bruin, D. Roman, G. M. Watson, C. M. Blood, to be published.

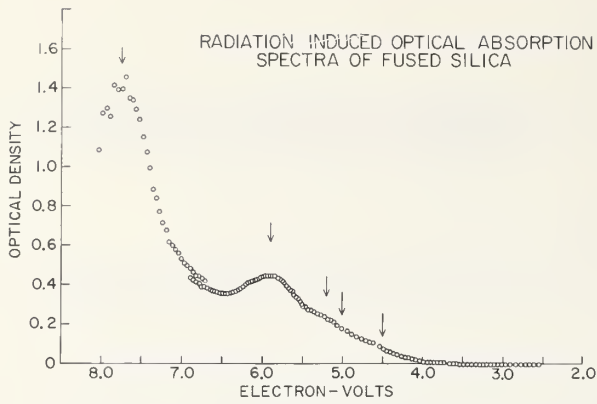


Figure 1. The color center spectrum produced by irradiating relatively pure fused silica. Very nearly the same spectrum is obtained by either gamma-ray or reactor irradiation. The arrows indicate the peaks of the more prominent absorption bands.

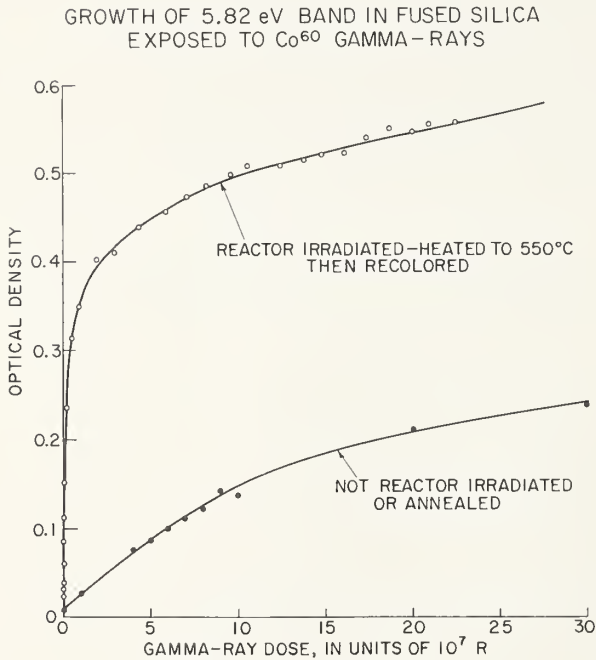


Figure 2. The growth of the 5.82 eV absorption band in fused silica when exposed to Co^{60} gamma rays. The upper curve was obtained from a sample that had been reactor-irradiated and then heated for the shortest time and at the lowest temperature that would remove the 5.82 eV band. The rapid initial growth can be attributed to the coloring of reactor-induced defects that remained in the sample after annealing. The lower curve was obtained from a pristine sample which originally contained very few uncolored defects.

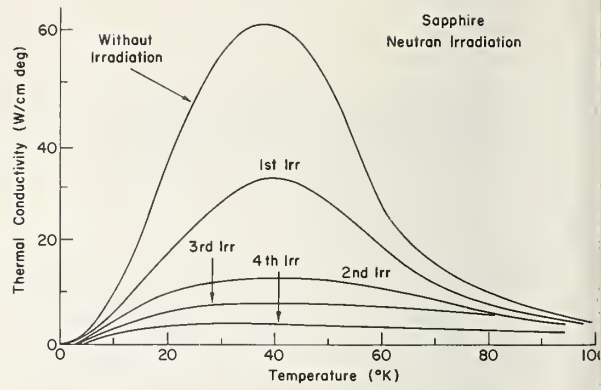


Figure 3. The low temperature thermal conductivity of synthetic sapphire, Al_2O_3 , before and after the indicated reactor irradiations. The doses were 1.5 , 8.9 , 20.2 , and 50.2×10^{17} nvt respectively.

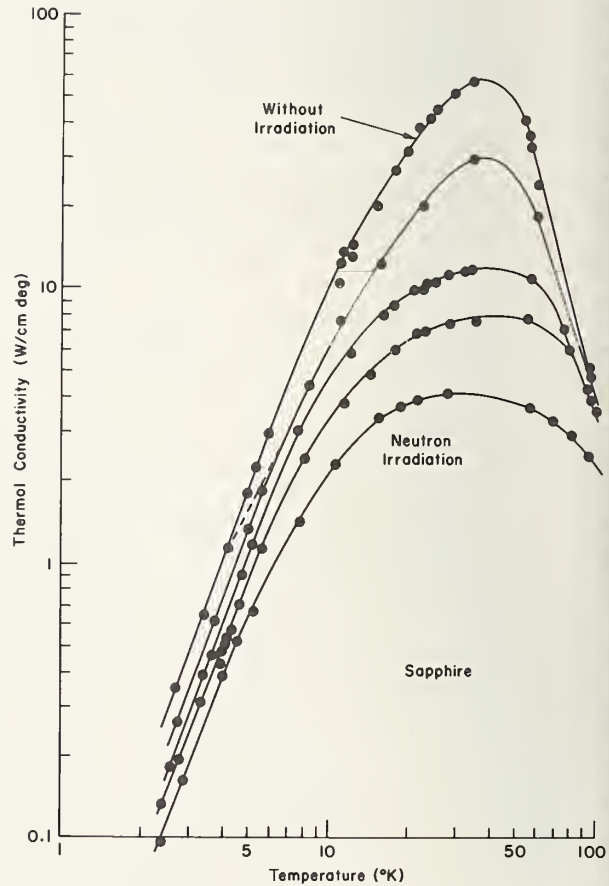


Figure 4. The thermal conductivity data shown in Fig. 3 plotted in a way that separates the linear low temperature boundary scattering contributions, the B/T^3 term, from the non-linear phonon-phonon contribution, the $(A/T) \exp(-\theta/2T)$ term, that dominates at higher temperatures.

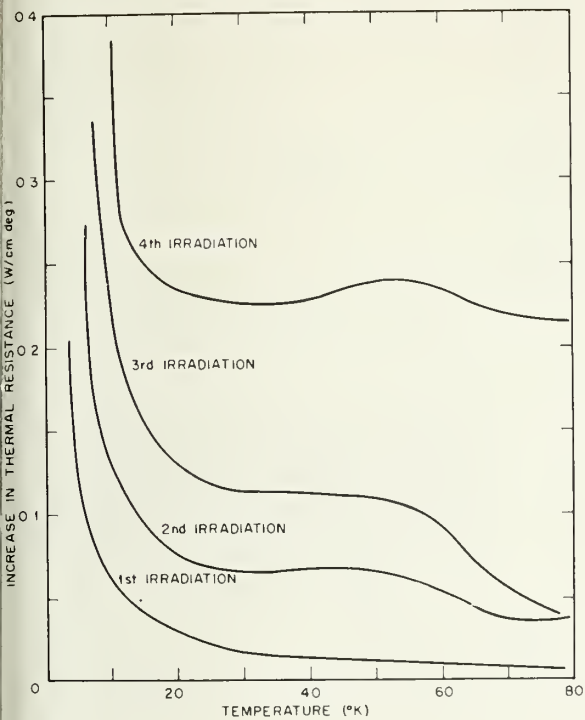


Figure 5. The radiation-induced change in the thermal resistance of Al_2O_3 computed from the data shown in Fig. 3.

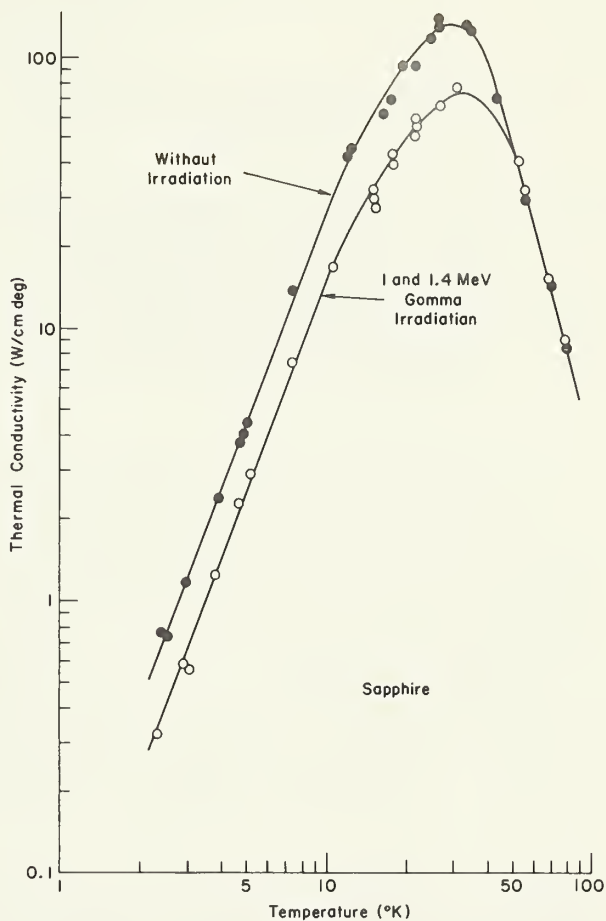


Figure 6. The thermal conductivity of Al_2O_3 before irradiation and after a 3×10^6 R Co^{60} gamma-ray dose.

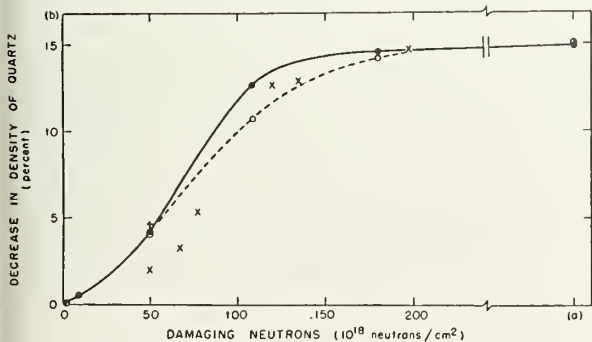


Figure 7. The change in density of crystal quartz exposed to reactor radiations. Except for the "crosses" the various points represent different kinds of physical measurements. The "crosses" are independent X-ray measurements. [15]

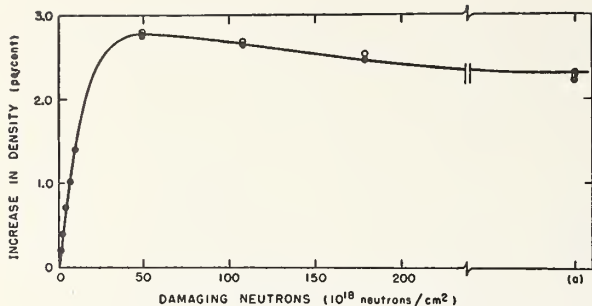


Figure 8. The change in density of fused silica exposed to reactor radiations. The various points represent different kinds of physical measurements. The half open circles are data from a "fused silica" sample that had been converted from crystal quartz by irradiation.

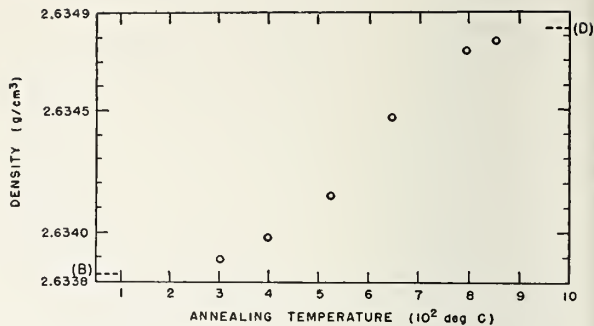


Figure 9. The increase in density of a quartz sample that had received a moderately heavy reactor irradiation, after heating for approximately 30 minutes at each progressively higher temperature point. (B) is the density after irradiation but before annealing. (D) is the density of unirradiated quartz.

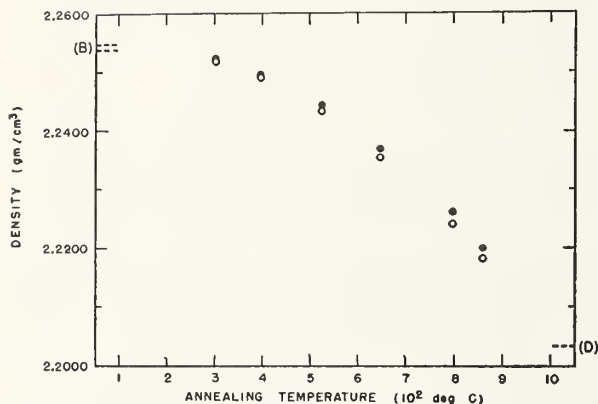


Figure 10. The decrease in density of a very heavily irradiated quartz sample (solid circles) and fused silica (open circles) after heating for approximately 30 minutes at each of the progressively higher temperature points. (B) indicates the densities after irradiation but before annealing. (D) is the density of unirradiated fused silica.

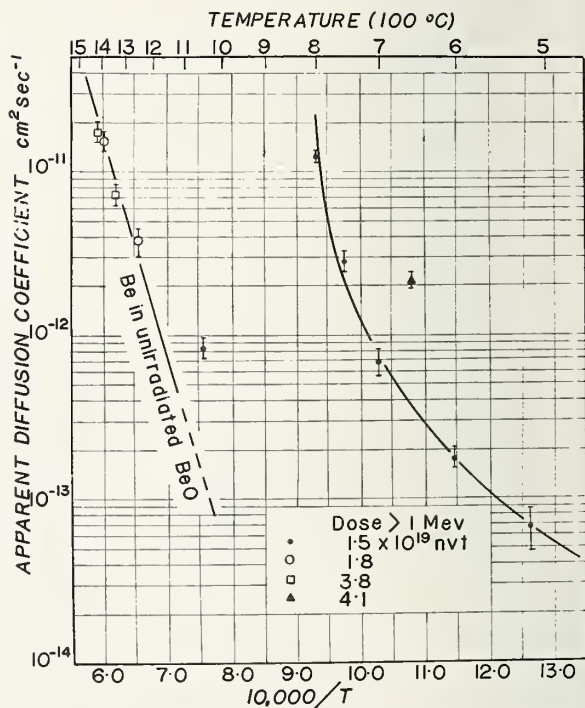


Figure 11. Apparent diffusion coefficients for the diffusion of Be (as radioactive Be^{10}) in polycrystalline BeO during the indicated reactor irradiations at the temperatures shown. The data below $800^{\circ}C$ indicates that the presence of the radiation flux has greatly enhanced the diffusion rate.

Chemical Problems Associated with Lattice-Defects.
Uranium Dioxide Phase

R. J. Thorn and G. H. Winslow

Argonne National Laboratory, Argonne, Illinois

1. Defects as Chemical Components

A. Thermodynamic Considerations

In most experiments and environments, a non-stoichiometric phase such as UO_{2+x} behaves reproducibly as a binary system. It is bivariant so that the pressure is a unique function of composition and temperature only. Thus

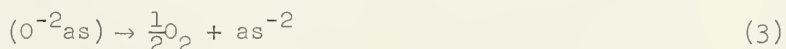
$$p = p(x, T) . \quad (1)$$

These statements are generally accepted as being so obvious that they suggest that any thing which follows them is frivolous. Their acceptance, however, without some enquiry tend to prejudice one in two important respects: Interesting experimental possibilities are excluded, and inconsistent relations are included in theoretical analyses. It is significant in these respects to recognize that if the uranium dioxide phase is to be described in terms of the defect-theory of non-stoichiometry, then one admits the real existence of other entities besides U and O. In fact, it has been demonstrated that the experimental results can be interpreted in terms of oxygen ions at the interstitial positions near the centers of the fluorite unit cells [1]¹ and the necessary concomitant vacancies in the anionic sublattice. Recognition of the condition expressed by equation (1) and of the existence of what effectively amounts to more than two components is required if one desires to analyze thermodynamically the non-stoichiometric phase. Yet a problem has been introduced. A clarification of this problem is outlined below by employing symbols for the defects as chemical components and by identifying conditions of restraint which in most experiments are an integral part of the system.

For a phase such as UO_{2+x} , one accomplishes a thermodynamic analysis which is more complete than that usually presented for non-stoichiometric phases by recognizing the following chemical symbols: U, O, -, +, cs, as, and is. Among these cs, as, and is refer to cationic, anionic, and interstitial sites respectively. In writing chemical reactions involving these possible components, one requires that the symbols are conserved. Thus one writes for the essential equilibrium within the solid the reaction:



which differs from the frequently used convention by the requirement that each symbol appears on each side of the equation. Of course, not all of the associated difficulties are solved by initiating the analysis thus, for to be rigorous one must recognize the existence of all the components in all the phases. The appearance of the components cs, as, and is in the gaseous phase may be rather unconventional but it is a difficulty which creates no impossibilities and which is set aside herein. In the situation being described the quantities $(O^{-2}as)$ and $(O^{-2}is)$ are similar to molecular entities or atomic groupings within other molecular entities or domains to be cited later. The reduction of the oxide can be represented by the reaction:



and a similar one for $(O^{-2}is)$. Such reactions, however, are probably more hypothetical than real because the charge on as or is undoubtedly relaxes practically

¹ Figures in brackets indicate the literature references at the end of this paper.

instantly or never even develops in a real sense. Whatever the situation may be, the general behavior suggests that thermodynamically this charge is so located that it corresponds to well defined valence states for the cations. For instance, Thorn and Winslow [2] have demonstrated that there exists a close parallel condition, for both divalent and trivalent states in the case of the elements in the first transitional row, between the energies in the oxides and those in aqueous solutions where one would expect the ions to be in well defined valencies. Consequently, one can represent the situation in UO_{2+x} by the equation:



The sum of reactions (3) and (4) represent more nearly than the individual reactions the process actually occurring. However, because of other factors, one of which is probably associated with localized charge-neutralization, the analysis must be carried at least one step further.

The seven possible components indicated by the symbols listed above suggest that for a diphasic system there are seven degrees of freedom. However, in most experiments several conditions of restraint exist. Thus one recognizes the following relations among the numbers of the various symbols:

$$N_+ = N_- \quad (5)$$

$$N_{cs} = N_u \quad (6)$$

$$N_{as} = 2N_u \quad (7)$$

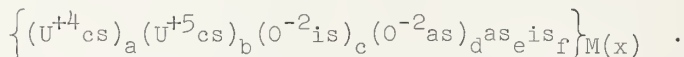
$$N_{+4} + N_{+5} = N_u \quad (8)$$

$$N_{is} = \alpha_1 N_{cs} \quad (9)$$

Depending on whether α_1 is a prescribed function, there are four or five conditions of restraint, and there remain either three or two degrees of freedom.

B. Roles of Valence-States and Their Energies

For binary systems of anions and cations which are compounded from what might be called Bravais "compounds", $cs_a as_b$, the primary contributions to the total energies are the cohesive energies which can be evaluated in terms of the Madelung formulation. A single Madelung constant suffices for each structure. In these cases there exists only a single valence-state for the cation. In non-stoichiometric phases, however, the presence of two valence-states for the cation introduces energies which cannot be described in terms of single Madelung constants and consequently features which simulate more nearly those corresponding to the conventional ternary system than those for a binary. Towards a more complete thermodynamical analysis, one must then recognize the existence of more complex structures which are variously identified in terms of enlarged unit cells, super-structures, lattice molecules, cooperative effects, domains, etc. For the present purposes one can indicate the situation by suggesting that the monophasic region is composed of subregions such as



Such units can serve as guides in further analyses which are directed towards the following features, among others: (1) Recognition of the continuous transition from one terminus to another of a monophasic region. (2) Recognition of defects as components or as conditions connecting Bravais "compounds". (3) Recognition of the likelihood of local neutralization of electrical charge. (4) Introduction of a basis for ternary systems generated from binary systems. The values of a, b, c, d, e, and f can be evaluated from the conditions of restraint given above. Thus for one compositional variable, $O/U = 2 + x$, one finds that

$$b = \left(\frac{2x}{1-2x} \right) a \quad (10)$$

$$c = \left[\frac{2\alpha_1(1-2x)+4x-1}{2(1-2x)} \right] a, \quad (11)$$

$$d = (2+x)(a+b)-c, \quad (12)$$

and

$$e = 2(a+b)-d. \quad (13)$$

Depending on one's interest, any one of the letter-subscripts in the unit can be divided out to determine the size of $M(x)$. Whatever one is accepted, the formula given above implies that there must be at least one of each of the entities given and that there exists a well defined configurational arrangement of the entities in a real material. Hence in most experiments there is only one variable, x , at the disposal of the experimentalist and a corresponding number of adjustable parameters available to the theorist. The quantities α_1 and $M(x)$ are determined by the energetics of the situation. Thus one writes that

$$\alpha_1 = \alpha_1(x, T), \quad (14)$$

and

$$M = M(x, T) \quad (15)$$

which are in a sense conditions of restraint also not at the disposal of the experimentalist. The number of "available" interstitial positions is fixed by the situation (x and T , x and p , or p and T). When a small amount of oxygen is added to stoichiometric uranium dioxide, the numbers of defects, as and $(O^{2-})_i$, are small at low temperature [3] and the size of the molecular unit is large if it is to contain at least one atom of each entity or it is small, i.e. comparable with a unit cell, if the situation is imagined to consist of defects dispersed throughout a matrix. In this region it can be meaningful to approximate the description in terms of point defects. However, as more oxygen is added the size of the molecular unit decreases and its resemblance to the original structure of the Bravais-compound cs_4as_8 becomes less. At some composition between 0 and 0.25 for x , the resemblance to another Bravais-compound cs_4as_9 begins to appear in the form of the corresponding molecular unit. Thereafter the second unit grows at the expense of the first one. At some point between the extremes there occurs the residues of a transition which is usually manifested in the form of inflections on a plot of pressure vs. composition. Such are undoubtedly the sources for the obscured x-ray diffraction patterns [4] for $0.08 < x < 0.13$, for the non-reproducibility for the partial molar entropy pointed out by Thorn and Winslow in this region [5], for the inflections observed by Aukrust, F rland, and Hagemark [6], and the turning point in a plot of the partial molar entropy of oxygen vs. the partial molar enthalpy [7]. The similarities and contrasts between this region and the diphasic region has been cited by Thorn and Winslow [2]. In the latter case one phase is converted into another; in the former one domain or molecular unit is converted to another but no surface energies are involved.

As cited above, the observations by Thorn and Winslow [2] indicate that the valence-states in the oxides of the elements in the first transitional row and the corresponding states in aqueous solution are sufficiently equivalent that one can represent, to the first order of approximation at least, the behavior of the oxides in terms of valence-energies which appear to exist in aqueous solution. Hence it should be possible to identify formally, to evaluate accordingly well defined valence-energies in solid oxides, and to develop therefrom a basis for solid state chemistry in general. Towards a limited aspect of these ends, further comparisons between the situations in oxides and in aqueous solutions are needed. An intercomparison among the valence-energies associated with the hyper-stoichiometric side of the fluorite-structured dioxides of the elements near uranium is not possible because such have not been measured in aqueous solution. An intercomparison is possible, however, for the hypo-stoichiometric side. Consequently, to illustrate some of the factors involved, we cite the role of the trivalent and tetravalent states in some of these compounds.

In Table 1 is compiled a comparison among the valence-energies of some actinide, and one rare earth, elements for which the electrode potentials in aqueous solution have been reported [8]. Therein one can observe the correlation between the increase in the quantity $\Delta F_f^0(M^{+3}, aq) - \Delta F_f^0(M^{+2}, aq)$ and the increase in the partial pressure of oxygen in equilibrium with an oxide having an arbitrarily selected composition. This relation indicates that one can predict the relative stabilities of solid oxides

from the energies for the valence-states observed in aqueous solution. Having once recognized the potential uses of such approximations to the situation existing in the solids, one can extend the description by recognizing that it is the relative energies of M^{+3} and of M^{+4} which determine the properties. Hence within certain limits imposed by the rigid parts of ionic electronic configurations, one can begin to treat different elements as manifestations of different valence-energies of essentially one element. Thus it is possible to describe symbolically the general situation corresponding to the molecular unit given above by replacing U^{+4} by E_i^{+4} or in general by E_i^{+4} which is some numerical value for the i th energy in the $+4$ state and similarly for the U^{+5} ; and to indicate the relative amounts of each energy one introduces compositional variables f_i and f_j for the valence energies E_i^{+4} and E_j^{+5} . Accordingly one represents a multicomponent system by the formula:

$$\left\{ \left(\sum_i f_i E_i^{+4} \right)_a \left(\sum_j f_j E_j^{+5} \right)_b (O^{-2})_c (O^{-2})_d^{as} e^{is} f \right\}_M(x) .$$

A more complete investigation of this formalism should yield the basis for predicting the behavior of ternary systems from the known behavior of binary systems and of the energies of the appropriate valence states. For instance, one observes by inspecting equation (4) that the more stable the lower valence-state is relative to the higher valence-state the larger is the partial pressure of oxygen. Consequently, to stabilize, in this sense of a lower partial pressure of oxygen, a non-stoichiometric oxide one adds a third chemical component having a more nearly positive value for the difference between the free energies of the valence-states than that for the host oxide. Thus the addition of magnesium to the wüstite phase produces effectively a reduction of the phase [See 2].

2. Defect Theory of Non-Stoichiometry

A. Basic Elements

Because the primary interest in the system at hand is, as indicated by equation (1), to ascertain how the composition of the solid is determined by the pressure of a gaseous phase, the appropriate statistical thermodynamic analysis is one employing an open system. That is, one considers a system, solid UO_{2+x} , containing energy states E_s and particles, not all of the various kinds of which are fixed, in contact with a reservoir, the gas, having fixed chemical potentials, μ_i 's. Accordingly, one writes for the probability that the system is in state E_s with $N_1 + N_2 + \dots + N_n$ particles of the various kinds:

$$P_{E_s, N_i}'s(\beta, \mu_i)'s) = \Omega_{E_s, N_i}'s e^{-\beta(E_s + pV - \sum_i \mu_i N_i)} . \quad (16)$$

In this expression $\beta = (kT)^{-1}$. If this system were composed of entities corresponding to the seven symbols as independent components, then the probability of the system would need to be normalized by summing over all seven components as well as the energies. However, as cited above, not all of entities corresponding to the symbols are independent because they are interrelated via equations (5) through (9). Thus, in the case of the uranium dioxide phase, one recognizes, as stated above, that the system is bivariant and consequently binary, i.e. there are only two N_i 's. Therefore, the construction of the appropriate partition function through the normalization of the probability must recognize this fact. For the purpose of describing the non-stoichiometric phase, these two components can be selected, of course, in several ways provided they are sufficiently independent to specify the composition of the phase. The analysis which is usually effected is one which considers not U and O as components but rather as and $(O^{-2})_s$. When the corresponding probability is normalized by equating the sum for P in equation (16) to unity one finds that

$$e^{\beta pV} = \Gamma(\beta, \lambda_o) = \sum_{E_s} \sum_{N_i, N_v} \Omega_{E_s, N_i, N_v} e^{-\beta E_s \lambda_o} N_i - N_v \quad (17)$$

in which N_i is the number of interstitial sites occupied, N_v is the number of anion sites vacant, and $\lambda_o = e^{\beta \mu_o}$, commonly identified as the absolute activity for oxygen. In this formulation, however, the N_i and N_v are not independent. At constant ratio of uranium to oxygen, oxygen ions can shift between lattice sites and interstitial

positions. Thus $dN_V = dN_i$ at constant x . And added oxygen is distributed between lattice sites and interstitial positions. Thus $(N_i - N_V)/N_u = x$.

The more complete analysis of the system through the evaluation of the semi-grand partition function Γ presents some logical problems which are not easily solved. For instance, one should recognize that energy states available depends on composition somewhat in accordance with the molecularity cited above. Hence Ω is a function of E_s as well as N_i and N_V . This fact implies that any interaction among the entities precludes the possibility of random distribution of them. To date, however, no general theory has been developed for the functional $\Omega(E_s(N_i, N_V))$. Consequently, an approximate evaluation has been accomplished by employing the elements of a randomized distribution in such a manner that it does not become catastrophically trivial or introduce several arbitrarily adjustable parameters. The functional Ω has been evaluated [See 5 and 13] by calculating all the possible arrangements of N_i and N_V and by including contributions of the defects to the vibrational part of the partition function, q_i and q_V . Thus, one writes that

$$\Omega = \frac{(\alpha_i N_u)!}{N_i! (\alpha_i N_u - N_i)!} \frac{(2N_u)!}{N_V! (2N_u - N_V)!} q_i^{N_i} q_V^{-N_V} \quad (18)$$

and following the usually presented arguments given by Heitler [14], one writes for the energies:

$$E_s(N_i, N_V) = E_V N_V - E_i N_i - \frac{E_{VV} N_V^2}{2N_u} - \frac{E_{ii} N_i^2}{\alpha_i N_u} \quad (19)$$

in which

E_V is the energy required to remove an oxygen atom from an anion site to a position of rest in the gas.

E_i is the corresponding quantity for an oxygen atom on an interstitial site.

$\frac{1}{2} E_{VV}/Z_V$ is the energy required to separate nearest neighboring pair of vacancies.

$\frac{1}{2} E_{ii}/Z_i$ is the energy required to separate a nearest neighboring pair of oxygen ions on interstitial positions.

Defining the fraction of the sites vacant as

$$\theta_V = N_V/2N_u \quad (20)$$

and the fraction of the interstitial sites occupied as

$$\theta_i = N_i/\alpha_i N_u, \quad (21)$$

and employing the usual procedures for maximization [13], one obtains the results:

$$\ln \lambda_O = \ln \left(\frac{1 - \theta_V}{\theta_V} \right) - \frac{E_V}{RT} + \frac{2\theta_V E_{VV}}{RT} - \frac{\partial}{\partial N_V} (\ln q_V) \quad (22)$$

$$\ln \lambda_O = \ln \left(\frac{\theta_i}{1 - \theta_i} \right) - \frac{E_i}{RT} - \frac{2\theta_i E_{ii}}{RT} - \frac{\partial}{\partial N_i} (\ln q_i) \quad (23)$$

The absolute activity of oxygen is related to the partial pressure of diatomic oxygen through the equation,

$$P_{O_2} = \lambda_{O_2}^2 k T Q e^{D/RT}, \quad (24)$$

in which Q is the partition function for molecular oxygen and D is its dissociation energy.

B. Application to UO_{2+x}

The energies and the Debye or Einstein temperatures associated with q_v and q_i , in equations (22) and (23) have been evaluated [5] by a procedure which involves the following items:

1. The value for the energy E_{ii} was obtained by equating $E_{ii}/2R$ to the critical temperature for the formation of U_4O_9 obtained by Roberts and Walter [15]. Thus $E_{ii} = 5.56$ kcal/mole.
2. The value for E_i was obtained through an averaging procedure which employs the measured relative partial molar free energy of oxygen. That is, equations (23) and (24) can be employed to obtain

$$2E_i + 4(x/\alpha_1)E_{ii} = -F_{O_2}^M + 2RT \left\{ \ln \frac{x}{(\alpha_1 - x)} \right\} - \ln q_i \Big\} + RT \ln(kTQ) + D, \quad (25)$$

from which one determines E_i . The value obtained is 93.95 kcal/mole.

3. The characteristic temperatures, θ_i and θ_v , used in the evaluation of q_i and q_v as functions of the temperature were determined from

$$-S_{O_2}^M = S_{O_2}^0 + 2R \left\{ \ln \frac{x}{(\alpha_1 - x)} \right\} - \ln q_i - T d \ln q_i / dT \Big\} \quad (26)$$

and the Debye-Waller factors observed by Willis [16]. The results are $\theta_i = 158.0^\circ K$ and $\theta_v = 542^\circ K$.

4. Values for E_{VV} were obtained in two ways. The melting temperature, $2760^\circ K$, for UO_2 corresponds to $E_{VV} = 16.47$ kcal/mole. A composition of $UO_{1.88}$ at $2200^\circ K$ for the lower phase boundary, UO_2-U , [10,17] corresponds to $E_{VV} = 16.87$ kcal/mole. The latter value was accepted.

5. A unique evaluation of E_v over the range of temperatures extending from 800 to $2400^\circ K$ is not possible within the formulation developed to this stage, but this difficulty appears to yield significant additional information concerning the phase. From a value, -170.53 kcal/mole, [10] for the relative partial molar free energy of oxygen at $2200^\circ K$, one obtains $E_v = 209.67$ kcal/mole. This value, however, is not consistent with the relative partial molar free energy observed [18,19] at $1100^\circ C$. An analysis of this difference suggests that a significant number of cationic vacancies in equilibrium at the higher temperature is frozen in at some intermediate temperature and consequently these vacancies are not at equilibrium at the lower temperatures. An analysis of the situation suggests that the fraction of uranium sites vacant and frozen in is 3×10^{-4} in the experiment by Markin and Bones [18]. The effective value for E_v , is under these conditions, 134.7 kcal/mole.

The results of the analysis sketched above yields a fairly complete thermochemical description [19] of the uranium dioxide phase for $0 < x < 0.10$ and $800 < T < 2400^\circ K$ and for the lower phase boundary. Two illustrative examples of the agreement between the experimental measurements and the analytical model are given in Figures 1 and 2. In the first figure, the calculated relative partial molar free energies are compared to the measured values at $1400^\circ K$. In the second one, calculated and measured lower phase boundaries are compared. There are, of course, places where the model is inadequate, but these inadequacies reveal features which are not entirely unanticipated. The possible role of the vacancies on the uranium sublattice has already been mentioned. Another insufficiency is displayed in Figure 3 in which a comparison is presented between the calculated and observed upper phase boundary. The discrepancy between the two could be associated with a dependence of α_1 on x as prescribed by equation (14). An attempt at this has been made by Hagemark [20], who has suggested that the occupation of a site of the type used in this model prevents the occupation of the twelve nearest neighboring sites of the same type. Thus he writes that

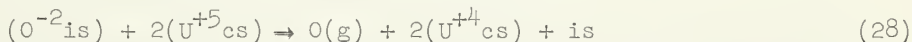
$$\alpha_1 = \frac{1}{1 + 12x} \quad (27)$$

On the other hand, Thorn and Winslow [5] have argued that $\alpha_1 = 1$ up to $x \sim 0.08$ and

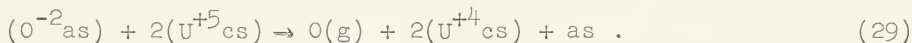
that α_1 then changes to the value 1/4, given by equation (27) at $x = 0.25$, already at $x \sim 0.12$.

The information concerning α_1 which has been revealed by the analysis effected by Thorn and Winslow illustrates the value of an analysis based on the concepts introduced in Section 1A and 1B given above, especially with respect to the suggested molecular units. It is expected that extensions of the significance of $\alpha_1(x,T)$ could be accomplished through mechanisms for structural changes which have been proposed by Rees [21] or via long range ordering parameters (See for example Elcock [22] and Green and Hurst [23]). It is particularly the latter which we choose to associate with the molecular units or domains. In further analyses of the situation in the uranium dioxide phase, one would be guided by such observations as those by Willis [1].

The energies E_1 and E_V are identified with the reactions:



and



The values obtained for these reactions are plausible ones. One would expect the potential energy for an oxygen ion on an interstitial position to be smaller than that for a vacancy. Further the values are ordered in the expected manner relative to θ_1 and θ_V . The direct significances of the energies E_{1i} and E_{Vv} , however, are not so readily identified with the actual processes occurring. The formalism presented herein suggests that the phases which separate out at the phase boundaries are assemblages of di-defects, $(O^{-2}is)_2$ and as_2 . The real phases are U_4O_9 and U respectively. A more complete investigation of this situation is obviously needed in terms of domains which can be made to approach more closely the real phases.

3. Kinetics at Equilibrium. Self-Diffusion.

A. Basic Elements

Thermodynamic formalisms have been developed for two general types of transport processes. They can be identified as (1) the transport in systems at equilibrium and (2) reversible, coupled transport in systems removed from equilibrium. In both cases the basic equation,

$$\frac{dS}{dt} = \frac{1}{T} \frac{dE}{dt} + \frac{p}{T} \frac{dV}{dt} - \sum_r \frac{\mu_r}{T} \frac{dn_r}{dt} \quad (30)$$

is applicable. The restricting conditions in the two cases are that (1) there is no net entropy produced in the first and (2) there is in the second. The first category can be identified as local thermodynamic equilibrium in the following sense: Each local region is considered to be at equilibrium in that an equilibrium equation of state can be written for it, and the unidirectional transport of entities from one region to another is calculated on the basis of an imagined unidirectional gradient rather than a net gradient. The equal flux in the opposite direction is ignored. Most of the theoretical treatments of transport properties are of this type, modified to account for relaxation, coupling, etc. which are introduced essentially after the derivations. Self-diffusion of atomic species in solids, however, approaches very closely a situation corresponding to local thermodynamic equilibrium. Consequently, the investigation of self-diffusion constitutes a useful basis for initiating studies of the inter-relationships between thermodynamic properties and atomic transport. One should be able to derive meaningful thermodynamic quantities from measurements of self-diffusion.

The factors which are considered to be significant for such processes have been discussed by Rice [24], among others. Thus he writes for the self-diffusion coefficient the equation:

$$D = \frac{1}{2} Z \langle \ell^2 \rangle v \theta_d (1 - \theta_d) e^{-U_d/RT}, \quad (31)$$

in which Z is the number of neighbors in the shell contained in the diffusion-complex-unit, $\langle \ell^2 \rangle$ is the mean squared jump-distance from defect to defect, θ_d is the concentration of the defects involved, v is the weighted mean frequency of

vibration of the shell surrounding the diffusing atom, and U_d is the energy needed to expand the shell sufficiently so that the atom can jump.

In the analysis [3] of the self-diffusion of oxygen in UO_{2+x} it has been assumed that the defects involved are the oxygen ions on interstitial sites. Accordingly, one can solve [3] the equations given above to obtain the expression

$$\theta_i \cong \frac{1}{2} \left\{ x + \left[x^2 + \frac{8q_i}{q_v} e^{-\frac{(E_v - E_i)}{RT}} \right]^{1/2} \right\}, \quad (32)$$

an approximation which is sufficiently exact to be applicable in the case at hand. In this equation the quantity q_i/q_v varies slowly with temperature.

B. Application to UO_{2+x}

In the case of the uranium dioxide phase, it is possible to evaluate all the quantities except U_d in equation (31) by measurements which do not involve self-diffusion.

1. The quantity $(Z/2) \langle l^2 \rangle$ was evaluated by assuming that a diffusing atom jumps from one interstitial position to another in the adjacent unit cell through a chain of atoms. This mechanism is suggested on the basis of Willis's analysis of the neutron diffraction. One imagines that the oxygen ion on an interstitial position itself cannot initiate the jump because either all possible adjacent positions are either blocked or there are too few vacancies. If, however, one of the four atoms surrounding the vacant interstitial position in the adjacent unit cell moves into the center of the fluorite cell, then a chain of events can occur in which the vacancy moves "backwards" into the interstitial position initially occupied by the extra oxygen ion. From the geometrical arrangement one deduces that $(Z/2) \langle l^2 \rangle = 22.4 \times 10^{-16} \text{ cm}^2$.

2. The analysis by Rice suggests that the weighted mean frequency is determined principally by the highest lattice frequency. Accordingly, the highest value observed in the inelastic scattering of neutrons [25] was selected for ν . The value is $18.10^{12} \text{ sec}^{-1}$.

3. The value for $E_v - E_i$ and consequently θ_i were determined from the analysis of the thermochemical properties. $E_v - E_i = 40.7 \text{ kcal/mole}$.

4. The energy U_d was evaluated from the measurements by Auskern and Belle [26] for values of x sufficiently large that the term $8(q_i/q_v) e^{-\frac{(E_v - E_i)}{RT}}$ in equation (32) was negligible. The result is 29.7 kcal/mole .

A comparison between the values for the self-diffusion coefficient of oxygen in UO_{2+x} measured by Auskern and Belle and the curves calculated from the model described above is given in Figure 4. The agreement between the two appears to be within the experimental errors. More accurate measurements are needed to examine the model further.

To compare self-diffusion in the three substances, UO_2 , ThO_2 , [27] CaF_2 , [28] (Figure 4), one notes the following items: (1) The partial pressure of oxygen (or fluorine) and the facility with which the composition can be changed are reflected essentially in E_v and/or E_i which are measures of the energies involved between the two valence-states, +4 and +5, according to equations (28) and (29). (2) The extent of the homogeneous region is determined primarily by E_i and E_{vv} . (3) It is $(E_v - E_i)$ which, especially near stoichiometry, reflects the equilibrium distribution of the anion between lattice and interstitial sites. (4) The energy U_d is a measure, in part at least, of the elastic moduli. The three substances certainly differ considerably with respect to items (1) and (2). The valencies in excess of +4 for thorium and +2 for calcium occur at energies which are much larger than the +5 state for uranium. The values for $(E_v - E_i)$ in the three cases, however, need not be very different. In the dynamics of the lattices, thoria and urania should be quite similar. The investigations of Willis [16,29] have demonstrated that the same kinds of displacements of the anions occur in all three substances. Willis has also obtained very nearly the same Debye temperatures for the first two substances. Consequently, one surmises that in stoichiometric uranium dioxide and thorium dioxide the energies involved in $U_d + 1/2(E_v - E_i)$ are very nearly the same. The actually reported values, 65.3 kcal/mole and 65.8 kcal/mole respectively, for the activation energy for self-diffusion of oxygen do agree. But the reported pre-exponential factors, $1/2 \times 10^3$ and $4.4 \text{ cm}^2/\text{sec}$ respectively, do not agree. If, however, one considers the experimental errors

and the difficulties associated with the reactions at the surfaces when particles of different sizes, 2.65 μ and 34.5 μ respectively, are employed, one surmises that the self-diffusion of oxygen in the two substances is very nearly the same so that both the energies and the entropies in the two cases are comparable. Calcium fluoride on the other hand, appears to differ from these two substances. But such is to be expected because not only is the displacement observed by Willis different for CaF_2 , but also the elastic constants for it are smaller than those reported for uranium dioxide. It may be significant to compare the change in slope of $\log D$ vs T^{-1} at about $T^{-1} = 10^{-3}$ for calcium fluoride with the analysis given herein. In the model, a similar change is predicted for the following reason: At low temperatures and sufficiently large values of x , the occupation of the interstitial positions is effectively saturated; in equation (32) this corresponds to the condition wherein $x > (8q_1/q_V) \exp [(-E_V + E_i)/RT]$. At high temperatures the occupation is accomplished by thermally shifting the equilibrium: $(\text{O}^{-2}\text{as}) + \text{is} \rightarrow (\text{O}^{-2}\text{is}) + \text{as}$, and the situation tends to approach that for $x = 0$. Such may be the source of the change in slope for calcium fluoride.

Since nitrogen probably dissolves interstitially rather than substitutionally in uranium dioxide, one anticipates that its diffusion is determined principally by the energies associated with the lattice dynamics. The value reported [30] for the diffusion of nitrogen is 33.4 kcal/mole. The solubility of nitrogen is probably relatively small so that the fraction of the interstitial sites occupied by nitrogen is probably much smaller than the fraction occupied by oxygen at stoichiometry. Consequently, one expects the observed rate of diffusion to be much smaller.

A detailed application of the results of this study to the technological aspects of the transport of material in urania is obviously not yet possible. Nevertheless, these studies should help to explain some of the problems of a basic nature which have arisen in attempts to understand the processes involved in sintering. As one example we cite the following: "As the volume diffusion coefficient for anions and cations generally differ, it has been normal to assume that the movement of the ion having the lower diffusion coefficient would be rate controlling. This assumption has led to serious discrepancies between theory and experiment, with sintering being more rapid than would be predicted from measured diffusion coefficients". The "final explanation of this puzzling discrepancy in apparent-diffusion coefficients is one of the most important problems in sintering theory today" [31,19]. The experimental results in the case of uranium dioxide consistently demonstrate that the sintering occurs at temperatures such that the self-diffusion of oxygen is measurable but such that the self-diffusion of uranium is not detectable. The former occurs at temperatures near 1000°K; the latter requires temperatures in excess of 2300°K to be measurable. Further, one observes experimentally that the rate of sintering increases with increasing oxygen dissolved in the solid phase. We surmise therefore that the fault lies with a theory in which it is assumed that the rate is controlled by the ion which moves more slowly. If successive steps are involved, then the slower one is determining. However, it appears doubtful that the process of sintering does involve successively the diffusion of oxygen and uranium or vice versa. Rather, the two occur simultaneously in parallel so that only the more mobile ions need to move. In this respect the analysis of the process by the methods of non-equilibrium thermodynamics serves to establish the criterion which resolves the apparent discrepancy, for the equations derived therein [3] enable one to predict that the chemical inter-diffusion is determined by the self-diffusion process having the larger coefficient. More precise measurements of the sintering process are needed particularly in the compositional range extending from 0 to 0.03 for x . At the present time one can hardly justify stating [32] otherwise than that for the former composition a rather large activation energy is required, perhaps as large as 76 kcal/mole and for the latter composition a value near 39 ± 4 kcal/mole is indicated, and that these are not in disagreement with the analysis presented herein.

Acknowledgements

The author wishes to acknowledge the typing of the manuscript by Marianne Ryan and Myrna Blasing and the preparing of the drawings by Ruth Lang.

This work was performed under the auspices of the U. S. Atomic Energy Commission.

References

- [1] B. T. M. Willis, *Nature* 197, 755 (1963); *J. Phys.* 25, 431 (1964).
- [2] R. J. Thorn and G. H. Winslow, *Advances in High Temperature Chemistry*, L. Eyring, ed., Academic Press, Inc., New York, to appear.
- [3] R. J. Thorn and G. H. Winslow, pp. 213-239, Vol. II, *Thermodynamics with Emphasis on Nuclear Materials and Atomic Transport in Solids*, International Atomic Energy Agency, Vienna, 1966.
- [4] L. Lynds, W. A. Young, J. S. Mohl, and G. G. Libowitz, pp. 58-65, *Non-stoichiometric Compounds*, R. Ward, ed., American Chemical Society, Washington, D. C., 1963.
- [5] R. J. Thorn and G. H. Winslow, *J. Chem. Phys.* 44, 2632 (1966).
- [6] E. Aukrust, T. Fjorland, and K. Hagemark, pp. 713-22, *Thermodynamics of Nuclear Material*, International Atomic Energy Agency, Vienna, 1962.
- [7] R. J. Thorn, unpublished manuscript.
- [8] M. Purbaix, *Atlas d'Equilibres Electrochimiques*, Gauthier-Villars and C¹e, Paris, 1963.
- [9] R. J. Ackermann, E. G. Rauh, R. J. Thorn, and M. C. Cannon, *J. Phys. Chem.* 67, 762 (1961).
- [10] R. J. Ackermann, M. S. Chandrasekhariah, E. G. Rauh, Argonne National Laboratory Report, ANL-7048, 1965.
- [11] L. M. Atlas and G. J. Schleman, pp. 407-421, Vol. II, *Thermodynamics with Emphasis on Nuclear Materials and Atomic Transport in Solids*, International Atomic Energy Agency, Vienna, 1966.
- [12] R. E. Ferguson, E. D. Guth, and L. Eyring, *J. Am. Chem. Soc.*, 76, 3890 (1954).
- [13] See R. H. Fowler and E. A. Guggenheim, *Statistical Thermodynamics*, Cambridge University Press, London, 1939.
- [14] H. Heitler, *Ann. d. Phys.* 80, 629 (1926).
- [15] L. E. J. Roberts and A. J. Walter, *J. Inorg. Nucl. Chem.* 22, 213 (1961).
- [16] B. T. M. Willis, *Proc. Roy. Soc. (London)* A274, 134 (1963).
- [17] A. E. Martin and R. K. Edwards, *J. Phys. Chem.* 69, 1788 (1965).
- [18] T. L. Markin and R. J. Bones, U. K. Atomic Energy Research Establishment, Harwell, Rept. R4178, Part 2 (1962).
- [19] See also, "Thermodynamic and Transport Properties of Uranium Dioxide," *Tech. Rept. Ser. No. 39*, International Atomic Energy Agency, Vienna, 1965. This report contains a summary of the known properties of the uranium dioxide phase.
- [20] K. Hagemark, Institutt for Atomenergi, Norway, Kjeller Rept. KR-67, 1964.
- [21] A. L. G. Rees, *Trans. Faraday Soc.* 50, 335 (1954).
- [22] E. Elock, *Order-Disorder Phenomena*, Methuen, London, 1956.
- [23] H. S. Green and C. A. Hurst, *Order Disorder Phenomena*, Interscience Publishers, New York, 1964.
- [24] S. A. Rice, *Phys. Rev.* 112, 804 (1958).
- [25] G. Dolling, R. A. Crowley, and A. D. B. Woods, *Can. J. Phys.* 43, 1397 (1965).
- [26] A. B. Auskern and J. Belle, *J. Nucl. Mater.* 3, 267 (1961).
- [27] H. S. Edwards, A. F. Rosenberg, and J. T. Bittel, Wright-Patterson Air Force Base, Ohio, Rept. ASD-TDR-63-635 (1963).
- [28] H. Matzke, *J. Nucl. Mater.* 11, 344 (1964).
- [29] B. T. M. Willis, *Acta Cryst.* 18, 75 (1965).
- [30] H. M. Ferrari, *J. Nucl. Mater.* 12, 142 (1964).
- [31] J. E. Burke and R. L. Colbe, p. 199, Vol. 3, *Progress in Ceramic Science*, Pergamon Press, 1963.
- [32] See I. Amato, R. L. Colombo, and A. M. J. Protti, *J. Nucl. Mater.* 11, 229 (1964).

TABLE 1. Comparison of valence-energies of some actinide elements

Element	Relative stabilities of valence states		
	In aqueous solution		Partial pressure of O ₂ for MO _{1.96} (s) at 1600°C
	Individual ^a values (kcal/mole)	Relative to U (kcal/mole)	
Th		-69 to 0	$\ll 10^{-18}$ atm ^b
U	14	0	5×10^{-22} atm ^c
Np	-4	18	
Pu	-22	36	7.1×10^{-11} atm ^d
Am	-50	64	
Pr	-66	80	$\gg 1$ atm ^e

References for Table 1:

- a $23[3E(M^{+3}) - 4E(M^{+4})]$; E is the electrode potential given by Pourbaix [7], which is the negative of the electrode potential commonly used in the U.S.A.
- b Ackermann et al. [9].
- c Ackermann et al. [10].
- d Atlas and Schlehman [11].
- e Ferguson, Guth, and Eyring [12].

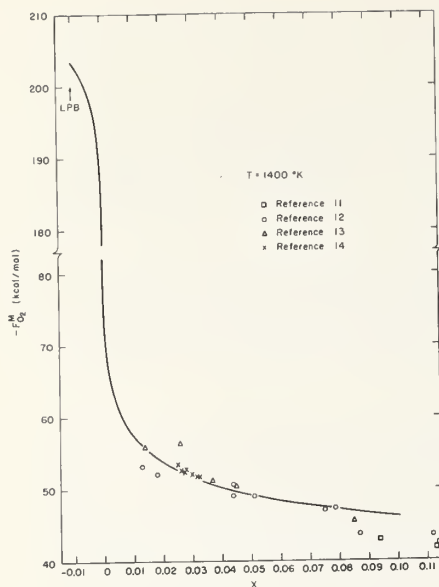


Figure 1. Comparison of relative partial molar free energy calculated at 1400°C with observation. See Ref. 5

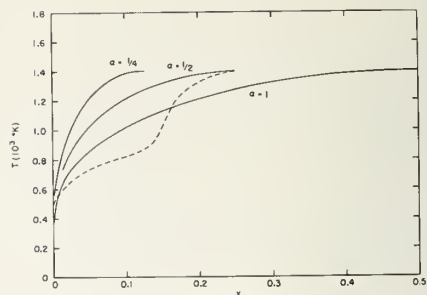


Figure 3. Comparison of the locations of the upper-phase boundary that would be calculated from this model, using various value of α_1 , with observed boundary. See Ref. 5

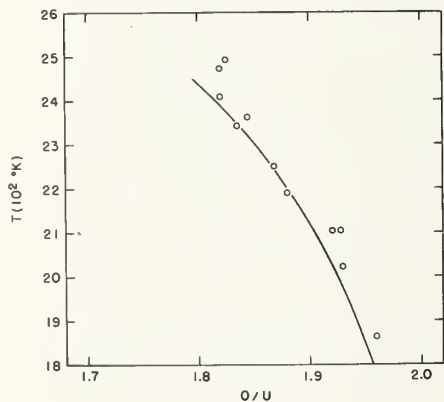


Figure 2. Comparison of calculated lower-phase boundary with observation. See Ref. 5, 10, and 17

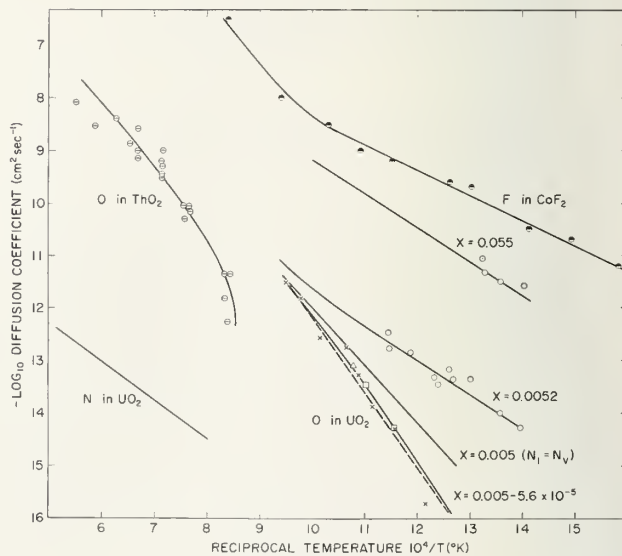


Figure 4. Intercomparison of self-diffusion coefficient. See Ref. 3

Nuclear Fuel Materials

D. W. Readey and J. H. Handwerk

Argonne National Laboratories

Argonne, Illinois

Abstract

Selection of a nuclear fuel material is dependent upon many compromises of material properties consistent with demands of the power generating system. Those properties which dictate the use of a given material for specific systems such as thermal and fast reactors, nuclear rocket engines, and direct conversion devices, are reviewed. Materials of interest are uranium, plutonium and thorium and their compounds either alone or combined with each other or with non-fissile materials. Technology at the present time is directed toward the utilization of primarily the oxides and carbides of fissile metals. However, their nitrides, sulfides, and phosphides show promise as potential fuel materials but the properties of these compounds must be more fully delineated before they can be considered for fuel purposes.

Nuclear Fuel Materials

D. W. Readey and J. H. Handwerk

1. Introduction

Ceramic materials possess certain properties which make them attractive as fuel materials for nuclear power generating systems. However, it should be pointed out at the outset that ceramics are not the only materials being considered. On the contrary, the state of the art of reactor design is constantly changing and other fuels under consideration are: solid and liquid metals, molten salts, solutions, slurries, and even gases. Each of the reactor design concepts, utilizing the different fuel types, has certain aspects which make some fuels more attractive than others.

To emphasize the property requirements for a nuclear fuel material, a summary of the physics, operation, and the environment encountered in nuclear power generating systems is presented. The properties and the behavior in the reactor environment of some of the more important ceramic fuel materials is compared. In general, those aspects of material-environment interactions peculiar to a nuclear power generating system are emphasized. Finally, the behavior of the actinide compounds which makes them interesting purely as materials is discussed. Throughout, the intent is not to give an exhaustive survey of all the design-environment-materials interactions but to emphasize the unique aspects of ceramic nuclear fuel materials.

2. Nuclear Power Generating Systems

2.1. The Fission Process

When a fissionable nucleus, such as U^{235} , undergoes fission after absorption of a neutron, two new nuclei are formed as fission products whose atomic weights are roughly half that of the fissioning nucleus. In addition, two or three neutrons, neutrinos, and β and γ radiation are emitted with a total energy of some 205 MeV. About seventy percent of the energy is released as kinetic energy of the fission product nuclei which quickly dissipate their energy within a few microns. This large release of energy as heat in a small volume causes a great deal of radiation damage to the crystal lattice. To illustrate the magnitude of energy liberated, the fissioning of one gram of U^{235} produces about one megawatt day of available energy [1].¹

As the process proceeds, the fission products accumulate in the fuel and affect its properties. Figure 1 gives a typical distribution of the yield of fission products from U^{235} , which consist mainly of Kr, Xe, Sr, Ba, Cs, I, Te, Zr, Mo, Ru, Ce and Nd [2].

2.2. Reactor Physics

In order for the process to continue, the neutrons released from a fissioning nucleus must be captured by other nuclei which subsequently fission, and so on, creating a "chain reaction". However, if the neutrons produced do not produce further fissions, the chain reaction and heat generation ceases. Neutrons can be lost from the fission process either by leakage from the reactor core (that part of the reactor containing the fissionable material), or by capture by non-fissionable nuclei. To help reduce the loss by leakage, a "reflector" material containing atoms of low atomic weight reflects neutrons back into the core via elastic nuclear collisions. To prevent loss by capture in non-fissionable nuclei, structural materials are utilized in the core which have low capture cross sections (a measure of the ability of a given nucleus to undergo the process in question) for neutrons. Therefore, a chain reaction will be maintained only if the rate of neutron production equals the rate of leakage plus the rate of absorption. To maintain a steady state of neutron production and loss, materials which easily absorb neutrons are inserted into the core via "control rods". Thus, a nuclear reactor can be defined simply as an assembly of fissionable material arranged in such a way that a chain reaction is sustained under control [1].

The neutrons emitted from a fissioning U^{235} nucleus have mean energies of about 2 MeV. The cross section of U^{235} for fission is about 1.59 barns ($1 \text{ barn} \approx 10^{-24} \text{ cm}^2$). Under these conditions, the critical mass (the minimum amount of fissionable material necessary for the sustained chain reaction) of pure U^{235} metal is about 20 kg. However, for neutron energies on the order of thermal energy (0.025 eV), the fission cross section is 582 barns. To reduce neutron energies, "moderators" are used. These are

¹Figures in brackets indicate the literature references at the end of this paper.

TABLE 1. Neutrons Available for Breeding from U²³⁵, Pu²³⁹ and U²³³ [6]

	U ²³⁵		Pu ²³⁹		U ²³³	
	Thermal	Fast	Thermal	Fast	Thermal	Fast
n	2.47	2.51	2.91	2.97	2.51	2.55
σ_f (barns)	582	1.59	746	1.83	527	2.37
σ_c (barns)	112	0.32	280	0.32	54	0.20
σ_c/σ_f	0.19	0.2	0.375	0.18	0.102	0.085
$\eta-1$	1.07	1.09	1.12	1.53	1.28	1.35

Thus, for maximum utilization of the world's potential fissionable power resources, fast breeder reactors are mandatory. At the present time, the Pu²³⁹-U²³⁸ cycle is economically preferable to the U²³³-Th²³² cycle because of its higher breeding ratio, higher fast fission bonus, and smaller critical mass requirements [7]. However, future power needs can make the U²³³-Th²³² cycle economically feasible.

Ultimately, fast breeder reactors will also become economically more favorable than thermal reactors because of the value of the fissionable material produced. However, most of the reactors existing and being built today are of the thermal type primarily because of the smaller fissionable material requirements, and subsequent reactor size and cost, for a given power rating.

2.3.3. Reactor Operation, Environment and Fuel Materials

To economize on the size and cost of the reactor core, it is desirable to use fuel materials which have a high fissile and fertile atom density. This is particularly true for fast reactors, such as a rocket engine, since the critical mass required is larger because of the smaller fission cross sections. Also, the other nuclei or atoms in the reactor core, be they in the moderator, coolant, fuel or structural members, should have a low neutron absorption cross section, again to economize on the critical mass and size of the core.

The coolant in a power reactor extracts the heat generated in the fission process. In thermal reactors the usual coolants are ordinary and heavy water, which also double as moderators, and CO₂ gas (in conjunction with graphite as moderator). For fast reactors, a non-moderating coolant with excellent heat transfer characteristics is required, hence, liquid sodium is most commonly used. To prevent corrosion of the fuel material and release of radioactivity into the coolant, the fuel is normally encased in a cladding. The combination of fuel-cladding is usually referred to as the "fuel rod or plate". The common cladding materials, chosen because of their corrosion resistance and neutron transparency, are aluminum, magnesium, zirconium alloys, and stainless steels. A cladding and fuel combination must be selected to minimize reaction between them to prevent cladding failure, and release of radioactive material into the coolant. In spite of the cladding, it is still desirable to use a fuel which reacts as little as possible with the coolant medium in case of cladding failure.

Coolant temperatures are usually limited to only a few hundred degrees centigrade because of structural strength and corrosion problems. Therefore, to extract the maximum heat flux from a reactor, a large thermal gradient must exist within fuel rods. These gradients may be as high as 1000°C/cm for some ceramic fuels. Hence, a high melting point and good thermal conductivity are of paramount importance for a fuel material.

As the reactor operates, fission product accumulation, thermal cycling, and prolonged operation in the steep thermal gradient change the overall properties of fuel rods. This limits the amount of "burnup", or the amount of fission energy available in the fuel material actually used (commonly expressed in megawatt days per metric ton of fuel) before it must be removed from the reactor core. Since fuel cost is an appreciable part of the cost of the power, generally the higher burnup, the lower the fuel cost. In fact, fuel costs decrease inversely proportional to burnup [8].

3. Properties of Ceramic Fuel Materials

3.1. General

Although ceramics possess many of the desired properties for a fuel, this does not necessarily imply that the fuel will be a massive, dense body. In some instances, this is the case, but in others the

ceramic is dispersed in a matrix of a metal or graphite or even another ceramic to give the overall fuel rod improved properties, such as higher thermal or electrical conductivity, or lower work function. Also, instead of relatively large dense pieces of fuel, some reactor designs utilize small, loosely compacted particles to permit easy release of gaseous fission products. Therefore, it is difficult to generalize processing and properties because of the multiplicity of reactor design concepts. Hence, an attempt will be made to discuss only those processing techniques and properties which are unique to ceramic nuclear fuel and are of reasonably general applicability.

From what has preceded, it is obvious that a nuclear fuel material must contain a certain percentage of the fissionable isotopes, U^{233} , U^{235} , or Pu^{239} . Usually about two percent is required for thermal reactors and about twenty percent or more for fast reactors with the rest the fertile U^{238} and Th^{232} . Since the Pu^{239} - U^{238} breeding cycle is presently of greatest interest, and plutonium is normally present in minor concentrations, the discussion of properties will be concerned primarily with the uranium compounds. This is not to say that the properties of the other actinide compounds and their combination with uranium compounds are not of interest. However, their properties and behavior are, in many respects, quite similar to those of the uranium compounds. Therefore, the uranium compounds are convenient vehicles for discussion and have also been the most thoroughly investigated.

3.2. Processing and Reprocessing

Some of the processing techniques utilized for ceramic nuclear fuels are quite conventional such as cold pressing and sintering. Others, such as arc melting and casting, are more unusual. Still others, such as pyrolytic graphite coating of fuel particles, are exotic. However, there are two areas peculiar to nuclear fuel materials worthy of special note: these are, (1) reprocessing the spent fuel to retrieve unused and bred fuel, and (2) nuclear safety.

3.2.1. Reprocessing

Normally, less than ten atomic percent burnup (equivalent to about 100,000 MWD/metric ton) can be sustained before a fuel rod must be removed from a reactor core because of degradation of its properties. To achieve maximum utilization, the unused and bred fissionable materials must be separated from the fission products and refabricated into new fuel rods. Many of the fission products are highly radioactive (the higher the burnup, the greater the radioactivity). Thus, reprocessing must wait until the activity subsides or be carried out in a shielded, remote facility, which is an expensive operation. Since fuel cost represents a sizeable fraction of the operating expenditures for a nuclear reactor, the expense of a remote reprocessing facility may override the cost of the large fuel inventory necessary if conventional facilities are used. Such a remote reprocessing facility is shown in Figure 3. This particular facility has been designed for reprocessing the metallic fuels for the EBR-II reactor. Reprocessing of ceramic fuel materials is still in its infancy. Nevertheless, the ease of inexpensive reprocessing is an important consideration in the selection of a fuel material for a given reactor application. Some of the reprocessing separation techniques under consideration are: solvent extraction; oxidation-reduction to remove volatile fission product oxides; vaporization of volatile actinide metal chlorides and fluorides.

3.2.2. Nuclear Safety

During both processing and reprocessing fuel materials, there are two everpresent safety hazards: (1) criticality, and (2) alpha particle activity of fissile and fertile nuclei.

With regard to criticality, about 20 kg. of pure U^{235} metal and 0.8 kg. of U^{235} in water, and even less for Pu^{239} and U^{233} , are necessary for a critical mass. Therefore, in any operation where there is any possibility, either intentional or accidental, of the fissionable material becoming intimately mixed with a good moderator, such as water, a total amount of fissionable material considerably less than a critical mass must be used. This limits handling and storing procedures to relatively small quantities of material, makes continuous processes difficult, and requires strict control, all of which contribute to the expense of fissionable material.

All the common isotopes of uranium, thorium, and plutonium undergo radioactive decay by alpha emission, and to a much lesser extent, by spontaneous fission. Alpha particles are strongly absorbed by most materials and can easily be protected against. However, since they are strongly absorbed, causing a great deal of damage to the absorbing material, alpha emitters are particularly dangerous if they enter the human body. Uranium, plutonium and thorium compounds tend to concentrate in bone material and, as a result, their maximum permissible body burden is set at a few tenths of a microcurie (1 curie = 3.7×10^{10} disintegration/sec) [9]. For most of the isotopes in question, this amounts to a few hundredths of a gram total body burden. However, Pu^{239} and U^{233} have much shorter half lives, and the permissible body burden for them is only about 0.1 microgram. Therefore, much more stringent precautions against inhalation, ingestion, and entrance through the skin must be taken and, as a result, work with these isotopes must be carried out in gloveboxes. A typical glovebox enclosure for plutonium work is shown in Figure 4. Gloveboxes give an added advantage in that many fuel materials react strongly with air and atmospheric moisture and with an inert, dry atmosphere in the glovebox, oxidation and hydration can be minimized.

3.3. Materials and Properties

3.3.1. General

Table 2 lists the properties of several uranium compounds which are of primary interest for fuel application. The list is by no means complete and is only meant to serve as an illustration of some materials being given major consideration and of representative property values. Other compounds such as aluminides, silicides and beryllides are not listed since they are generally being given less attention, and although the dicarbide is being considered for a dispersed fuel because of its compatibility with graphite, it is not listed. The primary purpose of the list is to compare the properties of the oxide, UO_2 , with the compounds having the sodium chloride structure.

TABLE 2. Typical Properties of Selected Uranium Compounds
(all values at room temperature unless specified)

	UO_2	UC	UN	US	UP
Crystal Structure	CaF_2	NaCl	NaCl	NaCl	NaCl
Density (gm/cc)	10.96[11]*	13.63[16]	14.32[11]	10.84[24]	10.23[24]
Uranium Density (gm/cc)	9.66	12.97	13.52	9.57	9.07
σ_a , thermal for second element (barns)	0.0002	0.0033	1.88	0.52	0.20
Lattice Parameter (Å)	5.47[11]	4.96[16]	4.88[16]	5.49[24]	5.59[24]
Melting Point (°C)	2730[10]	2500[17]	2750[14]	2450[24]	2240[24]
Thermal Conductivity (cal cm ⁻¹ sec ⁻¹ °C ⁻¹)	0.018-0.028[11]	0.05[17]	0.035[22]	0.026[24]	0.032[24]
Electrical Resistivity ($\mu\Omega$ -cm)	$\sim 10^{11}$ [13]	70[18]	160[22]	179[28]	325[24]
$-\Delta F_{298}^\circ$ (kcal/mole) [14]	264.6	24.5	74.3	98.6	67[29]
Vapor Pressure (atm at 2000°K)	$\sim 10^{-7}$ [12]	$\sim 10^{-10}$ [19]	$\sim 10^{-4}$ [23]	$\sim 10^{-8}$ [25]	$\sim 10^{-6}$ [29]
Thermal Expansion Coefficient (10 ⁻⁶ °C ⁻¹)	10.5[13]	11.1[19]	9.5[22]	11.6[24]	8.6[27]
Young's Modulus (10 ⁶ psi)	31[15]	30.4[20]	31[11]	24.2[26]	25.6[26]
Modulus of Rupture (psi)	$\sim 11,000$ [13]	$\sim 15,000$ [21]	—	14,000[26]	17,000[26]
Poisson's Ratio	0.30[15]	0.284[20]	0.1[11]	—	—

*Reference

3.3.2. Nuclear Properties

A high uranium density is desirable for a reactor system so that the reactor core size and cost can be minimized. It is particularly important for fast breeder reactors in which neutron conservation is important. Therefore, from this standpoint, UC and UN are most desirable for fast reactor applications.

The other parameter which concerns the nuclear properties of these compounds is the thermal neutron absorption cross section, σ_a , (thermal), for the second element. For a thermal reactor, one would like this to be as small as possible, for neutron economy. In this case, UO_2 and UC are the most favorable, whereas, UN is the least. For fast reactors, this is of less importance because the differences in the cross sections decrease with neutron energy.

3.3.3. Thermal and Chemical Stability

As was stated earlier, a high melting point is desirable in a fuel material in order to obtain a

large heat flux from the fuel element. All of the compounds in Table 2 have sufficiently high melting points to be of interest as reactor fuels. In most cases, it is undesirable for melting to occur in the fuel material for essentially two reasons. First, the major fraction of the fission products are gaseous at these temperatures and melting releases the gases which had been trapped in the solid fuel, either as bubbles or in solid solution. Second, there is usually a significant volume change which takes place on melting which may cause swelling or even rupture of the cladding material. These problems, however, can be circumvented by leaving a certain amount of void volume within the fuel element to allow for fission gas release and volume changes due to melting [30].

All of the compounds listed have sufficiently low vapor pressures at elevated temperature with, perhaps, the exception of UN. Naturally, the vapor pressure must be low to prevent swelling and rupture of the cladding material. Of course, this only becomes significant near atmospheric pressure. A low vapor pressure, however, is also desirable to prevent relocation of the fuel material within the fuel element via an evaporation-condensation process under the influence of the steep thermal gradient.

Migration and segregation of fission products and fissile and fertile materials can also take place by solid state diffusion and gas bubble migration under the influence of the temperature gradient [31]. This segregation of constituents can change considerably the overall properties of a fuel rod. One of the interesting effects of the temperature gradient extant in fuel materials is the observation of the so-called "amoeba" effect [32]. For certain reactor designs, carbon-coated (to retain fission products) UC_2 particles are dispersed in a graphite matrix. Under the influence of the temperature gradient, UC_2 dissolves more carbon on the high temperature side of the particles and precipitates it on the cooler side. As a result, the UC_2 migrates out of the carbon coating, up the temperature gradient, with a resulting microstructure which looks strikingly like an amoeba.

Compatibility between the fuel and cladding materials and corrosion resistance of the fuel in the coolant medium if the cladding material should fail are also important. A complicating factor is that most of the ceramic fuels exhibit wide ranges of stoichiometry. Thus, the reactivity of the cladding and coolant with the fuel depends strongly on fuel composition. As an example of the range of stoichiometry these materials can sustain, UO_2 has long been known to exist as a single phase up to about $UO_{2.25}$ above $1000^\circ C$ [33]. Recently, however, it has been shown that UO_2 may become hypostoichiometric at temperatures above $1500^\circ C$ and the single phase region extends down as far as $UO_{1.65}$ at $2400^\circ C$ [34]. Figure 5 [35] gives the phase diagram of the plutonium-carbon system as a typical example of the non-stoichiometry range in the sodium chloride structure compounds.

Another factor worth noting is that accumulated fission products may change the activity of oxygen or carbon, for example, in the fuel material and alter the compatibility and corrosion characteristics of the fuel [36].

Therefore, the reactivity of a fuel material with its cladding and coolant are dependent on a number of variables which include temperature, composition of fuel, cladding and coolant, and burnup. Compatibility of fuel and matrix materials is also an important consideration for dispersion type fuel elements with matrices such as the graphite used in a nuclear rocket engine [37] and the tungsten considered for thermionic emission. [38] The very large number of possible combinations of materials, compositions and environments precludes any detailed discussion of compatibility and corrosion. However, the following somewhat limited observations can be made. Uranium dioxide is far less reactive in air, water, steam and CO_2 than are the non-oxides. [39] Therefore, the oxide is a good choice for thermal reactors which are generally water cooled. On the other hand, uranium carbide is relatively stable in liquid sodium but its corrosion rate is strongly dependent on the oxygen content of the liquid metal. [39] Also, if the carbide contains any excess carbon or the chemical activity of the carbon is high, there can be compatibility problems with carbide-forming cladding materials such as stainless steels and zirconium alloys.

3.3.4. Thermal Properties

3.3.4.1. Thermal Conductivity

As was pointed out earlier, all else being equal, the higher the heat flux from a fuel rod, the higher the power rating of the reactor. Therefore, the thermal conductivity of the fuel material is a property of primary importance. From Table 2 it is seen that UO_2 has the lowest thermal conductivity of all the compounds listed. Therefore, the higher the desired heat flux, as in a fast reactor, the less desirable UO_2 becomes compared to the other compounds.

The reason for the higher thermal conductivity of the sodium chloride structure compounds is that a large fraction of heat is transported by electrons, whereas, thermal transport in UO_2 is entirely by phonons. Since the atomic weights of the metal and non-metal atoms in the actinide compounds are greatly different, phonon conductivity is low because of the anharmonicity of the lattice vibrations [40]. Figure 6 compares the thermal conductivity of UC with UO_2 [21]. The electronic contribution to the thermal conductivity for UC, k_e , was calculated from measured values of the electrical resistivity [21] with the Wiedemann-Franz law,

$$k_e = \frac{L_o T}{\rho} \quad (3)$$

where L_o is the Lorentz number, ($L_o = 5.72 \times 10^{-9}$ if k_e is in $\text{cal cm}^{-1} \text{sec}^{-1} \text{C}^{-1}$, T in $^{\circ}\text{K}$, and ρ in ohm-cm) T is the absolute temperature and, ρ , the electrical resistivity. It is seen that the phonon contribution to the thermal conductivity of UC is close to that for UO_2 and decreases with increasing temperature due to phonon-phonon scattering. Eventually, at some higher temperature, the electronic contribution will, for all practical purposes, equal the total thermal conductivity. For the other sodium chloride type compounds, such as UN, [22] the behavior is similar. However, for UN, the total thermal conductivity increases with temperature parallel to the electronic contribution. This implies that the phonon contribution, which is larger for UN, is relatively insensitive to temperature. This behavior parallels that of the transition metal monocarbides and nitrides which has recently been summarized by Williams. [41] Williams explains the insensitivity of the phonon contribution by phonon scattering from lattice defects, electrons and possible magnetic disorder on the metal sublattice. However, at higher temperatures, the phonon contribution should be expected to decrease since phonon-phonon scattering will eventually limit the phonon mean free path in the lattice.

Since solid fuel materials are generally polycrystalline bodies, there are interesting microstructural changes which have been observed to take place during operation with the steep temperature gradient. These changes significantly affect the overall thermal conductivity of the fuel elements. For example, the gaseous fission products produce lenticular voids in UO_2 , [30] with their short axes parallel to the direction of the heat flux. These voids are very effective in reducing the thermal conductivity. On the other hand, due to the migration of these voids up the thermal gradient, large columnar grains are formed [30] in UO_2 whose long axes are parallel to the direction of the heat flux. Figure 7 [42] shows an example of this columnar grain growth in UO_2 . It has been shown that photon conduction becomes the primary heat transfer process in single crystal UO_2 at temperatures above 1000°C [43]. Hence, it would be expected that the columnar grain structure would behave similarly to single crystal UO_2 and the thermal conductivity would increase at elevated temperatures. Whether or not this actually occurs is still open to question. [30]

Figure 8 [44] is an example of some of the micro- and macro-structural changes which take place during irradiation and illustrates the effect of increasing the overall thermal conductivity of the fuel material. Note the columnar grain growth and the large central void formation in the sample on the left. The central void has been formed by the migration of fission gas bubbles up the temperature gradient. In both cases, there is severe cracking of the fuel material with penetration of the lead bonding (light phase) into the cracks.

3.3.4.2. Thermal Shock Resistance

During the operation of a reactor, the fuel material is subjected to thermal cycling and thermal shock resistance is important to inhibit cracking and disintegration of the fuel. Cracking and disintegration is undesirable because: (1) a redistribution of fuel material may occur producing swelling or rupture of the cladding; (2) the surface area of the fuel increases, enhancing the release of gaseous fission products; and (3) the overall thermal conductivity of the fuel element decreases.

If the thermal stress resistance, R , is defined as: [40]

$$R = \frac{k S (1-\mu)}{E\alpha} \quad (4)$$

where, k = thermal conductivity
 S = fracture strength
 μ = Poisson's ratio
 E = Young's modulus
 α = thermal expansion coefficient

then roughly speaking UO_2 should exhibit the lowest thermal shock resistance of all materials listed in Table II because, while all other parameters are similar, the thermal conductivity is lowest for UO_2 . However, several of these properties such as S are strongly dependent upon microstructure, which varies with operating conditions, hence it is difficult to make predictions as to the thermal shock resistance of a given material under the environmental conditions present during reactor operation.

3.3.5. Mechanical Properties

As was pointed out above, there is little difference in the room temperature mechanical properties

of these compounds and they depend strongly on microstructure. The creep behavior of fuel materials at elevated temperature is of importance since the pressure of fission product gases in voids can cause deformation of the fuel and concomitant swelling and possible rupture of the cladding. Here again, creep rate depends greatly on the microstructure and its changes within the reactor environment.

The creep rate is also dependent on composition. For example, the creep rate of UO_2 increases with increasing hyperstoichiometry while the activation energy decreases [45]. There is a reasonable correlation between the activation energies for creep and for uranium self diffusion in UO_2 . Hence, on this basis and the fact that the strain rate is linear with stress, creep in UO_2 has been associated with the Nabarro-Herring mechanism. Recent constant strain rate experiments [26] on UO_2 have shown the nucleation and growth of grain boundary voids in tensile regions. This behavior is consistent with the Nabarro-Herring diffusional creep mechanism.

For the sodium chloride compounds, the slip system is the same as the fcc metals, $(111) \langle \bar{1}\bar{1}0 \rangle$, but slip is an activated process and apparently only slightly dependent on stoichiometry [21]. Creep in UC, [21, 46] UN, [46] US and UP [26] is probably limited by an activated nonconservative dislocation motion [21] but the situation is not at all clear at the present.

3.3.6. Electrical Properties

The electrical properties of fuel materials are of primary importance when being used in a thermionic power system. Here, a high electrical conductivity and low work function are necessary. However, any deficiencies can be circumvented by dispersing the fuel in a matrix possessing the desired properties such as tungsten.

4. Bonding and Electronic Structure

In this section a short discussion of the defect and electronic structure, and the bonding of the actinide nuclear fuel compounds will be given, again concentrating on the compounds of uranium as being representative. As will be seen, the situation is quite complex, and due to the lack of sufficient experimental and theoretical information, much of the discussion is tentative and even speculative.

The type of bonding in the actinide compounds is doubtless complex since it involves combinations of s, d and f electrons of the metal and s and p electrons of the nonmetal. The number of valence electrons available varies from eight for ThC to fourteen for PuS. The type of bonding certainly affects the electrical and magnetic properties, the defect structure and degree of nonstoichiometry in these compounds.

4.1. Dioxides

The dioxides are different from the sodium chloride type compounds in that they have high room temperature electrical resistivities and are semiconductors, that is, they possess a positive temperature coefficient of resistivity. Uranium dioxide exhibits both hyper- and hypostoichiometric deviations from the ideal $UO_{2.00}$ composition. Neutron diffraction results indicate that hyperstoichiometric UO_2 contains oxygen interstitials [47]. No information is available concerning the defect structure of hypostoichiometric UO_2 . A recent study of electrical conductivity and Hall mobility concludes that electronic conduction in UO_2 takes place by a "hopping electron" or small polaron mechanism [48]. It should also be pointed out that UO_2 undergoes an antiferromagnetic transition at 28°K [49].

Plutonium dioxide is known to deviate only hypostoichiometrically from the ideal PuO_2 composition. In this case, the electrical properties and stoichiometry changes are consistent with a hopping electron mechanism and oxygen vacancies in the lattice [50].

In many respects, the dioxides behave quite similarly to the semiconducting transition metal oxides such as NiO and TiO_2 , etc. and, hence, their bonding can be considered to be a mixture of covalent and, primarily, ionic.

4.2. Sodium Chloride Type Compounds

The NaCl type compounds, in general, exhibit semimetallic behavior in that they have positive temperature coefficients of resistance and high room temperature resistivities. In this respect, they are quite similar to the transition metal monocarbides and nitrides such as TiC and TiN. Certainly, the bond type in these compounds is not at all clear. In Table 3 are listed observed and calculated lattice parameters. From this table, it appears that US can be considered either covalent or ionic whereas the carbides definitely appear to be more covalent. That a certain degree of covalent bonding exists in these compounds is evidenced by their magnetic transitions. Table 4 lists the known magnetic transitions of the uranium compounds.

Another indication of the bond type and similarity to the transition metal monocarbides and nitrides is the deformation behavior of these compounds. For example, it has been shown that the slip system of UC at high temperatures is $(111), \langle \bar{1}\bar{1}0 \rangle$ [21] which is the same as the transition metal compounds but

TABLE 3. Calculated and Observed Lattice Parameters of NaCl-Type Compounds

Metal	Non-metal	Observed Lattice Parameter (Å)	Covalent [51]				Ionic [52]			
			Metal Radius (Å)	Non-metal Radius (Å)	Calculated Lattice Parameter (Å)	a_o/a_c	Cation Radius (Å)	Anion Radius (Å)	Calculated Lattice Parameter (Å)	a_o/a_c
Th	S	5.68	1.80	1.03	5.66	1.004	0.99	1.84	5.11	1.112
U	S	5.49	1.55	1.03	5.16	1.06	0.93	1.84	5.54	0.990
Pu	S	5.54	1.53(α)	1.03	5.12	1.06				
Th	N	5.16	1.80	0.71	5.02	1.03	0.99	1.71	5.40	0.955
U	N	4.89	1.55	0.71	4.52	1.08	0.93	1.71	5.28	0.925
Pu	N	4.91	1.53(α)	0.71	4.48	1.09				
Th	P	5.82	1.80	0.93	5.46	1.05	0.99	2.12	6.22	0.938
U	P	5.59	1.55	0.93	4.96	1.13	0.93	2.12	6.10	0.918
Pu	P	5.67	1.53(α)	0.93	4.92	1.15				
Th	C	5.34	1.80	0.77	5.14	1.04	0.99	2.60	7.18	0.743
U	C	4.96	1.55	0.77	4.64	1.07	0.93	2.60	7.06	0.705
Pu	C	4.97	1.53(α)	0.77	4.60	1.08				

TABLE 4. Magnetic Transitions of Uranium Compounds

Compound	Transition Type	Temperature (°K)	Reference
US	ferromagnetic	178	52
UN	antiferromagnetic	50	53
UP	antiferromagnetic	130	52
UC	none	—	—

quite different from the (110), $\langle 1\bar{1}0 \rangle$ glide in the alkali halides [54].

Although information on the defect structure of these compounds when they deviate from stoichiometry is lacking, it is generally felt that hypostoichiometry implies nonmetal vacancies and hyperstoichiometry. nonmetal interstitials.

In order to relate nonstoichiometry and electrical properties to bonding in these materials, it is tempting to carry the analogy between the actinide and transition metal sodium chloride compounds further. For example, Denker [55] discusses the nonstoichiometry and defect structure of TiC, TiN and TiO on the basis of an electronic density of states curve which contains both bonding and antibonding overlapping bands. His argument is essentially as follows. Titanium monoxide exhibits a wide range of stoichiometry from TiO_{0.8} to TiO_{1.2}. At stoichiometry, both the titanium and oxygen sublattices have about fifteen percent vacant sites and, throughout the range of composition, the number of valence electrons per titanium site always remains about 8.5. Stoichiometric TiO would have ten valence electrons per metal atom site, four from titanium and six from the oxygen. A density of states curve similar to that considered by Denker is shown in Figure 9. To arrive at this type of density of states curve, ionic and covalent bonding between metal and nonmetal were considered as well as covalent interaction between metal-metal and nonmetal-nonmetal atoms. Below the minimum in the density of states

curve, the electronic levels are largely all bonding levels whereas above the minimum, they are largely antibonding. If all the lattice sites were filled in the stoichiometric TiO, the Fermi level would occur at the indicated position deep within the antibonding band. Therefore, to stabilize the rock salt structure, about fifteen percent vacancies are permitted, dropping the Fermi level down to about the minimum in the density of states curve, near the bottom of the antibonding band, a decrease in the free energy of about 1.75 eV per molecule or 40.3 kcal per mole of TiO. Denker then calculates that the energy to form fifteen percent vacancies is about 0.62 eV per molecule or 14.4 kcal per mole of TiO. Hence, the sodium chloride structure can be stabilized and the free energy at absolute zero lowered by a net of about 1.1 eV per molecule or 25.9 kcal per mole if fifteen percent vacancies are allowed to exist in the structure.

Denker also points out that for TiC, the bonding band is not quite filled. Therefore, he postulates, that increasing the number of valence electrons by adding TiN in solid solution to fill the bonding band, will produce a material with the highest stability and melting point in the TiC-TiN system.

It is interesting to speculate that similar occurrences for the actinide metal compounds are possible since their behavior parallels the transition metal compounds in so many other ways. Postulating a density of states curve for these materials, similar to that in Figure 9, it would no doubt be even more complex because of the f electron contributions. Also, the number of valence electrons can vary from eight for ThC to fourteen for PuS. Therefore, with this type of model and the large variation in the number of valence electrons in these compounds, a number of interesting possibilities arise.

1. Widely varying degree of nonstoichiometry from compound to compound,
2. large defect concentrations on both sublattices near stoichiometry,
3. possibility of semiconductivity where bands do not overlap and the lower ones are filled,
4. wide variations in stability, deviations from stoichiometry and electrical properties with solid solution.

Evidence that the actinide compounds behave in this manner is shown by the maxima in melting points found in the UP-US [24] and UC-US [56] systems in line with Denker's suggestion of maximum stability with filled bonding bands.

5. Conclusion

Nuclear ceramic fuel materials have certain desirable properties which make them attractive for use in nuclear power generating systems. Although a great deal of information has been generated on the properties of these materials, because of the complex interactions between the fuel and its reactor environment, much more needs to be done. From a fundamental standpoint, the actinide compounds are exciting vehicles for the study of solid state phenomena because of their apparent similarities, yet also their vast differences which arise from their complex electronic structure and bonding.

These are materials in which there is a strong correlation between the understanding of the basic physical phenomena and their engineering usefulness. Some of the areas of further study which would yield a better understanding of the materials themselves and provide useful design data are:

1. The chemical potentials of the various constituents in the materials as a function of composition and temperature,
2. mechanism of fission product retention in the solid state,
3. atomic diffusion in chemical and thermal gradients,
4. fission gas void formation and migration,
5. the effect of thermal gradients on microstructural changes such as grain growth,
6. variations in all of the above with solid solutions between various fuel compounds and fission products.

Certainly ceramic nuclear fuel materials merit a good deal of consideration since it can be estimated that in the not too distant future the value of the annual production of plutonium metal alone, will exceed one billion dollars [5]. Therefore, it does not take a great deal of imagination to foresee that the nuclear fuel industry will make a sizeable contribution to the gross national product within a few short years.

Acknowledgments

Thanks are extended to Mr. J. E. Schumar for his helpful comments and enlightening discussions. This work was performed under the auspices of the United States Atomic Energy Commission.

References

- [1] A. Glasner, Introduction to Nuclear Science, p.90, Van Nostrand, Princeton, N. J. (1961).
- [2] H. Soodak, editor, Reactor Handbook, 2nd Ed., Vol. III, Part A. Physics, p.10, Interscience, New York (1962).
- [3] *ibid.*, p.275.
- [4] *ibid.* p.285.
- [5] Plutonium Survey, 1963, Edison Electric Institute, New York (1963).
- [6] R. G. Palmer and A. Platt, Fast Reactors, p.3, Temple Press, London (1961).
- [7] F. J. Leitz, p.105, Fast Reactor Technology, Report No. ANS-100, American Nuclear Society (1965).
- [8] R. B. Gordon, Nuclear Fuel Elements, ed. by H. H. Hausner and J. F. Schumar, p.20, Reinhold, New York (1959).
- [9] Maximum Permissible Body Burdens and Maximum Permissible Concentrations of Radionuclides in Air and Water for Occupational Exposure, National Bureau of Standards Handbook 69 (1959).
- [10] T. D. Chikalla, J. Am. Cer. Soc., 46 323 (1963).
- [11] G. F. Burdi, editor, Snap Technology Handbook, Vol. III, Refractory Fuels and Cladding, Report No. NAA-SR-8617, Vol. III, April (1965).
- [12] R. J. Ackermann and R. J. Thorn, Paper No. SM-66/80, Thermodynamics (Proceedings of the IAEA Symposium on Thermodynamics with Emphasis on Nuclear Materials and Atomic Transport in Solids, Vienna, July 22-27, 1965). Vol. I, p.243, Int. Atomic Energy Agency, Vienna (1966).
- [13] J. Belle, editor, Uranium Dioxide: Properties and Nuclear Applications, Chapter 5, "Physical Properties of Uranium Dioxide," p.173, Naval Reactors, Division of Reactor Development, USAEC (1961).
- [14] M. H. Rand and O. Kubaschewski, The Thermochemical Properties of Uranium Compounds, Oliver and Boyd, Edinburgh (1963).
- [15] S. M. Lang, "Properties of High Temperature Ceramics and Cermets, Elasticity and Density at Room Temperatures," U. S. National Bureau of Standards, Monograph 6, March (1960).
- [16] N. R. Gardner, Nuclear Reactor Fuel Elements, Metallurgy and Fabrication, A. R. Kaufman, ed., p.194, Interscience, New York (1962).
- [17] A. Strasser, Nuclear Eng., August (1960).
- [18] J. A. Leary, R. L. Thomas, A. E. Ogard, and G. C. Wonn, Carbides in Nuclear Energy, Vol. I., p.365, Macmillan, London (1964).
- [19] M. A. De Crescente and A. D. Miller, *ibid.*, p.342.
- [20] L. J. Graham and R. Chang, Compounds of Interest in Nuclear Reactor Technology, p.409, Nuclear Metallurgy, Vol. X, AIME, IMD Special Report No. 13 (1964).
- [21] S. C. Carniglia, p.403 of Ref. 18.
- [22] E. O. Speidel and D. L. Keller, "Fabrication and Properties of Hot-Pressed Uranium Mononitride," Report No. BMI-1633, May (1963).
- [23] J. Bugl and A. A. Bauer, p.215 of Ref. 20.
- [24] Y. Baskin and P. D. Shalek, p.457, Ref. 20.
- [25] E. D. Cater, R. J. Thorn, and R. R. Walters, p.237, Ref. 20.
- [26] C. R. Tottle, "Mechanical Properties of Uranium Compounds," Report No. ANL-7070, November (1965).
- [27] "Reactor Development Program Progress Report," Report No. ANL-7017, February (1965).
- [28] P. D. Shalek, J. Am. Cer. Soc., 46, 155 (1963).
- [29] K. A. Gingerich and P. K. Lee, J. Chem. Phys., 40 3520 (1964).
- [30] T. J. Paskar, D. R. Dehalas, D. L. Keller, and L. A. Neimark, Proc. 3rd Intern. Conf. on the Peaceful Uses of Atomic Energy, Geneva, August 31-September 9, 1964, p.472, Vol. 11, United Nations, New York (1965).
- [31] I. D. Thomas, Current Trends in Nuclear Power, proceedings of a symposium held at Tucson, Arizona, February 26-March 12, 1962, p.52, published by Argonne National Laboratory (1962).
- [32] W. V. Goettel, Materials and Fuels for High-Temperature Nuclear Energy Applications, M. T. Simnad and L. R. Zumwalt, eds., p.130, MIT Press, Cambridge, Mass. (1964).
- [33] H. R. Hoekstra, p.229 of Ref. 13.
- [34] A. E. Martin and R. K. Edwards, J. Phys. Chem., 69, 1788 (1965).
- [35] R. N. R. Mulford, *et al.*, Plutonium, 1960, p.301, Cleaver-Hume, London (1961).
- [36] M. H. Rand and L. E. J. Roberts, Paper No. SM-66/29, Ref. 12, Vol. I, p.3.

- [37] R. W. Spence, International Science and Technology, No. 43, p.58, July (1965).
- [38] A. F. Weinberg, L. Young, and R. G. Hudson, p.73 of Ref. 32.
- [39] see Ref. 11.
- [40] W. D. Kingery, Introduction to Ceramics, John Wiley and Sons, New York (1960).
- [41] W. S. Williams, J. Am. Cer. Soc. 49, 156 (1966).
- [42] L. A. Neimark and J. H. Kittel, "The Irradiation of Aluminum Alloy-Clad Thoria-Urania Pellets," Report No. ANL-6538, June (1964).
- [43] J. L. Daniel, J. Matolich, Jr., and H. W. Deem, "Thermal Conductivity of UO_2 ," Report No. HW-69945, September (1962).
- [44] L. A. Neimark, J. H. Kittel, and C. L. Hoenig, "Irradiation of Metal-Fiber-Reinforced Thoria-Urania," Report No. ANL-6397, December (1961).
- [45] W. M. Armstrong and W. R. Irvine, J. Nucl. Maters., 12 261 (1964).
- [46] M. H. Fossler, F. J. Huegel, and M. A. De Crescente, "Compressive Creep of UC and UN," Report No. PWAC-482, Pt. 1, October (1965).
- [47] B. T. M. Willis, Nature, 197 755 (1963).
- [48] P. Nagels, et al., J. Appl. Phys., 35 1175 (1964).
- [49] p.212 of Ref. 13.
- [50] L. M. Atlas, private communication.
- [51] P. Costa and R. R. Conte, p.3 of Ref. 20.
- [52] M. Allbutt, A. R. Junleison, R. M. Dell, ibid, p.65.
- [53] P. Costa, R. Lallement, F. Anselin and D. Rossignol, p.83 of Ref. 20.
- [54] W. S. Williams, Science, 152, p.34, April (1966).
- [55] S. P. Denker, p.51 of Ref. 20.
- [56] P. D. Shalek and G. D. White, p.266 of Ref. 18.

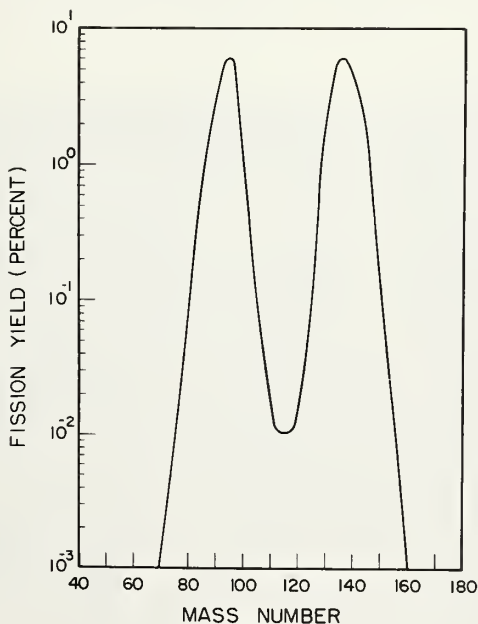


FIGURE 1. Fission product yield from U^{235} [3].

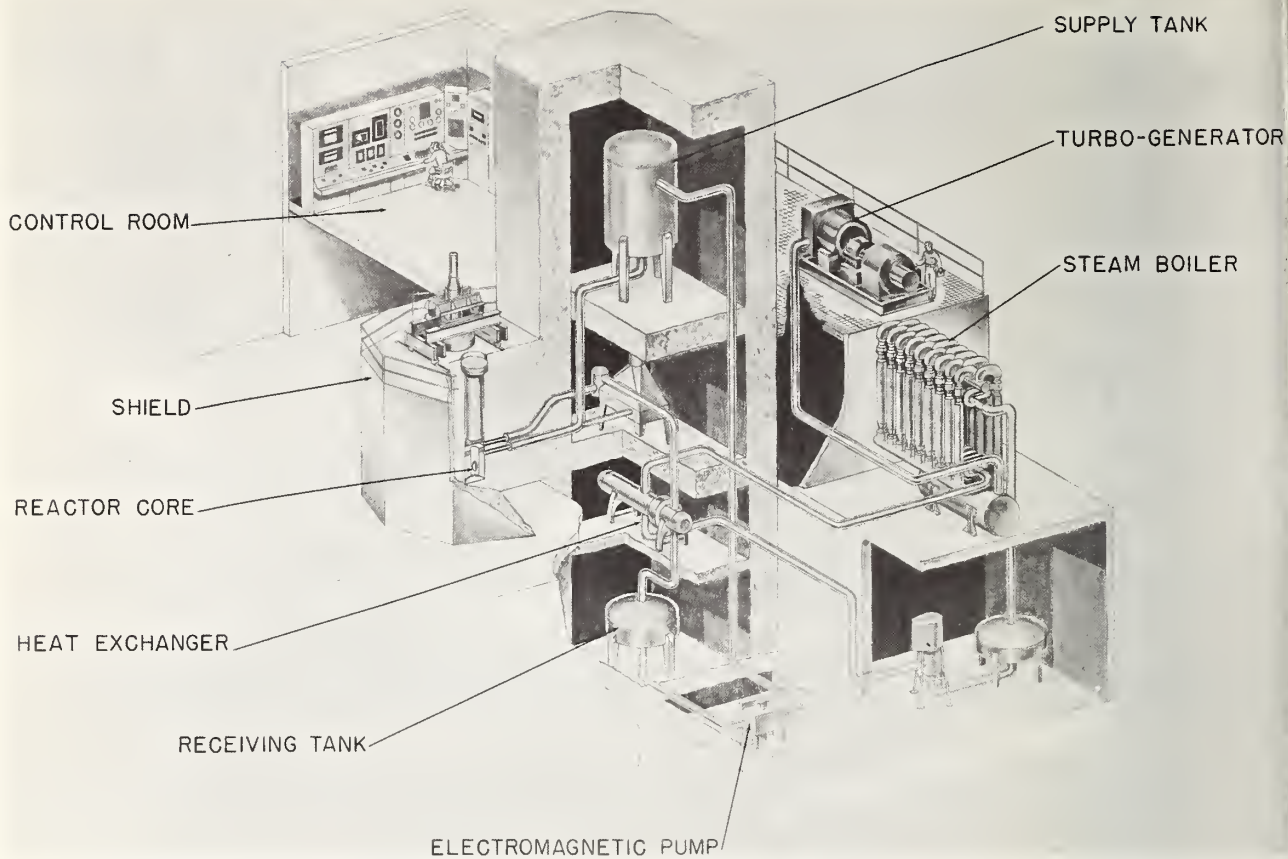


FIGURE 2. Schematic diagram of a typical liquid-metal-cooled reactor power generating system.

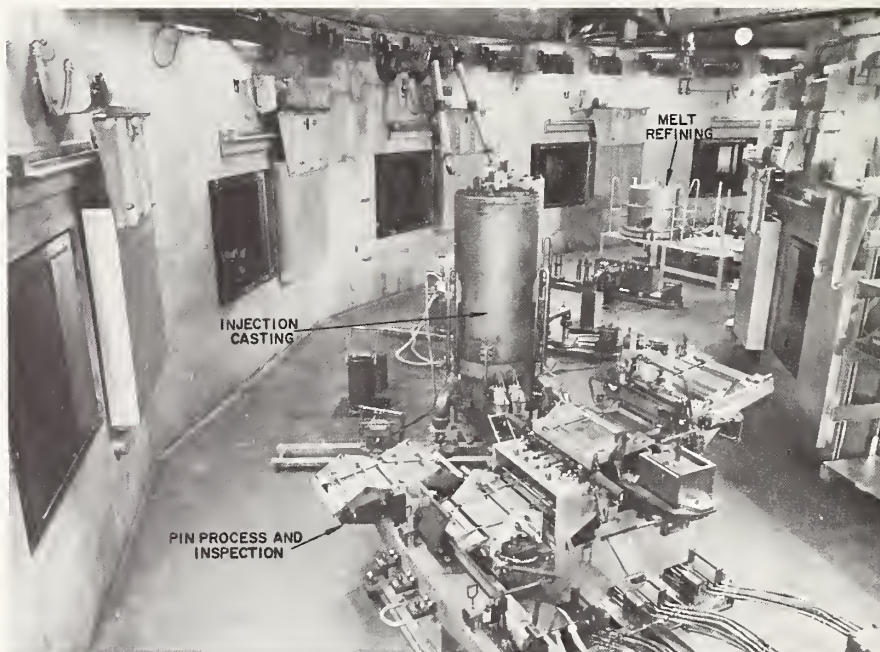


FIGURE 3. Interior view of the remote reprocessing facility for the EBR-II reactor showing the equipment used for pyrometallurgical reprocessing of the metallic fuel. Operating personnel are behind the wall (biological shield) running from the left to the rear of the photograph.

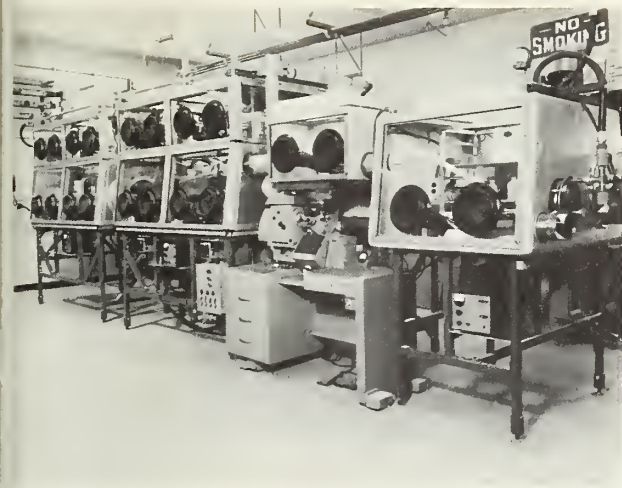


FIGURE 4. Plutonium metallography glovebox installation at Argonne National Laboratory illustrating a typical glovebox facility.

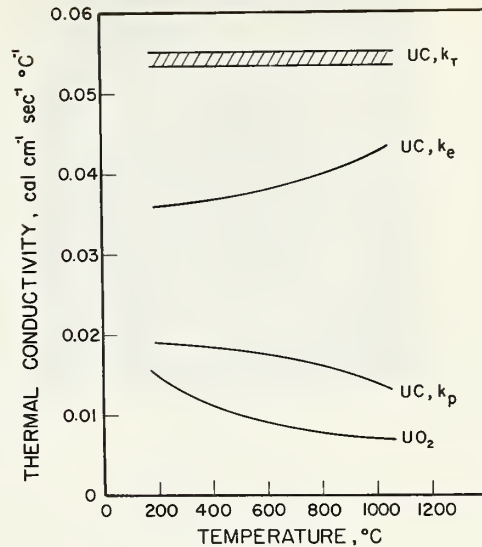


FIGURE 6. Comparison of the thermal conductivity of UO_2 and UC; k_T , k_p , and k_e are the total, phonon, and electronic thermal conductivities of UC respectively. Note the large electronic contribution in UC which increases with increasing temperature.

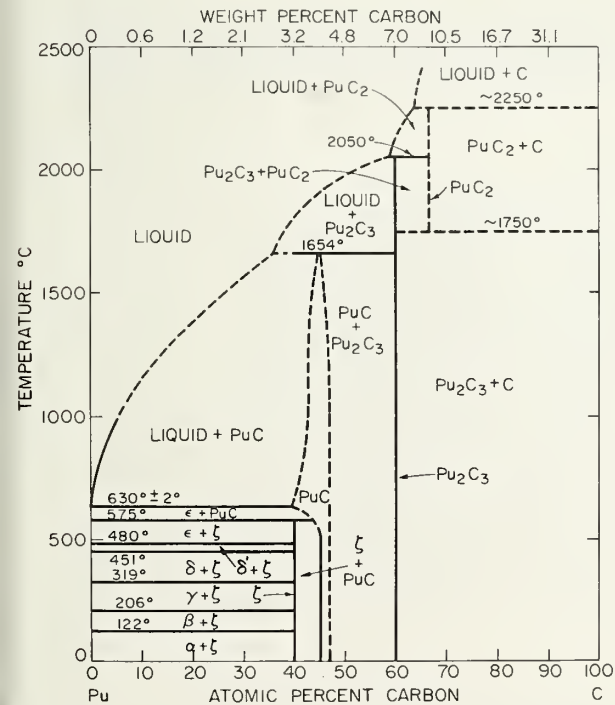


FIGURE 5. Plutonium-carbon phase diagram [35] illustrating typical deviation from stoichiometry of the sodium chloride type compounds.



FIGURE 7. Longitudinal section through UO_2 -25.6 w/o ThO_2 pellet showing columnar grain growth (dark) and molten area (gray) after 28,500 MWD/metric ton burnup. [42]



Unfibred
 $k d\theta = 86 \text{ w/cm}$
 20,000 Mwd/T
 $\text{ThO}_2 - 10 \text{ w/o UO}_2$



10 w/o Mo Fibers
 $k d\theta = 115 \text{ w/cm}$
 20,000 Mwd/T
 $\text{ThO}_2 - 30 \text{ w/o UO}_2$

FIGURE 8. Effect of increasing the overall thermal conductivity (measured by $k d\theta$) of an irradiated oxide fuel rod by insertion of molybdenum fibers. Note the large central void and columnar grain growth in the sample on the left produced by fission gas migration up the thermal gradient. The light areas are the lead bonding phase which has penetrated cracks formed in the fuel by thermal cycling [44].

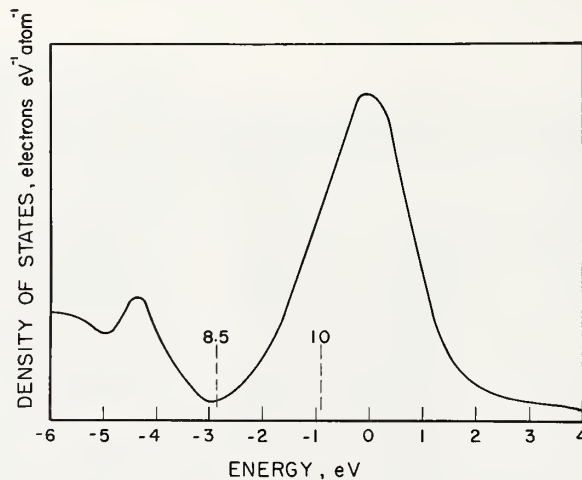


FIGURE 9. Density of electronic states curve in the transition metal monocarbides, nitrides and oxides. The position marked "10" would be the Fermi level in TiO if both sublattices were full. The position marked "8.5" indicates the Fermi level in stoichiometric TiO with fifteen percent vacancies in both sublattices. The top of the bonding band falls at about the minimum in the density of states curve; above the minimum the states are largely antibonding [55].

Reactor Materials Design

D. R. de Halas, W. C. Morgan, and M. D. Freshley

Battelle Northwest
Richland, Washington

Abstract

Design problems in the use of graphite as structural and moderator materials in a nuclear reactor are discussed. The type of graphite to be used is controlled by the service temperature and type of atmosphere. Dimensional stability under irradiation is controlled by graphite structure. Effects of radiation damage, service temperature and atmosphere on the use of beryllium oxide are outlined. A summary of the several types of irradiation damage to nuclear control materials are given. Engineering aspects of ceramic fuel element design are used as a basis for discussion of materials coupling problems in reactor design. Stresses introduced by changes in the core often cause clad failure. Compatibility between the core and clad material, and effects of impurities in the core as acting on the clad, are also important. Service conditions affect the choice of materials, due to effects on performance of failed fuel elements, corrosion, and fission gas release.

Reactor Materials Design

D. R. de Halas, W. C. Morgan, M. D. Freshley

1. Introduction

This paper covers four independent subjects: graphite, beryllium oxide, ceramic control materials, and the design of ceramic fuel elements. The first three sections cover the properties of nonfuel ceramic materials used in reactor design and discuss limits of application and design considerations for use in these materials. The fourth section discusses the influence of the properties of ceramic fuel materials on the design of nuclear reactor fuel elements.

2. Graphite

Introduction

The choice of graphite as a moderator material in the first nuclear reactors was predicted on the large ratio of neutron scattering cross-section to absorption cross section, the availability of large amounts of material at relatively low costs, and the ease of forming and machining to the shapes and sizes required for construction. These "traditional" reasons are still valid and govern the choice of graphite over other materials for certain applications, but other special properties are becoming more important in specific designs. The high strength-to-weight ratio, increased strength at elevated temperatures and wide range of available thermal conductivities, are examples of some of the special properties of artificial graphites.

Artificial carbons and graphites are aggregates of, approximately randomly oriented graphite crystallites, which are literally glued together with nongraphitic carbon atoms. Graphite crystals are composed of hexagonal planes of carbon atoms, stacked in an A-B-A- sequence as shown in Figure 1, with rather weak bonding between the planes. Thus, the physical properties of the crystals are very anisotropic, as is shown in Table I. The physical properties of the artificial aggregate can be varied over a wide range depending on the choice of raw materials and processing conditions, which control the alignment of crystallites, the bulk density, and the amount of nongraphitic carbon.

TABLE I. Physical Properties of Crystals

	Single Crystal	
	<u>a-direction</u>	<u>c-direction</u>
Coefficient of Thermal Expansion		
0-500 ° C (x 10 ⁻⁶ per ° C)	-0.5	28.2
500-1000 ° C (x 10 ⁻⁶ per ° C)	+0.8	29.4
Electrical Resistivity (ohm-cm)	4 x 10 ⁻⁵	0.3
Thermal Conductivity (watts/cm °C)	4.0	0.8

Limitations on Use

As with any material some of the properties impose limitations on the environments in which graphite can be used. The reaction of graphite with oxidizing gases has perhaps received the most attention. The amount of oxidation which is considered permissible in a given application is usually limited by reduction of strength rather than the gross amount of graphite removed. The loss of strength with oxidation is disproportionately large for graphite; for example, a homogeneous weight loss of 10% may result in 50% reduction in compressive strength. Oxidation rates are of course dependent on controllable properties, such as porosity and impurity content, but as a general rule, reaction rates are considered excessive above about 300 °C in air and 600 °C in CO₂. The problems associated with oxidation can be eliminated by the use of nonoxidizing gas atmospheres, such as helium or nitrogen, or protective coatings, such as pyrolytic carbon or silicon carbide. Coatings must of course be chemically stable in contact with graphite at the operating temperatures, but even more important, the coating

and artificial graphite grade must be carefully chosen to eliminate any significant mismatch in thermal expansion coefficients or dimensional changes under irradiation.

The design of nuclear reactors often requires that structural or cladding materials operate in contact with graphite for long periods of time. The choice of materials for such applications, especially at elevated temperatures, must be carefully made since most metals and their oxides react with carbon far below their melting point. In this regard, it is fortuitous that the oxides of thorium, uranium, and plutonium do not react with graphite below about 1800 °C; and likewise the oxides of aluminum, beryllium, magnesium, and zirconium are usable over about the same temperature range.

One of the most important phenomena associated with graphite is the fairly large dimensional changes which are produced during neutron irradiation. Irradiation of graphite crystals results in an expansion in the direction perpendicular to the basal planes and contraction in the direction parallel to the planes. However, the behavior of the artificial graphites is dependent not only on the changes occurring in the crystallites, but also on the changes in the nongraphitic portions of the aggregate. In general artificial graphite bodies initially contract in all directions when irradiated at temperatures above 300 °C; at higher exposures contraction ceases and the aggregate begins to expand. The contraction rates and other phenomena depend on the type of graphite and the irradiation temperature. These effects will be discussed in more detail in a following section of this paper.

Examples of Usage and Reactor Design

The prime use of graphite in reactors has been as the neutron moderator. Some typical graphite moderated reactor designs are listed in Table II, the listing is not meant to include all reactors, but represents different types which have evolved.

TABLE II. Graphite Moderated Reactor Types

	Coolant	Reactors
Horizontal Channels	Air	X-10 (ORNL) BGRR Windscale Reactors (UK)
	Water	Hanford Production Reactors NPR
	CO ₂	G-2 and G-3 (French)
	He	UHTREX (Los Alamos)
Vertical Channels	Water	APS (USSR) Urals Power Station Reactors (USSR)
	CO ₂	Calder Hall Reactors (UK) Tokai Mura (Japan) AGR (UK)
	He	EGCR (ORNL) Dragon (UK-EURATOM) Peach Bottom
	Sodium	Hallam
	Molten Salt	MSRE (ORNL)
Pebble-Bed	He	PBR (West Germany) PBRE (ORNL)

The first reactors were built of graphite bars stacked in horizontal layers. This arrangement allows the fuel and coolant tubes to be solidly supported by the graphite moderator, but distortion of the stack at high exposures can result in maintenance or fueling problems.

One of the most unusual graphite moderated reactors ever conceived is the Ultra High Temperature Reactor Experiment (UHTREX). The core consists of 24 wedge-shaped graphite blocks; each a 40-inch high block containing 13 radial fuel channels. The blocks are keyed together, producing a cylinder 70 inches in diameter with a 12-inch diameter axial hole, and pinned to a graphite base disk. The entire core can be rotated to charge fuel elements and discharge them through the central hole. The unclad fuel elements consist of graphite tubes impregnated with uranium oxide. Fuel temperatures of

1820 °C and exit helium coolant temperatures of 1315 °C are expected during operation.

One means of reducing the distortion problem is to turn the stack on end as was done with the Calder Hall Reactors. As variation of this configuration one can interlock the bars with keys, as was done at Takai Mura, use monolithic multihole columns as in the EGCR, or position the fuel channels between bars as in the Hallam Reactor. All of these configurations reduce the effect of graphite distortion; in addition, means can be provided in the design for periodic replacement of the moderator if the distortion is expected to become excessive.

Another alternative is to make the moderator replaceable with the fuel, as a monolithic fueled column as in the Peach Bottom and Dragon Reactors, as fueled segmented blocks as in the Colorado Reactor types.

The Dragon and Peach Bottom Reactors both make extensive use of graphite in their designs. Both are helium cooled and are fueled with U-Th carbides in graphite-clad elements. Maximum graphite temperatures of about 1650 °C are expected at coolant outlet temperatures of 730 - 750 °C. The main differences in the two reactor designs are in the arrangement of the replaceable fuel-moderator elements and in the methods used to scavenge fission products which are released from the fuel.

The Pebble Bed Reactors are of another unusual design. The uranium or thorium oxides or carbide fuels are contained in graphite spheres, which serve the dual purpose of containing the fission products and acting as moderator.

In the Molten Salt Reactor Experiment (MSRE) at Oak Ridge, the fuel is a solution of fluorides of uranium, thorium, Li⁷, beryllium, and zirconium, circulated through channels in the graphite moderator. This design provides a possibility of reducing fuel costs and shut-down time for a power-generating reactor.

Graphite is useful for reactor shielding either in purified form as a neutron reflector, or as a neutron absorber by adding a neutron poison such as boron. Porous carbon or carbon felt is an excellent material for heat shielding if protected from fast neutrons or if the design allows large dimensional changes in these parts.

Dimensional Changes During Irradiation

To understand the effects of neutron irradiation on artificial graphite, it is helpful to consider how the material is made. The normal nuclear grade graphites are composed of small particles of a ground petroleum coke filler; about half of the particles, by weight, are less than 0.1 millimeter on a side, each containing literally millions of graphitic carbon crystallites. The filler particles are mixed with about 25 weight-percent coal-tar pitch, which binds the particles together, then the mass is extruded to the desired shape. During the extrusion process, flow of the mass through the dies generally aligns the long axis of the particles parallel to the axis of extrusion. Since the basal planes of the crystallites are generally oriented parallel to the long axis of the filler particles, this results in a preferred orientation of crystallites within the bar and a higher degree of orientation near the surface of the bar.

After extrusion, the bars are baked to pyrolyze the binder pitch, then heated in a graphitizing furnace to a temperature between 2400 and 3000 °C. Some shrinkage and cracking occurs during the heating and the crystallites grow in perfection.

During the period of cooling-down from graphitization temperature, the anisotropy of the thermal expansion coefficients results in generation of internal stresses in the temperature range below about 1800 °C. These stresses are partially relieved by formation of microscopic cracks, called Mrozowski-cracks, parallel to the crystallite basal planes.

Thus, the resultant body is composed primarily of graphitic crystallites, but contains some non-graphitic bonding carbon, some residual internal stresses, and a system of cracks parallel to the crystallite basal planes.

During neutron irradiation, the volume change of the crystallites is always positive; the expansion in the "c-direction" is larger than the contraction in the "a-direction" by a factor which varies from about 10 at room temperature to about 2.5 at 650 °C. The dimensional changes of an artificial graphite are dependent not only on the changes of the constituent crystallites but also on how much of these changes are transmitted to the aggregate, how much is absorbed in closure of the internal cracks or in deformation of nongraphitic portions of the aggregate, and on the effect of the changes in internal stresses. Typical behavior of a graphite under irradiation is illustrated in Figure 2.

The general features of the dimensional change resulting from exposure to neutron irradiation for graphites have been postulated to result from the following phenomena:

- (1) Low-exposure transverse expansion due to relief of internal stresses.
- (2) "Linear contraction" dependent on "a-direction" contraction, with much of the "c-direction" expansion being absorbed in closure of cracks.
- (3) Transmission of "c-direction" expansion to the aggregate and re-orientation of crystallites within the body, after closure of the cracks.

Two other phenomena, associated with irradiation-induced dimensional changes, can be of prime importance to reactor designers, arising from the effects of external stress and of sample size. Externally applied stresses produce significant creep rates in artificial graphites during irradiation. For example, compressive stresses of only a few hundred psi are required to increase the apparent contraction rates by a factor of 2. The steady-state creep is apparently accommodated in the inter-crystalline bonding regions since the crystalline dimensional changes do not appear to be affected by the applied stresses.

It has been observed that the dimensional change rates of large bars of graphite are about 2.5 times the rates obtained on small samples. Two effects have been postulated to explain this observation:

- (1) in large bars, a "skin" of highly oriented graphite exists due to the effect of the extrusion process; this skin may contract at a more rapid rate than the interior graphite, thus producing stresses which accelerate the contraction
- (2) in smaller samples, cracks, which intercept the surface, may partially relieve the internal stresses generated between crystallites.

3. Beryllium Oxide

Introduction

Beryllium oxide has always been an attractive material for thermal nuclear reactors even prior to the demonstration of criticality at Stagg Field, Chicago. Its principal attributes are good moderating characteristics, relatively high thermal conductivity, and relative inertness. The interest in beryllium oxide is still high for advanced reactor applications where it is the aim to increase efficiency by using higher temperatures.

The applications for beryllium oxide fall in two categories; those in which it is used only as a moderator, and those in which it is used as a fuel matrix material. In the latter applications, it also acts as a moderator material.

Use as a Moderator

Extensive investigations in the United States and Europe have delineated the limitations and the applications of beryllium oxide. Under certain power reactor conditions the BeO can be physically degraded due to the neutronic production of helium gas in the lattice and the effects of fast neutrons on the crystallographic structure of the BeO. If irradiations are carried out at too low a temperature the BeO is subject to physical disintegration by microcracking. Factors that influence the radiation degradation of BeO include grain size, impurities or additives, and if it is used as a fuel material, the extent of fuel loading.

The resistance of BeO to neutron irradiation degradation improves as the temperature is increased above 500 °C. At the present time there are only limited data concerning the effects of irradiation above ~ 1100 °C. It appears that for certain reactor applications BeO may possess suitable radiation integrity starting in the range from 700 to 1000 °C.

Use as a Fuel Matrix

Fueled BeO can take many forms. Much of the work has been done with spherical UO₂ particles, of maybe 200 to 300 μ diameter, enclosed by BeO. Figure 3 shows a micrograph of such a fuel structure. Similar structures have been made using UO₂-ThO₂ and even UC₂ or UC₂-ThC₂ particles.

When BeO is used as a fuel matrix one of its principal requisites is good retention of fission products. In general, the amount of fission products released from a BeO matrix has been 2 to 3 orders of magnitude higher than reactor designers prefer. The higher amounts released appear to result from the porosity of the matrix even though greater than 98% of theoretical density has been achieved. Poor fission product retention has been one reason for a lessening of interest in BeO as a fuel material.

However, recent work at General Atomic has shown that improvements in the fabrication techniques for BeO have markedly improved fission product retention at temperatures as high as 1400°C. Values that are quite close to those that are desired are now obtained. The improved retention characteristics are due mainly to closing of pores in the BeO matrix by the production of a material having a density of > 99.3% of the theoretical value. The high density appears to be related to two factors: the current availability of more highly sinterable grades of BeO powder; and development of the technique of hot pressing during sintering. This latter technique is excellent for overcoming the limitations of less sinterable powders and reducing variability from batch to batch of the same powder. The resulting structures have a grain size of 5 μ or less which probably not only enhances fission product retention but also reduces the effects of radiation on physical degradation. To date the results on these improved materials are preliminary, but high exposure irradiations have been started.

Cost

The cost of material and its fabrication has always been greater for BeO than for graphite. This has placed some limitations on the competitive position of BeO as a solid moderator material. However, due to recent demands of the aerospace and electronics industries, BeO can now be obtained in large quantities for approximately \$10/lb. This compares with the cost of \$20/lb. five years ago. This reduced cost aids in making fueled BeO competitive with other high temperature fuel systems, particularly coated particles. The recent improvements in fabrication methods have reduced the cost of fueled BeO compacts so much that there is now a much less pronounced differential between coated particle fuels and fueled BeO than there used to be.

4. Ceramic Control Materials

Control materials are used in nuclear reactors to absorb neutrons and control reactivity. Their primary requirement, therefore, is that they have a high absorption cross section for neutrons. The very fact that control materials have high cross sections means that they are highly susceptible to reaction and potential damage from neutrons.

Control materials have been used in reactors in forms of alloys (for example, cadmium-indium-silver alloy), as dispersions (for example, B₄C in aluminum), or as pure ceramic (for example, B₄C). The pure ceramic materials have little structural strength and must be supported by the control rod components. A basic design might consist of encapsulated doughnut-shaped ceramic wafers strung on a water cooled tube. Alternately, the control rod could be fabricated by vibrational compaction of sized ceramic powder.

Desirable properties of control materials include:

- *high cross section for neutron cross-section,
- *dimensional stability at high temperature,
- *good radiation damage resistance,
- *ease of fabrication,
- * mechanical stability,
- *decay after neutron absorption to a daughter material also possessing a high cross section for neutron absorption.

Common forms in which ceramic control materials are used are listed in Table III.

TABLE III. Common Ceramic Control Materials

Material	Melting Point	Macroscopic Cross Section	May be Used
B ₄ C	2450 °C	83.6 cm ⁻¹ (B ¹⁰ C 443.8 cm ⁻¹)	{ in Al (boral) in stainless steel in graphite
HfO ₂	2130 °C	2.9 cm ⁻¹	
Gd ₂ O ₃	2330 °C	1134.4 cm ⁻¹	{ in Zr, Ti, stainless steel
Eu ₂ O ₃	2050 °C	116.8 cm ⁻¹	
Sm ₂ O ₃	2300 °C	141.1 cm ⁻¹	

A prime consideration in the use of control materials is damage by neutrons. The damage principally falls into two categories; characterized by (n, α) and (n, γ) reactions.

Examples: Types of Reaction

(n, α)



(n, α)



The (n, α) reactions with thermal neutrons are generally limited to the light elements. The damage to the control material is principally caused by the products of this reaction. In the case of boron, the lithium atom that is formed has a larger atomic radius than the boron and causes lattice strain as it accumulates. However, the principal cause for damage is the helium atoms. At the higher temperatures these diffuse and agglomerate into small bubbles. With continued burnup, the pressure in the bubbles becomes considerable and causes appreciable swelling of the boron (B₄C). Damage is also produced in the crystal lattice by displacements resulting from collisions with recoil atoms. However, these displacements, creating interstitial atoms and vacancy clusters in the lattice, tend to be annealed out at higher temperatures.

The (n, γ) type of reaction is generally much less damaging to control materials. First of all, there is no helium generated. Also, the ionic radius of the product tends to be similar to that of the parent, so that there is less lattice distortion.

The means of controlling the damage lie in the design of the control rods. A particulate ceramic such as B₄C may be dispersed in a metal. The metal matrix acts first to provide restraint on the swelling of the ceramic particles. It also acts to lower the temperature of the ceramic phase, thereby reducing helium atom agglomeration and swelling. It is also possible to allow for swelling of the particles by using a low density particle in a dense metal matrix. Use of vibrationally compacted powder with a gas plenum for helium collection would also circumvent irradiation damage.

It is worthwhile to mention that the choice of control materials in fast reactors is much more limited than for thermal reactors. The control materials must have a high cross section for neutron absorption at high energies and this essentially limits the choice to the lighter elements, in particular, boron. Thus, in spite of the problems created by the (n, α) reaction in boron, these problems will have to be overcome by clever design and materials development. It is likely that much more effort will

be needed in the development of improved dispersion-type boron-based control materials.

5. Design of Ceramic Fuel Elements

Introduction

Although several kinds of ceramic systems hold promise as fuel for power reactors, oxides, carbides, and cermets have received the most attention and are being investigated most actively. Each fuel system has advantages and disadvantages and, ultimately, the service conditions dictate the choice of material. Fissile materials include Uranium, Thorium, and Plutonium with uranium receiving most attention. Recently, however, the use of plutonium as enrichment has received more emphasis and hence mixtures of uranium with plutonium, either for the oxide or carbide systems, are being investigated more earnestly.

Many factors must be considered in the design of reactor fuel elements and one of the complicating considerations is that the properties of the fuel material are continually changing throughout its reactor lifetime. The primary fuel design considerations are dimensional stability and compatibility and reactions between core and cladding and coolant, fuel relocation, solid and gaseous fission product accommodation, fission product and plutonium migration, fuel swelling and thermal expansion, among others. All of the ceramic fuel materials are prone to the same kinds of irradiation effects and the basic problems are essentially the same for each fuel type.

A satisfactory fuel design must provide structural integrity of the fuel for long operating lifetimes in the reactor environment and hence, the fuel material and its cladding must be considered as an integral unit.

Oxide Fuel Design

Dramatic structural changes occur during irradiation of high specific power oxide fuel elements. The postirradiation structure of oxide fuels is relatively insensitive to the fabrication technique, whether involving pelletizing or the use of packed particles. Sintering, grain growth, and densification of oxide fuels occur in the reactor at fuel temperatures above 1600 °C. This sintering and densification of the fuel causes the formation of a void in the thermal center of the fuel region. The densification process causes radial redistribution of the fuel. At fuel temperatures above melting, axial displacement or slumping of the oxide fuel has been observed. The degree of slumping depends upon the fuel geometry (rod diameter), the operating conditions, and the initial bulk fuel density.

These structural changes within the reactor affect the thermal conductivity of the fuel, altering the temperature profiles as irradiation proceeds.

Adequate accessible porosity must be provided within the fuel rods to accommodate swelling due to the accumulation of fission products and the thermal expansion of the fuel material. Fuel swelling is due to the combined effects of retained fission products and thermal expansion. At high burnup, UO_2 fuel changes in composition due to the accumulation of massive amounts (over 20%) of fission products, which causes swelling. The volume of UO_2 irradiated at relatively low temperatures increases 0.7% per 10^{20} fissions/cm³. This expansion rate is not attained until the initial porosity of the fuel is occupied. The thermal volume expansion of UO_2 from room temperature to the melting temperature is 15% and it experiences an additional increase of 10% in passing through the melting transition. Hence, a total volume increase of about 25% must be accommodated between room temperature and the fully molten condition. The effects of these large volume increases are particularly important in areas of a fuel rod which may have increased bulk density due to slumping or axial fuel relocation. Swelling in these regions then would cause interaction between the fuel and the cladding, and deformation or failure of the cladding.

Fuel rod swelling is reduced by using annular pellets or low density powder in the range of 80 to 85% of the theoretical density. However, the void space provided to accommodate swelling increases the potential for fuel redistribution.

Since approximately 30% of the fission products formed during the fission process are gases which may be released from the fuel at high operating temperatures, the fuel must be designed to accommodate the release of gases without allowing excessive pressure buildup within the rod to stress the cladding. Fission gas release values as high as 88% have been measured in $\text{UO}_2\text{-PuO}_2$ fuel rods operating under high power generating conditions. A reasonable fission gas release model for oxide fuels assumes 100% gas release from the fuel volume operating at temperatures above 1800°C and approximately 10% release for that fuel volume operating below this temperature. Excessive internal pressures within the fuel rod are avoided by the provision of adequate void space to accommodate the release of gases. Another solution to the problem of excessive pressure buildup that is receiving attention for high burnup fuels is the continual venting of the gases from the rod during operation through such devices as porous plugs.

Fuel property measurements made outside the reactor for nonirradiated ceramic fuel specimens should not be considered completely indicative of the performance capability of that fuel. The most important example of this is the differences in UO_2 thermal conductivity that are measured in and out of the reactor. These differences are apparently related to the oxygen potential within a completely canned fuel element, the magnitude of the thermal gradients, and at low temperatures, irradiation damage. Fuel composition also effects thermal conductivity. High O:U ratios, in particular, seem to adversely affect heat transfer rates.

Interactions Between Fuel and Cladding

Cladding strains are caused by external (coolant) pressures. This effect becomes important in the large diameter tubular elements and rods clad with thin-walled collapsible cladding. Thermal cycling of collapsed cladding would probably lead to early fatigue failure in the reactor. Cladding strain produced by thermal expansion of the fuel can rapidly limit fuel element performance.

Fuel-cladding interactions at high burnup are also affected by the chemical and radiation cladding material. In some cases, impurities in the oxide fuel material, such as water, carbon compounds, and halogens have a dramatic effect on the compatibility between the core and the cladding. Hydrocarbon impurities in the ceramic fuel can cause massive hydriding and subsequent rupture in the Zircaloy cladding in a relatively short period of time. The failure of some Zircaloy-clad rods after irradiation is characterized by a tree-like corrosion penetration from the inner surface of the cladding, a small crack, and no metallographically discernible zirconium hydride. Failures of this type have been tentatively attributed to fission product iodine attack on the Zircaloy. If such a failure mechanism is real, then fuel element exposure would be limited by fission product iodine buildup and temperature. These failures have been isolated cases and there is no statistical evidence that such a limit may be a real one.

Behavior of Fuel After Penetration of the Cladding

Penetration of cladding need not in itself limit the useful life of an oxide or ceramic fuel element and in fact, satisfactory failure behavior is an important fuel design consideration. Operating experience in several power reactors, test reactors, and experimental reactors has shown that fission product loss from the failed fuel rods can be accommodated without creating intolerable operating problems. Irradiations of oxide fuel rods containing intentional defects have shown that fission product activity bursts generally occur after changes in reactor power level. Steady-state release of fission products has been sufficiently low to cause no concern. One of the major concerns associated with the operation of oxide fuel rods with defects is the possibility that extensive fuel washout may occur as a result of waterlogging. This problem has been of particular concern for packed particle fuels which are more susceptible to the intake of water; however, operating experience with regard to lack of fuel washout has been very favorable.

Carbide Fuel Design

Uranium carbide or mixtures of uranium carbide and plutonium carbide fuels have application in liquid-metal-cooled thermal and fast reactors. In common with oxides, the carbides have the advantage of high melting point and good dimensional stability.

The thermal conductivity of the carbides is 4 to 10 times higher than that of uranium dioxide or mixed oxide fuel. The power generation rate limit may therefore be higher for carbides than for lower conductivity fuel materials. There are several ways to take advantage of this property with fewer, larger diameter fuel rods, higher specific power operation, and lower fuel temperatures to decrease fuel redistribution, swelling, and fission gas release.

The disadvantages peculiar to carbides are based on their thermodynamically reactive nature. The carbide fuels are less compatible with cladding materials than are the oxides. The poor oxidation resistance of carbides requires that they be handled in low oxygen and low moisture content atmospheres. Stoichiometry control is particularly important in carbide fuels. For example, free uranium or free-metal may cause enhanced fission gas release.

One of the most successful cladding materials for carbides is stainless steel, either type 304 or 316, since it is readily available and compatible with the sodium coolant. Medium nickel content alloys such as Hastelloy-X or Incoloy have higher strength but their compatibility with carbide is unknown. High nickel alloys such as Nimonic or Inconel-X are not compatible. Refractory alloys based on niobium, vanadium, molybdenum, and tantalum are reasonably compatible with the carbide but are likely to be unstable with respect to the coolant. Reaction with sodium is sensitive to impurities in the sodium. In order to take advantage of the high thermal conductivity of carbides, sodium bonding of the carbides to stainless steel cladding has been intensively investigated. However, this poses carburization problems with hyperstoichiometric fuel. Sodium helps reduce the higher carbides in the fuel and transfers the carbon to the stainless steel at temperatures as low as 650 °C. With hypostoichiometric UC fuel

sodium causes reactions to occur between free uranium and stainless steel cladding at temperatures of 760 to 870 °C.

One of the major problems to be solved for carbides as well as oxides is the accommodation of fuel swelling at high burnups without disruption of the cladding and without excessive fuel temperatures. Even the small diametral increases of 0.6% per percent burnup of fissile atoms amount to sufficiently large changes at 10 atomic percent burnup to put the cladding under severe strain.

Cermet Fuel Design

Cermet type fuels are utilized in small compact reactors operating at high specific power. A PuO₂-stainless steel cermet is being considered as the driver fuel for the Fast Test Reactor. One of the major reasons for the selection of the cermet as a reference fuel for the FTR is the large thermal expansion characteristic which produces strong, prompt negative temperature and power coefficients of reactivity.

Cermet type fuels disperse the fissionable ceramic phase as discrete particles in a continuous matrix of nonfissile material. To minimize radiation damage and provide metallic properties, the matrix should predominate in volume and exist as a continuous phase surrounding the fissile particles. The matrix metal, in effect, acts as a structural material in the fuel element.

A prime objective is to concentrate the irradiation damage in the dispersed phase and in a highly localized region surrounding the dispersed fissile particle, leaving a fission-product-free region of matrix metal around the zone of damage. The design of an ideal dispersion fuel includes a dispersed particle size large compared to the fission product range, uniform dispersion of particles in the metal matrix, a continuous matrix of maximum possible volume fraction, and high fissile particle density.

Other areas to be considered in cermet fuel design are the combined effects of residual stress, thermal stress, pressure from fission gases, volume expansion of the ceramic fuel particles, and fast flux irradiation damage to the matrix and cladding.

Because of the reduced fissionable atom density in cermet type fuels, the specific damage to individual particles is very great. With high density ceramic fuel particles tightly held in a dense matrix, very high fission gas pressures can result as the burnup become appreciable. It has been proposed to use low density fuel particles in a high density matrix to provide void space for the accommodation of fission gases generated during the irradiation process. The use of low density particles would also provide expansion space for swelling resulting from the accumulation of fission products within the particle at the very high burnups.

6. Acknowledgments

The authors would like to acknowledge the assistance of R. J. Lobsinger and J. B. Burnham of this Laboratory in the preparation of the information on ceramic control materials.

R. A. Meyer of General Atomic kindly furnished the up-to-date information on the status of beryllium oxide technology used in preparation of that section of this report.

This paper includes work performed by Battelle Northwest for the United States Atomic Energy Commission under Contract AT(45-1) - 1830.

7. Selected References

R. E. Nightingale, Nuclear Graphite,
Academic Press (New York, 1962)

M. T. Simnad and L. R. Zurwalt,
Materials and Fuels for High-Temperature
Nuclear Energy Applications, MIT Press
(Cambridge, Mass., 1964)

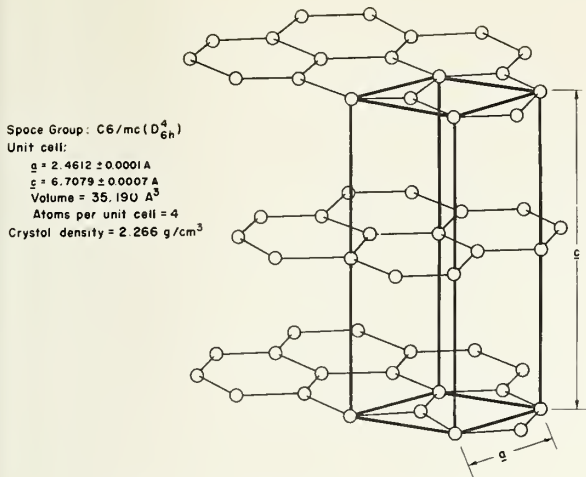


FIGURE 1. Graphite Crystal Lattice.

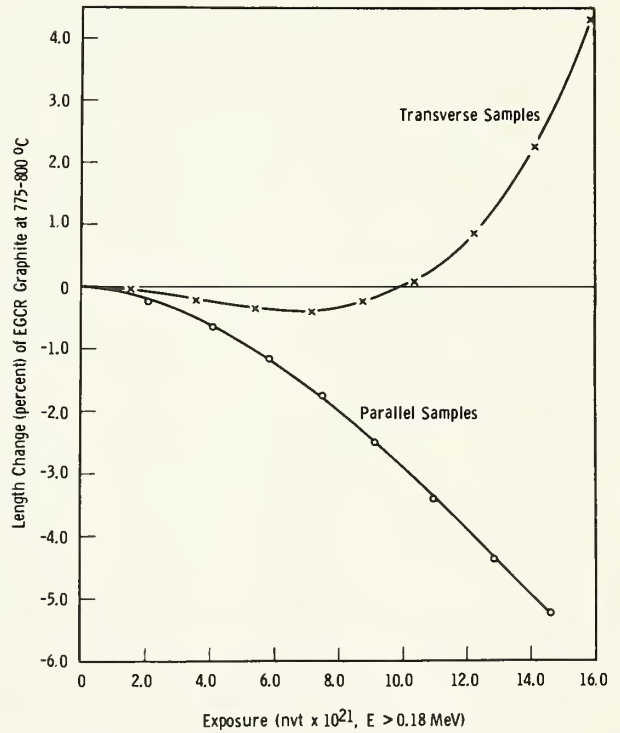


FIGURE 2. Dimensional Change of graphite under irradiation.

FIGURE 3. Microstructure of fueled BeO. White spheres are UO_2 particles in the BeO matrix.



